ENZYME IMMOBILIZATION INTO POLYMERS AND COATINGS

by

Géraldine F. Drevon

BS, Chimie Physique Electronique Lyon, 1997

Submitted to the Graduate Faculty of

School of Engineering in partial fulfillment

of the requirements for the degree of

Doctor of Philosophy

University of Pittsburgh

2002

UNIVERSITY OF PITTSBURGH

School of Engineering

This dissertation was presented

by

Géraldine Drevon

It was defended on

November, 2002

and approved by

Eric J. Beckman, Professor, Chemical and Petroleum Engineering Department

Toby M. Chapman, Associate Professor, Department of Chemistry

William Federspiel, Professor, Chemical and Petroleum Engineering Department

Krzysztof Matyjaszewski, Professor, Department of Chemistry, Carnegie Mellon University

Douglas A. Wicks, Professor, Department of Polymer Science, University of Southern Mississippi

Dissertation Advisor: Alan J. Russell, Professor, Chemical and Petroleum Engineering Department

ABSTRACT

ENZYME IMMOBILIZATION INTO POLYMERS AND COATINGS

Géraldine F. Drevon, PhD

University of Pittsburgh, 2002

In this study, we have developed strategies to immobilize enzymes into various polymer and coatings. Three categories of bioplastic matrices were investigated. The first type of bioplastics was prepared by irreversibly incorporating di-isopropylfluorophosphatase (DFPase) into polyurethane (PU) foams. The resulting bioplastic retained up to 67 % of the activity for native enzyme. The thermostability of DFPase was highly affected by the immobilization process. Unlike native enzyme, immobilized DFPase had biphasic deactivation kinetics. Our data demonstrated that the initial rapid deactivation of immobilized DFPase lead to the formation of a hyper-stable and still active form of enzyme. Spectroscopic studies enabled a structural analysis of the hyper-stable intermediate.

Biopolymers were also prepared via atom transfer radical polymerization (ATRP) using acrylic and sulfonate-derived monomers. ATRP ensured the covalent and multi-point immobilization of enzyme within polymer matrices. However, this approach was only partially successful, as no activity retention was obtained after polymerization

Enzyme-containing PU- and Michael adduct (MA)-based coatings correspond to the last category of bioplastics that was investigated. DFPase was irreversibly incorporated into PU coatings. The distribution of immobilized DFPase as well as activity retention were homogeneous within the coating. The resulting enzyme-containing coating (ECC) film hydrolyzed DFP in buffered media at high rates retaining approximately 39% intrinsic activity. DFPase-ECC had a biphasic deactivation profile similar to that of bioplastic foams. The synthesis of enzyme-containing MA coatings was performed in a two-step process using carbonic anhydrase (CA, E.C. 4.2.1.1). CA was first covalently immobilized into NVF-based water-soluble polymer (EP). The resulting EP was further entrapped into the matrix of MA coating. The so-formed ECC's exhibited approximately 7% apparent activity. CA-ECC showed good stability under ambient conditions and retained 55% activity after 90 days of storage.

TABLE OF CONTENTS

Page

LIST OF TABLES

LIST OF FIGURES

NOMENCLATURE

ATRP	Atom transfer radical polymerization
bpy	Bipyridine
BTP	Bis-tris propane
CA	Carbonic anhydrase
DFP	Diisopropylfluorophosphate
DFPase	Diisopropylfluorophosphatase
ECC	Enzyme-containing coating
EP	Enzyme-polymer
MANVF	Michael adduct from N-vinylformamide and methyl acrylate
MA	Michael adduct
NHS	N-Hydroxysuccinimide
NVF	N-Vinylformamide
NaSS	Sodium styrene sulfonate
PEG	Poly(ethylene glycol)
PEG-NCO	Poly(ethylene glycol)-monoisocyanate
PEG-$(NCO)_2$	Poly(ethylene glycol)-diisocyanate
PU	Polyurethane
TMATf	2-(N,N,N-trimethylammonio)ethyl methacrylate trifluoromethanesulfonate
Tris-HCl	Tris(hydroxymethyl)aminomethane-HCl

1.0 INTRODUCTION

Enzymes are attractive catalysts as they are highly effective and specific under ambient conditions. A major drawback is their short lifetimes. Research over the last four decades has focused on understanding the modes of enzymatic deactivation, as well as developing methods to overcome this shortcoming of the biocatalytic approach. Most enzymes are stable when stored at low temperatures and neutral pH's in aqueous media. This state is fragile and can be easily disturbed by means of external stresses such as high pressures and temperatures, extreme pH's, organic solvents, freezing, drying, and by oxidative, chelating, or denaturing agents. Conformational changes as well as chemical processes at the level of the polypeptide chains may be induced, leading to the enzyme inactivation. The resulting activity loss may be reversible or irreversible. The severity of these effects varies with the type of enzyme and the nature and the intensity of the stress. The main structural and covalent mechanisms in biocatalyst inactivation include the disulfide intra- and inter-exchanges, the deamidation of asparagine residues, the decomposition of disulfide bridges by b-elimination, the hydrolysis of peptide chains, the b-isomerization of asparagine and aspartic acid residues, and amino acid racemization.

A first approach to prevent deactivation consists of changing the enzyme environment, for example, by means of soluble additives such as metals, surfactants,

polyols, PEGs and sugars. Stabilization results from the non-covalent interactions between the additive, the biocatalyst and the solvent. Stabilizing effects of similar origin have often been observed for enzymes that are entrapped within a solid matrix or physically adsorbed onto a support. Other strategies rely on the alteration of the enzyme primary structure using one of the following methods: chemical modification; covalent immobilization; protein engineering; or directed evolution.

Immobilization refers to the preparation of insoluble biocatalytic derivatives and involves the coupling of enzymes to solid supports that are either organic or inorganic. It has been increasingly used in industrial applications as it facilitates the separation of biocatalysts from the effluents and, hence, the recovery and purification of the products. Moreover, solid biocatalysts offer the major advantage of being reusable. The large variety of matrices that can be used ranges from natural and synthetic polymers to silica beads. Covalent immobilization often proceeds by the reaction of specific functionalities at the support surface with amino acid side chains that are readily available on the enzyme surface. The covalent coupling may induce drastic changes in the enzymatic kinetics especially when it occurs near the active site. Another important effect is to reduce the enzyme flexibility. As the number of linkages between the enzyme and the support increases, so does the enzyme rigidity. By providing a maximum rigidity, multi-point covalent immobilization is likely to prevent enzyme unfolding upon heating or in the presence of a denaturant. A non-conventional strategy to achieve multi-point covalent immobilization within a polymer network is by

copolymerizing the enzyme with monomers capable of a chemical reaction with specific functionalities on its surface. During polymerization, the enzyme acts as a monomer and is, thus, expected to be uniformly distributed within the resulting biopolymer.

A large range of polymer matrices have been employed for enzyme immobilization. In this study, enzymes were inserted into various polymer networks. To optimize the catalytic efficiency and stability of the resulting biopolymers, the attempt was made to understand the immobilization effects on enzymatic properties. Polyurethane foams are attractive supports, and can be used to prepare highly active and stable bioplastics via multi-point and covalent immobilization. Therefore, their potential as matrices for the immobilization of the agentase diisopropylfluorophosphatase (DFPase) was investigated. Atom transfer radical polymerization (ATRP) is another potential method for the mutli-point and covalent immobilization of enzymes, as it is compatible with a large variety of functionalized monomers and can be performed under mild conditions. It was determined whether ATRP could be used for the incorporation of biocatalysts into polymer matrices. The third category of polymers that were tested includes polyurethane- and Michael adduct-based coatings. One important challenge in preparing enzyme-containing coatings (ECC's) was to reduce the internal diffusional limitations and, hence, assure good apparent activity retentions. A method to facilitate the access of immobilized enzyme to substrate for bio-PU coatings was developed. When working with Michael adduct-based coatings, the main aim was to

incorporate homogeneously the enzyme within the hydrophobic blend used for the casting of films. Given the enzyme hydrophilicity, the enzyme properties had to be altered to enable its dispersion in the coating bulk.

2.0 BACKGROUND AND LITERATURE REVIEW

2.1 Biocatalyst Deactivation and Regeneration

Biocatalysts offer major advantages over traditional metallic and organometallic catalysts such as high specificity and high efficiency under mild conditions of temperature, pressure and pH. However, their storage and operational instability limit considerably their use for industrial applications. Therefore, important efforts have been made to develop stabilization strategies, which rely on the rational understanding of the causes and pathways involved in their deactivation.

In this chapter, we will consider the reversible and irreversible deactivation of biocatalysts. At this point, it is necessary to specify that we will preferably use terms such as enzyme, protein, proteinase and protease instead of the more general term biocatalyst. We will describe the various modes of irreversible inactivation, and more especially, the deactivation induced by heat, extreme pH, organic solvents, freezing, antagonist additives such as detergents, salts, specific chemicals and metal ions. We will further examine the techniques that have been developed to prevent or minimize biocatalyst deactivation. Stabilization in aqueous media can be achieved by altering the water–protein interactions by means of external excipients, and by chemically or genetically modifying specific amino acids. Protein immobilization is another major strategy.

2.1.1 Reversible Denaturation

The denaturation of an enzyme corresponds to the unfolding of the enzyme by disruption of noncovalent intramolecular interactions. This can be induced by any change in the enzyme environment such as an increase in temperature or the addition of a denaturing agent. The process is reversible when the native conformation of enzyme (E) and, hence, the original biological activity are spontaneously recovered by simply returning to the initial external conditions. After extensive unfolding, an enzyme is predominantly randomly coiled, and hence inactive. The highest extent of protein reversible unfolding has been obtained at room temperature in the presence of denaturant chemicals such as urea, guanidine hydrochloride ($GdnH^+$, GdnHCl) and guanidine thiocyanate. Heat results also in extensive loss of ordered secondary and tertiary structures, as opposed to extreme pH, organic solvents and inorganic salts.[1]

Reversible unfolding involves a very cooperative two-state transition, $E \leftrightarrow U$, where the partially unfolded intermediates between folded and unfolded stages (U) are usually thermodynamically unstable and are not present in a significant proportion of total enzyme molecules.[2] The conformational stability is determined from the equilibrium studies and is given by the Gibbs energy of folding.[1]

Protein unfolding is often followed using techniques such as fluorescence, circular dichroism, UV-difference and raman spectroscopies as well as nuclear magnetic resonance, proton exchange and gel filtration.[3] Conformational changes can

also be evaluated from the changes in viscosity and sedimentation velocity of protein. Other chemical methods based on, for example, non-specific labeling of exposed amino residues, radioactive labeling and the reactivity of free thiol groups for specific reagent such as iodoacetate are available.[3]

2.1.2 Modes of Inactivation

Proteolysis. Proteases have the ability to catalyze the hydrolysis of protein chains at specific peptide bonds. Some proteases exhibit high selectivity. An example is the endoproteinase V8, which cleaves the peptide bonds at the COOH-terminal side of glutamic acid residues. Similarly, trypsin only recognizes and cuts the Lys-X and Arg-X bonds, where X can be any amino acid. Other proteases such as chymotrypsin and subtilisin show broader specificity. Enzymatic digestion is more efficient when the protein-substrate is unfolded, thus making the targeted sites more accessible.

2.1.2.1 Thermoinactivation. As the short lifetime of enzymes in heated systems represents a major drawback for their application to industrial processes, a major effort has been made since the 70's to understand and prevent irreversible enzymic thermoinactivation.

Most enzymes follow first order deactivation kinetics, where the enzyme deactivation is proportional to the time in a semi-logarithmic scale:

$$\frac{d[E]}{dt} = -k_d[E]$$

k_d corresponds to the deactivation rate constant, while $[E]$ represents the concentration of active enzyme, and is determined by activity assay.

It has been established in some cases that the reversible protein unfolding precedes the step of irreversible inactivation:

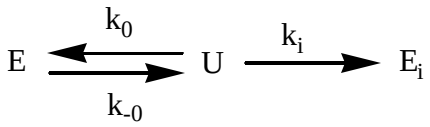

As mentioned in the previous section, the folding/unfolding transition is highly cooperative and, the unfolded enzyme (U) is inactive. When the system is kept at high temperature for a short period of time, only reversible inactivation occurs and the native activity is fully recovered by resuming the initial conditions. As the high temperature is maintained for longer periods of time, irreversible inactivation of the reversibly unfolded enzyme occurs, leading to the inactivate form of enzyme (E_i). Depending on the enzyme properties, irreversible inactivation may be attributed to diverse mechanisms either structural or chemical. The latter can both proceed via the unfolded form of enzyme U. However, the chemical modifications, which lead to covalent

changes on the enzyme molecules, can also directly occur on the native form E. We will present the different modes of enzyme inactivation and the inactivation processes involved in details later in this section

The time-dependent enzymatic activity loss exhibits a first order profile when the equilibrium between the enzyme forms U and E_i is rapid. The resulting apparent rate of deactivation, k_{app}, is a function of the rates for reversible folding/unfolding, k_0 and k_{-0}, as well as the rate for irreversible deactivation, k_i:[4]

$$k_{app} = \frac{k_i}{1 + K}$$

Hence, the estimation of the true rate of irreversible deactivation, k_i, relies on the determination of the equilibrium constant between folded and unfolded forms, E and U, ($K = \frac{k_{-0}}{k_0}$).

Biphasic irreversible deactivation is less commonly observed and can usually be modeled using multi-step kinetic mechanisms.[5,6] One useful model assumes the existence of an intermediate enzymatic state, E_1, with a reduced activity, a_1, and a deactivated form of enzyme (E_2) with a reduced activity, a_2:

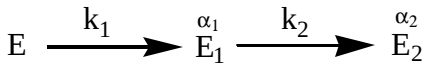

The expression for enzymatic activity is derived analytically, and is easily solved for the kinetic parameters:

$$[E] = [E]_0 \left\{ \left(1 + \left(\frac{a_1 k_1 - a_2 k_2}{k_2 - k_1} \right) \right) exp(-k_1 t) + \left(\frac{k_1 (a_2 - a_1)}{k_2 - k_1} \right) exp(-k_2 t) + a_2 \right\}$$

Where t is the time of thermoinactivation and $[E]_0$ the initial concentration of active enzyme. This model was successfully applied to the thermoinactivation of several enzymes such as, for example, phosphoglycerate kinase.[6] Some thermoinactivation patterns are well described using a simplified form of the two-step deactivation mechanism presented above where the final deactivated form E_2 is considered inactive $(a_2 = 0)$. Another simplified form of the two-step deactivation model assumes that the native enzyme E inactivates to a deactivated form, E_1, with a relative activity a_1 (a_2=0; k_2=0).[5]

Another simple kinetic scheme stipulating the presence of two different states of native enzyme with different deactivation pathways was used to describe the deactivation profiles of enzymes such as isozymes :[5,6]

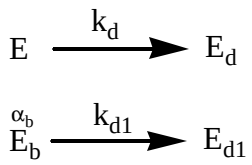

Once again an analytical solution for the enzyme activity course over time is available:

$$[E]_0 = \frac{\left([E]_0 \exp(-k_d t) + a_b [E_b]_o \exp(-k_{d1} t)\right)}{\left([E]_0 + a_b [E_b]_0\right)}$$

Where $[E_b]_0$ is the initial concentration of active enzyme form E_b, and α_b its initial relative activity.

Clearly, the main advantage of these kinetic schemes over more complex models is to provide an appropriate overview of the enzyme deactivation pathways using simple analytical techniques. If the chemical or conformational mechanism involved in an enzyme deactivation are known, kinetic analysis can serve as a useful tool to determine to which extent each of these processes occurs.

Proteases often exhibit non-first order thermoinactivation patterns. As protease molecules unfold upon heating, they become less resistant to self-digestion. Therefore,

their thermoinactivation can be thought as the result of the simultaneous intramolecular deactivation and autolysis:

When structural mechanisms are involved, irreversible thermoinactivation relies on either the protein aggregation or the protein spontaneous and incorrect refolding upon cooling often referred as scrambling.[7] Aggregation is caused by the intermolecular interactions between the hydrophobic areas of reversibly unfolded protein molecules. One potential route for aggregation is the disulfide interchange reaction between a free thiol group of one protein molecule and a disulfide bridge of another protein molecule.[2]

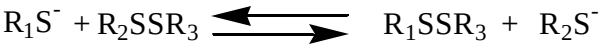

Scrambled structures of proteins have been shown to result in some cases from monomolecular disulfide exchange reactions.[8] Disulfide interchange can be minimized by maintaining a low pH.

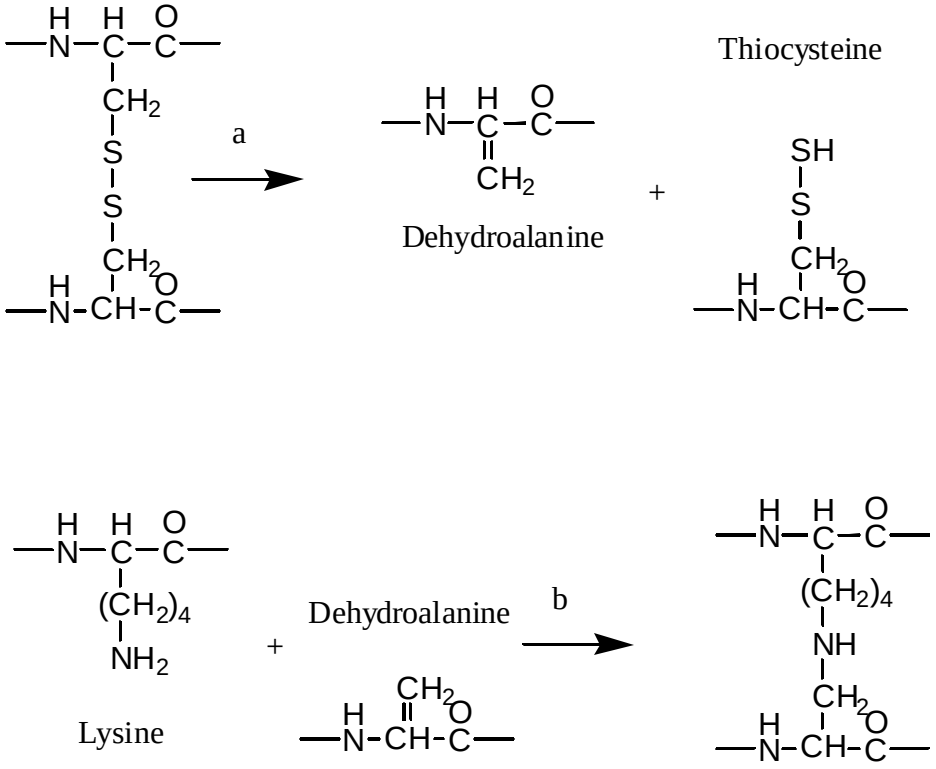

Figure 1 Decomposition of disulfide bridge

Several thermoinactivaton modes involve monomolecular chemical alterations of the enzyme primary structure. One possible cause is the decomposition of disulfide bridges into dehydroalanine and thiocysteine by β-elimination, which was reported, for example, at 100 ^{o}C for alkaline and acidic pH's ($4 \leq pH \leq 8$) (Figure 1; step a). [8,9] Peptide cross-linking further relies on the reaction of dehydoalanine with a lysine residue (Figure 1; step b).[8,9] Deamidation of asparagine residues can also largely contribute to protein thermoinactivation. It has been reported at alkaline and neutral pH's under both severe and mild heating conditions.[10] The proposed mechanism assumes the base-catalyzed attack of the side chain carbonyl carbon by the α-amino group, leading to the formation of a cyclic imide intermediate (Figure 2; step a).[11] The unstable five-membered succinimide ring further hydrolyzes into α- and β- aspartyl residues (Figure 2; steps b and c) with a typical isoaspartic acid to aspartic acid ratio of 3.[11] Deamidation of asparagines also takes place at acidic pH's, and is believed to result in the formation of α- aspartyl residues via direct hydrolysis.[11] The deamidation rate is greatly influenced by the type of residue present at the C-terminal side of asparagine. In fact, Asn-Gly and Asn-Ser sequences have been found to be particularly favorable to asparagine destruction.[11] Glutamines have been found to deamidate to a lesser extent than asparagines.

Another route is the hydrolysis of peptide bonds, which occurs at the Aspartic acid residues upon heating at acidic pH's. The cleavage at aspartic acids has been observed for several enzymes such as ribonuclease, RNase A, lysozyme,[12,8] and

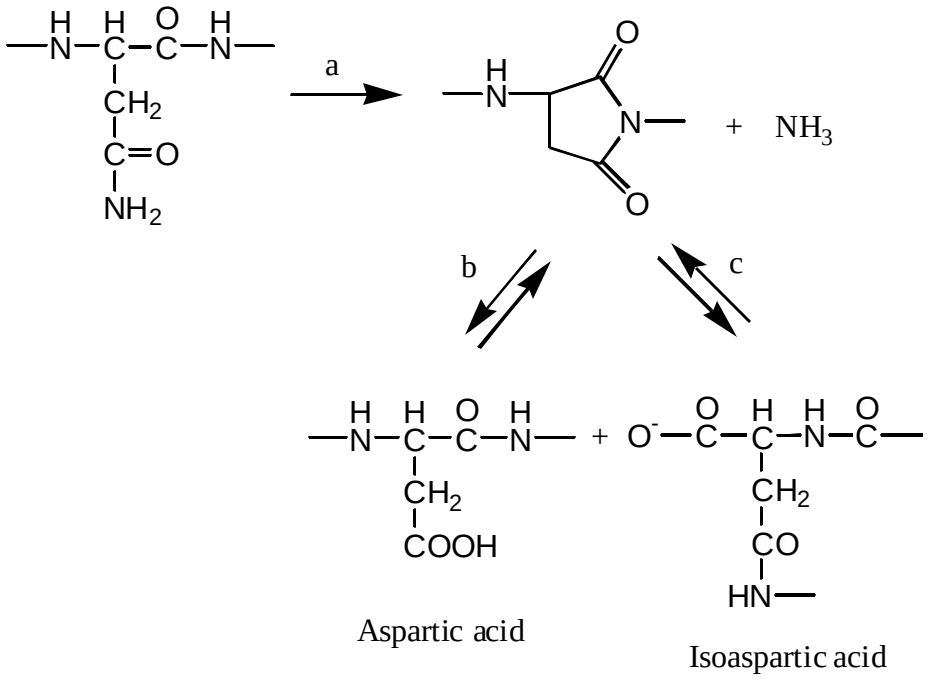

Figure 2 Deamidation of asparagines residues

peptides such as wool-polypeptide,[13] at pH's ranging between 2.5 and 4, and temperatures equal to at least 90 °C. Inglis suggested that the COOH- and NH_2- fissions follow distinct pathways.[13] The hydrolysis of carboxyl-terminal peptide bonds occurs via the formation a five-member ring as proposed for the deamidation of asparagine residues under acidic conditions. The hydrolysis at the NH_2-terminated bond is believed to rely on the formation of a six-member intermediate. Under neutral and alkaline conditions, the only reaction taking place is the cleavage of protein chain at the C-terminal sides of aspartic acid residues.[11]

Lysine may also undergo cross-linking via its *e*-amines with COOH- and $CONH_2$- containing residues (Asn, Gln, Asp and Glu) at elevated temperatures (Figure 3).[8] As this covalent reaction occurs at a slow rate, the formation of isopeptide bond necessitates severe and prolonged heating conditions.[14]

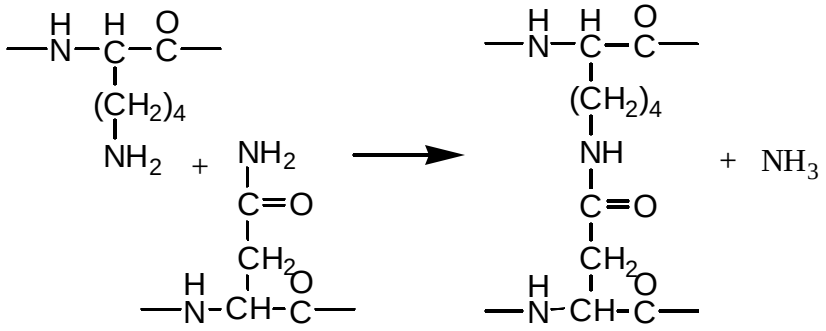

Figure 3 Lysine residues cross-linking

Asparagine and aspartic acid as well as, to a lesser extent, glutamine and glutamic acid are the principal amino acids subject to isomerization. The *b*-isomerization of asparagine at physiological and alkaline pH's results from the residue deamidation as previously mentioned (Figure 2; steps a, b and c).[15] Similarly, aspartic acid *b*-isomerization is believed to proceed via a five-membered succinimide intermediate (Figure 2; steps b and c).[15] Cis-trans isomerization of the peptide bond preceding a proline residue has also been reported, and may play a consequential role in enzyme inactivation at high temperatures.[10]

Proteins are solely composed of L-amino acids. Racemization of amino acids in the primary structure of proteins is known to take place under severe heating at alkaline, acidic and physiological pH's.[16] The reaction starts by the abstraction of *a*-proton from the amino acid, leading to the formation of a planar carbanion intermediate (Figure 4). A proton is subsequently readded to the intermediate (Figure 4).[16] Since the attack by the proton occurs on both side of the carbanion plan at a similar rate, a final stochiometric mixture of L and D configurations is obtained.

An important cause of themoinactivation in the food industry involves the reaction of reducing sugars such as glucose, lactose or maltose with the ε-amino groups of Lysine residues, and is referred as the Maillard reactions.[17] Mild heating (or even storage) induces mainly the formation of the stable deoxy-ketosyl derivative (Figure 5).

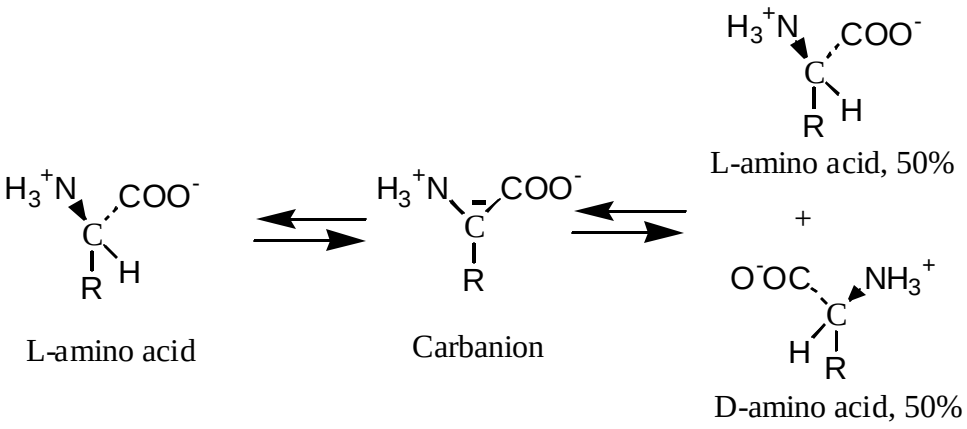

Figure 4 Racemization of amino acids

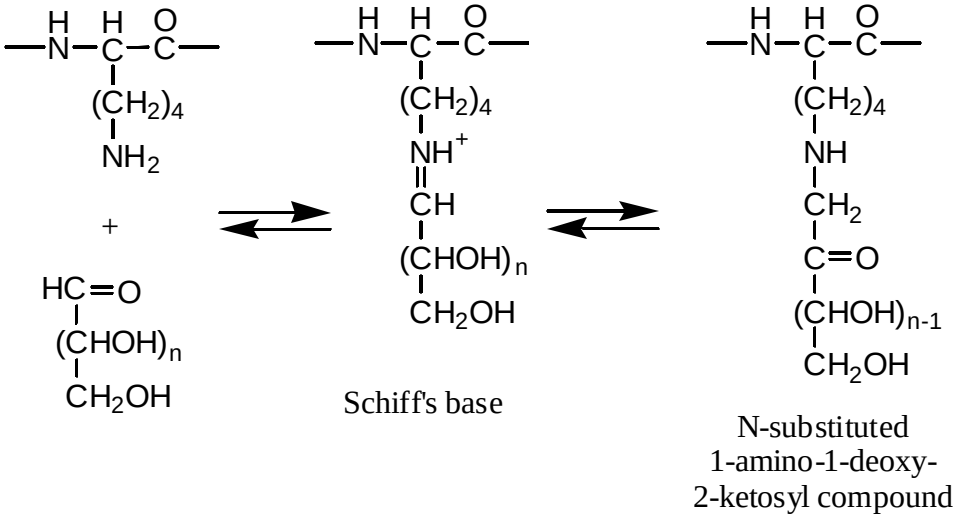

Figure 5 Maillard reaction

The process is quite complex, and is thought to start with the addition of *e*-amine to the carbonyl function of reducing sugar to generate an unstable and detectable Schiff's base. A serie of reactions called Amadori rearrangements further takes place to give the stable deoxy-ketosyl compound. Under severe heating, the Maillard reactions involve the transformation of deoxy-ketosyl intermediate into brown colored polymers, and may also occur at other amino acid residue such as arginine.[14]

2.1.2.2 <u>Oxidation.</u> Oxidative events are a major cause of enzyme inactivation in industrial applications requiring oxidizing agents and, more especially, laundry detergents or bleaches. As subtilisin, chymotrypsin and similar proteases are generally employed for these processes, their stability and activity in the presence of oxidants have been extensively studied.[18] Oxidation may occur at the sulfur-containing residues, cysteine and methionine, as well as histidine, tyrosine and tryptophane residues, although the rate of oxidation of histidine, tyrosine and tryptophane is slower.[10] Treatment with hydrogen peroxide, H_2O_2, or other mild oxidants results primarily in the conversion of methionine into methionine sulfoxide (Figure 6).[11] Harsher oxidation conditions lead to the formation of methionine sulfone (Figure 6).[11]

The oxidation of cysteine depends on the strength of oxidant.[13] As described previously, heating in the presence of dissolved molecular O_2 promotes the spontaneous interchange of free thiols with disulfide bridges. The spontaneous reaction of free thiols

with reactive oxygen species such as superoxide anions, $O_2^{\cdot -}$, $OH^{\cdot}$ and H_2O_2 also yields the formation of cystines. Sulfenic acid can be produced under similar oxidation conditions (Figure 7). Thiol oxidation predominantly proceeds by the intermediary thiyl radicals, $RS^{\cdot}$,[19,20] and can be mediated by transition metal ions including copper ions, Cu^{2+}, and iron ions, Fe^{3+}. Other radicals such as sulfoxyl species ($RSO^{\cdot}$, $RSOO^{\cdot}$, $RSO_2^{\cdot}$) and radical anion complex ($RSSR^{\cdot -}$) can be generated. The oxidation process is significantly accelerated at alkaline pH's. [11] Stronger oxidants lead to the conversion of thiol groups into cysteic acid (Figure 7).[11]

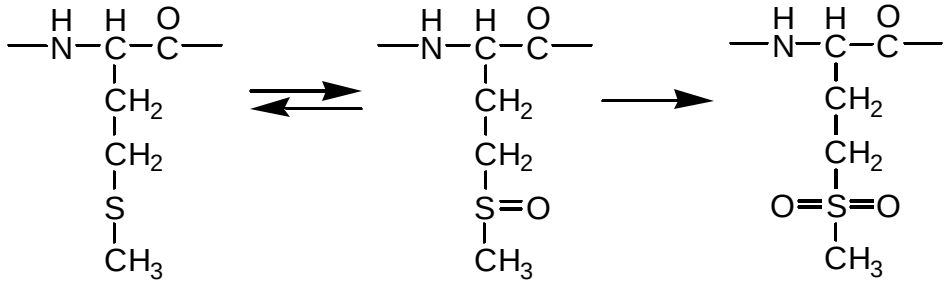

Figure 6 Oxidation of methionine

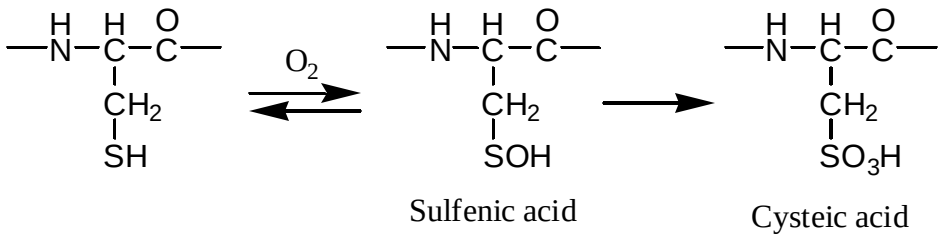

Figure 7 Oxidation of cysteine

2.1.2.3 <u>Inactivation by pH.</u> As mentioned earlier, shifting the pH in the alkaline or acidic range can induce protein inactivation, which involves in many cases a first reversible step followed by a second irreversible step. As implied by this two-step mechanism, short treatments lead to instantaneous, partial and reversible denaturation. Hence, returning to the initial pH restores the native form of protein. Protein propensity to reversibly unfold increases as the pH of its surrounding is moved away from its isoelectric point. At extreme pH's, amino acids, that are buried and uncharged in the native state of protein, ionize, and the resulting electrostatic repulsions between like charges disrupt the native state of proteins, provoking unfolding. A central factor at basic pH's is the ionization and exposure of cystidyl residues. At alkaline pH's, protein tendency to unfold arises from the ionization of amino acids such as tyrosine, as well as the disulfide bridge instability.[2,9] Irreversible inactivation usually take place during prolonged periods of incubation at extreme pH's, and may result from conformational mechanisms, either monomolecular or intermolecular, and covalent processes. Aggregation and protein molecule scrambling are the main conformational modes

encountered. Covalent inactivation often occurs when proteins are simultaneously exposed to extreme pH's and heating at elevated temperatures. Disulfide bridge destruction by β-elimination (Figure 1), racemization (Figure 4), β-isomerization of asparaginly/aspartyl residues (glutaminyl/glutamyl residues) (Figure 2), deamidation of asparagines (or glutamines) (Figure 2), and the partial hydrolysis of peptide bonds can proceed at alkaline, neutral and acidic pH's, as described in the prior section. Peptide bond hydrolysis with release of aspartic acid occurs at acidic pH's. Autolysis is also influenced by pH, although the corresponding pH-dependence varies from one protease to another.

2.1.2.4 <u>Inactivation by Organic Solvents.</u> Organic solvents constitute attractive media for biocatalysis over water.[21] Processes rely on the use either of non-polar or water-miscible organic solvents. The enzyme behavior in non-aqueous systems highly depends on whether the medium is hydrophobic (non-polar) or hydrophilic (polar). Hence, as different concerns arise for each category of organic solvents, we will consider them separately. We will further briefly discuss the possible effects of biphasic liquid/liquid systems on enzyme stability.

As compared with water, non-polar solvents offer the advantage of better solubilizing organic substrates. Another interesting property is to enable reactions that are thermodynamically unfavorable in aqueous phase. Given the absence or low water content (less than 5% (v/v)), water-induced side reactions are minimized and even suppressed. Finally, as enzymes are usually insoluble in organic solvents, they are

easily recovered after synthesis. Overall, switching to non-aqueous biocatalysis ensures dramatic increase in process efficiency. Solid enzymes prepared by lyophilization or immobilization are generally employed. These enzymes in the solid state are still tightly associated to essential water molecules. Although they may undergo some conformational alterations during preparation, they usually retain significant catalytic activity. Subsequent suspension in hydrophobic organic solvents does not disrupt their interactions with essential water molecules as a result of the solvent non-polarity.[22, 23] Consequently, the enzymes remain active. It is believed that water molecules do not always form a true solvation shell around the enzyme, and serve primarily to hydrate the charged amino acids.[24] For example, chymotrypsin suspended in octane is bound to as little as 50 water molecules when at least 10 times more would be required to form a water shell around the enzyme.[24] Enzymes suspended in such non-aqueous systems exhibit considerably enhanced thermostability.[25] As mentioned in a previous section, the high flexibility of enzymes dissolved in aqueous phase facilitates their unfolding. In the case of non-polar organic solvents, the number of water molecules surrounding the enzyme is not sufficient to provide high flexibility to the polypeptide. The resulting relative structural rigidity reduces the risks of denaturation. Moreover, the covalent mechanisms commonly encountered during thermoinactivation in aqueous media (deamidation, peptide hydrolysis…) are almost inexistent in non-polar organic solvents due to the absence (or low content of) water. Lastly, we should mention that, in some particular cases, enzymes may be solubilized in anhydrous organic phase, while retaining good catalytic properties. For example, α-chymotrypsin was dissolved in

micromolar amounts in the non-polar organic solvents, n-octane, cyclohexane and toluene, by following appropriate procedures.[26] The resulting α-chymotrypsin-containing organic solutions exhibited high enzymatic activity and stability.

Unlike non-polar organic solvents, hydrophilic organic solvents interact with the essential water layer of enzyme that is required for maintaining the proper polypeptide conformation. Indeed, they have been shown to strip away the water molecules tightly associated to the enzyme.[23] By doing so they disturb the non-covalent and hydrophobic interactions, which hold the enzyme in the proper folded state. Most polar solvents are unable to compensate for the water molecule removal by maintaining the hydrophobic interactions involved in the enzyme active conformation.[27] As a result, partial unfolding as well as inactivation occur. As the proportion of a specific water-miscible organic solvent increases in the enzyme surrounding, so does the extent of inactivation.[27] Catalytic activation is sometimes observed for small solvent fractions (below 50 % (v/v)).[27] Large volumes of solvent (above 60 % (v/v)) often provoke complete inactivation.[27] The induced denaturation is reversible, and refolding is achieved by diluting the enzyme/organic phase in an aqueous medium. The denaturation ability of hydrophilic organic solvents is inherent to their physiochemical properties (hydrophobicity, solvating ability, molecular geometry), and, hence, varies from one solvent to another.[23] Water-like hydrophilic solvents such as glycerol or ethylene glycol have the least dramatic effects on enzymes.[27]

Liquid/liquid systems composed of a water- and a water-immiscible organic phases, as well as micelle and reverse micelle systems are quite complex. Inactivation may result from the enzyme interactions with the solvent dissolved in the aqueous phase and with the interface between the water and organic phases. The accepted theory for inactivation at the interface involves the enzyme diffusion from the bulk aqueous phase to the interface, and its subsequent adsorption and relaxation.[28] The relaxation arises from the tendency of organic solvent to attract the enzyme hydrophobic amino residues. As the hydrophobic residues are mainly buried in the native conformation, the enzyme's hydrophobic side chains achieve a better contacting with the organic solvent surface via unfolding. Multi-layers of relaxed and entangled polypeptides are usually present at the interface, leading to interfacial gels.[29] Denatured enzyme molecules with significant cysteine content are believed to form intermolecular disulfide bonds, and, hence, strong interfacial films.[29] It is hypothesized that only enzyme relaxation allows significant decrease in the interfacial tension.[30] Loss of catalytic activity can be partial or complete. This process is irreversible, and the inactivated enzyme is released by destruction of the interface as insoluble aggregates. As expected, interfacial inactivation is proportional to the interfacial area.[31] Therefore, it highly depends on properties such as the degree of agitation and the identity of the organic solvent. Despite the high complexity of these biphasic systems, there have been some attempts to correlate the interfacial inactivation with solvent characteristics such as polarity and interfacial tension.[28] Clearly, it is difficult to account for all the mechanisms involved, and, especially, the variations in interface properties resulting from enzyme adsorption and

unfolding.[32] Moreover, the extent of inactivation depends not only on the solvent identity but also on the enzyme physicochemical characteristics.[29] Moreover, proteins originated from thermo- and hyperthermophiles are of particular interest for biocatalysis biphasic systems as they exhibit higher resistance toward interfacial inactivation than their mesophilic relatives.

2.1.2.5 Metal Chelators. Metalloenzymes are associated by non-covalent interactions to specific metal ions, which participate in the maintenance of their catalytically active conformation. Metal-chelators such as EDTA or EGTA strip the metal ions of the enzyme metal-binding site(s), usually leading to partial unfolding and inactivation. The enzyme activity can be recovered to some extent by re-introducing the specific metal ion in the enzyme surrounding. Metal ion(s) bound to an enzyme can be with located near the active site and play a direct role in the kinetic steps. Therefore, in this case, incubation with metal chelators provokes inactivation but not necessarily denaturation.

2.1.2.6 "Salting-in" Effect. When used at high concentrations, non-specific ions may either stabilize or destabilize proteins.[33] Destabilization of protein structures relies on the interaction of ions with the polypeptide chain and, more specifically, the charged groups as well as peptide bonds. As a result, the unfolded form of protein is stabilized, and the protein solubility enhanced. This phenomenon is called "salting-in". By opposition, "salting-out" refers to protein precipitation by high salt concentrations. The process of "salting-out" is related to the stabilization of the folded structure of protein. During precipitation, salts reduce the solubility of hydrophobic groups on the protein

surface and, hence, favor their association with other molecule hydrophobic groups via intermolecular interactions. The aggregated protein retains its native and active conformation. The extent of stabilization (or destabilization) of common anions and cations is given by the Hofmeister series as follows:

$$(CH_3)_4N^+ > NH_4^+ > K^+ > Na^+ > Mg^{2+} > Ca^{2+} > Ba^{2+} > GdnH^+$$
$$SO_4^{2-} > Cl^- > Br^- > NO_3^- > ClO_4^- > SCN^-$$

Anions and cations on the left of both series stabilize protein structures and can be used for salting-out, while those on the right are known for their destabilization and denaturant effects.

2.1.2.7 <u>Sulfhydryl-Reducing Agents.</u> Enzyme inactivation by heavy metals such as mercury (Hg^{2+}), cadmium (Cd^{2+}) and lead (Pb^{2+}) proceeds by the reduction of thiol group in cysteine residues with the formation of mercaptides.(34) Reduction of disulfide bridges also occurs, leading to the S-Hg-S bonds.(34) Heavy metals may as well interact with other residues especially tryptophans or histidines.

Common sulfhydryl agents such as 2-mercaptoethanol, 5,5' –dithiobis(2-nitrobenzoic acid) (DTNB; Ellman's reagent) and dithriothreitol (DTT) reduce disulfide bridges to regenerate two SH groups. The treatment of proteins with 2-mercaptoethanol

or DTNB may also lead to the formation of new intra- and intermolecular disulfide links with the possibility of protein aggregation.[35,36] Reducing sugars have also been shown to protect proteins from oxidative inactivation.

2.1.2.8 <u>Mechanical Modes of Inactivation.</u> The inactivation of an enzyme in solution during either shaking or ultrasound is believed to follow one common pathway. Shaking involves the creation of air bubbles in the enzyme solution, leading to an increase in the air/water interface and a possible irreversible denaturation of the enzyme at the interface.[9] The rational for enzyme irreversible unfolding at the interface is similar to that described for liquid/liquid systems. In the case of ultrasound, gas dissolved in the aqueous medium is released as microbubbles, leading to an increase in the gas/liquid interface area and, hence, a risk of enzyme inactivation.[9]

Pressure-induced inactivation often involves a first reversible inactivation step followed by irreversible inactivation. The reversible denaturation of monomeric proteins usually requires pressurization to at least 10 kbar. Unfolding results from the disruption of ionic interactions, the rupture of hydrophobic interactions with exposure of hydrophobic residues and the favored formation of hydrogen bonding.[37,38,39] The changes in non-covalent interactions, polypeptide hydration and conformation involve a decrease in the protein volume. Pressures in the 1-2 kbar range promote the dissociation and inactivation of oligomeric and multimeric proteins. This pressure-induced dissociation of protein subunits arises, most probably, from the destabilization of ionic and hydrophobic interactions at the subunit interfaces. Subunit unfolding may further

take place. Pressure release usually allows the re-association of subunits. Few cases of irreversible pressure-induced inactivation have been reported, and may be attributed to either aggregation or covalent mechanisms.

2.1.2.9 Radiation. Both ionizing (γ-rays, X-rays, electrons and α-particles) and non-ionizing radiations (UV, visible light) can cause damages in protein primary structure and result in irreversible inactivation.[11] Ionizing radiations induce the formation of intermediary radicals either on the polypeptide chain or in the protein surrounding (water, salts…). The active agents further lead to covalent changes in the polypeptide chain. Non-ionizing radiations generate photons, which are adsorbed by photosensitive agents such as dyes and oxygen, or labile residues including cysteine, tryptophane and histidine.[11] The photoionized species can further initiate the chemical alteration of protein.

2.1.2.10 Cold, Freezing and Lyophilization. Despite the common belief that enzyme stability increases with decreasing temperature (in the absence of freezing), many enzymes exhibit less activity at low temperature. The corresponding inactivation mode involves either spontaneous unfolding, often referred as cold denaturation, or dissociation of subunits in multimeric enzymes. Both processes are usually reversible and results from changes in the physical properties of aqueous medium including the viscosity, acid/base balance and hydrogen bonding.[40,41] The central force for cold denaturation is thought to be the increasing affinity between enzyme apolar clusters and water, and the resulting disruption of hydrophobic interactions.[40,41] Another reason

may be the better solvation of polar and ionic residues by water via hydrogen bonding.[41] One well-documented effect of temperature lowering is to affect the pH of buffered media. This tendency is driven by the temperature-dependence of buffer pKa's.[42] Changes in pH during chilling have been shown to be the primary cause for the dissociation of some multimeric proteins.[42] Chilling may also induce shifts in the pKa's of specific ionizable amino residues, which are critical for the maintenance of protein quaternary structure.[40] The resulting change in protonation of such specific residues disrupts the subunit association.[40,42] Unlike chilling, freezing involves not only temperature lowering but also the transfer of water from the liquid to the crystallized state, while amorphous solutes including most salts and enzyme stay in a residual liquid phase.[9] Consequently, the enzyme and other water-soluble species are significantly concentrated in the non-ice glassy phase, where a significant proportion of unfrozen is still present (20 %). Irreversible deactivation, which is likely to arise from the drastic changes in the enzyme micro-environment, has been reported to occur by aggregation as well as thiol-disulfide exchange and cysteine oxidation.[9] The process is taken one step further during lyophilization as the ice phase is evaporated. Although freeze-drying is a more complex process, the principles developed for irreversible inactivation during freezing are still valid. Additional phenomena may impose new stresses to the protein.[43] For example, the release of dissolved air may provoke protein adsorption and inactivation at the liquid/gas interface. The significant decrease in the amount of residual unfrozen water during the final stage of lyophilization (from 20 to 5 %) may as well affect the protein.

2.1.3 Strategies to Minimize Inactivation

2.1.3.1 <u>Soluble Stabilizers.</u> A large panel of additives have been proposed as stabilizers including salts, metals, surfactants, natural and synthetic polymers, polyols, sugars and amino acids. Stabilization may result from the additive-biocatalyst and (or) additive-solvent interactions. Protection against inactivation may also be achieved by doping the biocatalyst with another agent that either competes for the destabilizing reagent or react with protein side-chains targeted by the destabilizing reagent.

A given enzyme exhibits specific affinities for its substrates as well as substrate analogues and competitive inhibitors, referred as specific ligands (L). The complex formation between the enzyme and one of its specific ligands (E-L) tends to shift the equilibrium between the enzyme native (E) and unfolded states (U) towards the folded conformation:[33]

By favoring the folded conformation, the irreversible events, which take place on the unfolded enzyme and lead to inactivation are less likely to occur. The ligand-binding is believed to confer a more rigid structure to the enzyme.

Non-specific additives may have stabilizing effects by disturbing the enzyme-water interactions, affecting the water properties, or directly interacting with the enzymes.[44,36] Structural stabilization by soluble additives usually obeys the well-accepted principles of preferential interactions.[45] Any enzyme exhibits different affinities for water and additives. A higher affinity for water results in the preferential exclusion of additive from the enzyme surface. Being preferentially hydrated the enzyme is usually stabilized. On the contrary, the preferential binding of additive to the enzyme leads to destabilization in most cases.

Stabilization by preferential hydration relies on changes in the thermodynamic properties of enzymes. In the absence of stabilizer, reversible unfolding is associated with an increase in the enzyme chemical potential, which is thermodynamically unfavorable. Upon the introduction of stabilizer, the chemical potential of folded enzyme increases. As the stabilizer induces an unfavorable shift in the chemical potential of folded enzyme, denaturation of preferentially hydrated enzyme should be more unfavorable than that of native enzyme. Moreover, the enzyme surface area increases upon denaturation and the exclusion of stabilizer from the enzyme surface becomes even more unfavorable. Consequently, the stabilizer causes as well an increase in the positive change in chemical potential associated with unfolding.

A first proposed scenario for the preferential exclusion of stabilizer involves the interaction of additive with water, and relies on the steric exclusion of stabilizer from the enzyme core and (or) the participation of stabilizer in the structural re-organization

of water. The influence of stabilizer on water structure usually leads to an increase in the water-enzyme interfacial tension and medium viscosity. In a second scenario, the preferential hydration of the enzyme is controlled by the direct chemical repulsion between the exposed residues of polypeptide and the stabilizer. Exclusion of weakly charged additives is most likely to proceed by solvophobic effects, whereas that of ionic additives is determined by like-charges on the enzyme surface.

Although preferential exclusion is a necessary condition for stabilization, it is not always sufficient. Indeed, some excipients preferentially excluded from the enzyme hydration shell may still be able to bind some sites at the enzyme surface and to provoke destabilization. As previously briefly described, stabilization or destabilization of an enzyme by an additive is the net result of various mechanisms taking place at the enzyme level. Moreover, as enzymes with distinct properties will either stay inert or interact (binding, repulsion) with a given additive, the latter influence may well dramatically differ from one enzyme to another. Therefore, it may be difficult to predict the effects of a given additive on a specific enzyme.

Polyhydric alcohols including glycerol, erythritol, and sorbitol, as well as sugars such as sucrose and mannitol have usually non-specific stabilizing effects. They follow the general principles mentioned previously, and are preferentially excluded from protein vicinity.[33] Reducing sugars such as glucose and lactose often stabilize protein conformations. However, their application as stabilizers should be avoided, as they are likely to induce covalent inactivation via the Maillard reactions. The influence of

poly(ethylene glycol)s (PEGs) on proteins highly depends on the polymer molecular weight and on the protein characteristics. Despite the widespread use of PEGs, the underlying mechanisms are not well understood yet. It has been suggested that ethylene glycol is likely to stabilize polar proteins, while destabilizing non-polar ones.[33] PEGs with high molecular weights are believed to prevent protein-protein interactions, leading to stabilization. Stabilization by large natural polyols such as polysaccharides and other polymers such as dextran has also been reported, and involves several mechanisms including preferential exclusion and hindrance of protein-protein interactions. Non-specific salt-induced stabilization results mainly from electrostatic shielding and changes in water properties. The stabilizing salts to the left of the Hofmeister serie (section "Salting-In") act by reducing the solubility of hydrophobic regions in proteins, and by favoring the protein preferential hydration.

Sugars and polymers can serve to stabilize proteins during lyophilization. The additive should stay amorphous during the process of freeze-drying in order to maintain its interactions with the protein in the non-ice liquid phase. Stabilization relies on the prevention of unfolding during chilling, freezing and drying.[42] Surfactants constitute another interesting category of additives. Given their ability to reduce interfacial tension between organic and aqueous phases, they have been use to prevent enzyme interfacial inactivation in biphasic systems.[44] Nonionic surfactants are preferred to ionic surfactant as they are less likely to bind strongly to enzymes and lead to destabilization.

2.1.3.2 Chemical Modification. Chemical modification corresponds either to protein crosslinking using bi- and poly-functional reagents or to the conjugation of protein to smaller mono-functional reagents via covalent linkages.[46,47,48] These techniques have been the focus of much interest in biotechnical and biomedical sciences, as they are quite simple, inexpensive and do not necessitate an intensive knowledge on the protein sequencing and conformation.

Protein crosslinking involves formation of inter- and intra-molecular covalent linkages between protein molecules. Water soluble carbodiimides and glutaraldehyde are common bi-functional reagents, which covalently bind to amino and carboxyl groups. The rational for stabilization of monomeric proteins is the rigidification of conformation by crosslinks and, hence, the prevention of unfolding. Inter-crosslinking between subunits plays also a central role in the stabilization of oligomeric and multimeric proteins, as it prevents protein dissociation and favorizes re-association of subunits. Despite these attractive features, a main disadvantage of chemical crosslinking is to stabilize proteins in unpredictable ways.

During chemical modification with mono-functional reagents, protein alteration occurs at targeted amino residues.[49] Since polar amino acids are present in majority at the protein surface, they are easily accessible and, hence, commonly chosen as specific sites for modification. Cysteine and Lysine are the most reactive amino residues under mild conditions, but the chemical modification of other residues such arginine, histidine, aspartic and glutamic acid, asparagine, arginine, tyrosine and tryptophan has

also been reported.[47,48] Modifiers can be small chemicals in the 100 g/mol molecular weight range to large polymers such as PEG's, polysaccharides and dextrans. Full modification is not necessarily achieved, as the selected amino groups that are buried or not easily accessible do not take part into the reaction. The efficiency of the chosen covalent process is given by the extent of conversion of native enzyme, i.e. the yield of modification. Moreover, chemical modification often leads to a heterogeneous mixture of bioconjugates characterized by various degrees of modification, where the degree of modification is defined as the number of covalent alterations per protein molecule. Since modified enzyme molecules from a same batch may have with different extents of conjugation and, hence, may exhibit different properties, it is recommended to isolate each variety of modified enzyme for further analyses.

Chemical modification usually perturbs the enzymatic activity. The changes in kinetics are described assuming the enzyme follows the Michaelis-Menten mechanism:

$$E + S \underset{k_{-1}}{\overset{k_1}{\rightleftharpoons}} ES \xrightarrow{k_2} E + P$$

In the proposed mechanism, the enzyme, E, and the substrate, S, associate reversibly to form a complex, ES, which further breaks down as the product, P, is

released. Assuming the concentration of ES is at steady-state, the Michaelis-Menten equation is derived:

$$u = \frac{k_2[E_T][S]}{K_M + [S]}$$

$[E_T]$ is the total enzyme concentration and K_M equals $\frac{(k_{-1} + k_2)}{k_1}$. k_{cat} is the turnover number of the enzyme and represents the enzyme maximal catalytic activity. K_M represents the affinity of the substrate for the enzyme. Chemical modification usually results in an increase in the K_M value and a decrease in the k_{cat} value. Loss of activity is more often encountered than enzyme activation, and results from several mechanisms including conformational distortions. Inactivation increases with the extent of modification in the general case. Modification of amino groups located in or near the active site has the most dramatic effects of enzyme activity. Complete inactivation is expected when the modified amino residues play a vital role in the enzymatic reactions. Obstruction of the active site by modifier chains with prevention of the enzyme-substrate complex formation reduces also significantly the catalytic activity. Protection against activity loss may be achieved to some degree by conducting the modification in the presence of substrate or a competitive inhibitor. Not only can chemical modification change enzyme kinetic constants, it can also alter the pH dependence of enzymatic

activity. Therefore, an exhaustive characterization of modified enzyme may give a better idea on the efficiency of chemical modification.

A major goal of chemical modification is to enhance enzyme thermostability.[47,48] Chemical modification has been successfully used for the prevention of autolysis, which plays a major role in the thermoinactivation of proteases. The strategy relies on the specific modification of amino groups preceding the sites targeted for the cleavage of peptide chain. As a result, the modified residues are not recognized by the protease, and do not serve as templates for peptide bond hydrolysis. This principle was, for example, applied to the thermolabile protease, trypsin. The lysine and arginine residues, at which polypeptide cleavage occurs, were covalently altered. As expected, this specific chemical modification led to the enhancement of protease resistance to heat.[50] Chemical modification may not be as effective at minimizing the self-digestion of less specific proteases. Thermostability may be dramatically affected by changes in protein surface properties including polarity, hydrophobicity (or hydrophilicity), and number of positively (and negatively) charged groups.[47,48] However, there is no general rule to correlate the observed effects and predict further covalent modifications. Hydrophilization of protein surface tends to provoke enhanced thermostability in many cases and especially in the case of alpha-chymotrypsin. Increase in hydrophilicity has been performed either by covalently altering hydrophobic residues such as proline with hydrophilic chains or by covalently coupling primary amines of lysine residues to more hydrophilic reagents. The degree of

stabilization depends on protein properties and extent of modification. Hydrophilization, however, does not systematically ensure stabilization, as shown by several studies where it caused protein destabilization. As suggested by R. Tyagi and coworkers,[48] it may be possible that a given protein reaches an optimal extent of stabilization at a specific ratio between surface hydrophobicity and hydrophilicity, and that this optimum is protein-dependent.

Chemical modification of proteins with PEG derivatives, also called PEGylation, has driven a lot of interest especially in drug delivery and enzyme chemistry.[51,52] PEG molecules are non-toxic amphiphiles. Once covalently linked to proteins, and if the extent of PEGylation is sufficient, PEG's confer their ability to be soluble in both aqueous and organic phases to the bioconjugates. PEGylated proteins are soluble, active and highly stable in various organic solvents such as benzene, toluene and trichloroethane. PEGylation also enhances stability of enzymes in emulsion systems. Another attractive property of PEG's is to repel large polymers from their vicinity and, hence, to be non-immunogenic. This property is translated to proteins via PEGylation. Consequently, PEG-proteins exhibit reduced immunogenicity and increased blood clearance time (*in vitro* stability).

2.1.3.3 <u>Immobilization.</u> Immobilization refers to the preparation of insoluble derivatives of enzymes.[53,54,55] Immobilization techniques have been increasingly used in industrial applications in order to ease the separation of biocatalysts from the effluents and, hence, the recovery and purification of products. By switching from

homogeneous to heterogeneous biocatalysis via immobilization the costs of downstream processing can therefore be considerably minimized. Moreover, solid biocatalysts offer the major advantage of being reusable. Interestingly, immobilization can dramatically affect enzyme properties such as pH-dependence, temperature profile, resistance to proteolytic digestion and denaturants, as well as kinetics, and has often been observed to enhance thermostability.

Immobilization can be performed by entrapping the enzyme of interest into polymers, gels, microcapsules made of semi-permeable membranes, and hollow fibers. The immobilized enzyme may exhibit altered characteristics as a result of the changes in its micro-environment and its possible non-covalent interaction with the matrix. Immobilization involves otherwise the coupling of the enzyme with a selected solid support via covalent and (or) non-covalent interactions. Several non-covalent linkages can be specifically favored, including ionic and metal bindings as well as physical adsorption.[56] With the exception of physical adsorption, the support has to be activated prior to enzyme binding. Immobilization by adsorption results from weak forces between the protein and the solid surface, such as electrostatic and hydrophobic interactions or hydrogen bonds. Adsorption may proceed via conformational rearrangements, depending on the enzyme nature.[57] Increase in enzyme thermostability is often explained by the hydrophilicity/hydrophobicity of the selected support.[56] As adsorption constitute a mild immobilization process with respect to covalent linkage, it is expected to have less effect on enzymatic kinetic behavior. Despite its simplicity, immobilization by physical adsorption is significantly limited by the tendency of

enzyme to desorb from the support. A smaller extent of leakage is observed when the enzyme is attached onto a solid support via stronger linkages such as ionic and affinity bindings.[56]

Affinity binding occurs in a confined region of the protein surface, and, hence, is not likely to influence enzyme properties unless the binding site is close to the active site. Structural changes may possibly result from indirect and non-specific interactions with the support itself. Immobilization via affinity binding is a powerful technique, which has been, for example, successfully applied to the purification and concentration of proteins, leading to the development of techniques such as affinity liquid chromatography. The particularity of affinity liquid chromatography relies on the activation of the stationary phase with a specific ligand such as an antibody or a metal ion. The process requires first the column loading with the protein mixture. Proteins weakly adsorbed are then easily rinsed out while the protein of interest stays bound to the specific ligand. Release of the targeted protein from the column usually necessitates an increase in the ionic strength of the elution buffer or the addition of a competitor for the binding site in the mobile phase. Native conformation of enzyme is recovered in the general case.

More efficient immobilization methods involve the covalent attachment of the enzyme onto or into a solid support. The effect of covalent immobilization is usually exhibited by the enhancement of thermostability in aqueous media and is often associated with the alteration in pH optima and dependence of enzymatic activity on

pH.[58,59,60,61] It is also noted that covalent bonding leads to an increase in the intrinsic K_M value combined with a decrease in k_{cat} value.[62] The improvement of true biocatalytic stability via immobilization may be explained by the modifications in enzymatic conformational structure. The polymeric microenvironment and the covalent interactions connecting the biocatalyst to the support lead to a reduction in the enzyme mobility. Therefore, the formation of enzyme-polymer systems helps prevent against denaturing and instability resulting from conformational fluctuations. Traditionally, functionalities present at the support surface are chemically modified in such way that they can further react with some specific side chains such as primary amines, carboxylic or hydroxyl groups at the enzyme surface under mild conditions. Given the steric hindrance between the enzyme and the support, only few (one or two) covalent linkages can be formed. Each point of covalent attachment brings some rigidity to the enzyme structure. Multiple covalent bindings between the enzyme and support provide a maximum rigidity; thus, they are most likely to prevent unfolding upon heating or in the presence of a denaturant. One way to achieve multipoint covalent immobilization is by copolymerizing the enzyme with monomers capable of reacting with some specific functionalities at the enzyme surface. During polymerization, the enzyme acts as a monomer, and is thus expected to be uniformly distributed within the resulting biopolymer. To ensure an efficient immobilization process the rate of bond formation between monomer functionalities and targeted enzyme groups should be at least as fast as that between monomer molecules. One should keep in mind that extensive covalent modification may, however, significantly alter the enzyme kinetic characteristics and

lead to loss of catalytic efficiency. The principle of multipoint irreversible immobilization was, for example, successfully applied to the incorporation of enzymes such as phosphotriesterase (EC. 3.1.8.1),[63] and aminoacylase (EC. 3.5.1.14)[64] into polyurethane foams via the favorable reaction between isocyanates and primary amines at lysine residues. No significant enzyme leakages from the foams were observed. Moreover, the immobilized enzymes exhibited good activity retention and enhanced thermostability.

The mass transfer of substrate and product is a major concern for the characterization of immobilized enzymes. In the general case, the substrate, initially present in the liquid phase, diffuses to the enzyme-containing solid support and is transformed into product at the enzyme active site. The product is further released from the enzyme active site and diffuses back from the solid phase to the liquid bulk. When the enzyme is immobilized onto the support surface, only external diffusional limitations can occur. Systems containing enzyme entrapped or covalently incorporated into a solid matrix may be limited by both external and internal diffusions. In the presence of diffusional limitations, apparent enzymatic characteristics are obtained that may not reflect the true effects of immobilization on the enzyme properties. For example, during thermoinactivation experiments, the immobilized enzyme does not apparently loose any activity over time as long as its activity is diffusionally limited. Apparent losses of activity and, hence, thermoinactivation are only recorded as the

system becomes kinetically controlled. Consequently, an apparent thermostability enhancement may be recorded when there is no true increase in thermostability.

Sol-gel materials have been increasingly employed as support for protein immobilization in the last ten years since they exhibit interesting physico-chemical properties and can be used for a wide range of applications including coatings, gels and fibres.[65,66] Sol-gel materials result from the hydrolysis of the silicon alkoxide initiator, $(RO)_4 Si$, in the presence either of an acidic or alkaline catalyst at room temperature.[67]

$$n(RO)_4Si \xrightarrow{\text{Hydrolysis}} (SiO)_n$$

Other metal alkoxide precursors can be used too.[67] Subsequent processing of the resulting gel may include steps of condensation, drying and annealing, depending on the application for which the inorganic matrix is to be used.[67] Variants of SiO_2-based materials are obtained by initiating the hydrolysis with precursors of the type $R'Si(RO)_3$. Proteins can be either covalently immobilized onto the sol-gel matrices or encapsulated within the inorganic gel particles.[67] Many examples have been reported where the immobilization process resulted in good enzymatic efficiency and stability.

2.1.3.4 <u>Protein Engineering.</u> Enzyme inactivation correlates with structural and (or) chemical mechanisms. As discussed previously, enzyme inactivation can primarily

result from the covalent alteration of specific residues such as methionines, asparagines, glutamines and free cysteines. In such cases, the enzyme can be stabilized by replacing the labile residues in the amino acid sequence by other more resistant residues via site-directed mutagenesis (protein engineering).[68]

Much effort has been made in the last decade to determine the structural rational for the high thermostability of thermophilic and hyperthermophilic proteins, as compared with mesophilic proteins. Several potential causes have been determined from the direct comparison between the structures of various homologous meso- and thermophilic enzymes, and can be further applied to the stabilization of proteins by protein engineering.[69,70,46] Although no general principles are available yet, it has been shown that stabilization may occur by increasing the number of hydrogen bonds, the electrostatic interactions, the protein compactness, the α-helix content, the ratio of polar to unpolar external area, the number of disulfide bridges and the number of prolines.[68,69] Optimizing the hydrophobic interactions, as well as other parameters such as the stability of metal-binding sites (in the case of metalloenzymes) may result in stabilization too.[68,69] The importance of each of these properties differs from one enzyme to another. The stabilization of a given enzyme requires first to carefully analyze the protein four structural levels (primary, secondary, tertiary and quaternary), to subsequently combine this knowledge to fundamentals on protein thermostability and estimate the amino acids that need to be replaced by site-directed mutagenesis. The process is quite complex. Moreover, the effects of selected mutations on enzyme characteristics, including thermo stability, are not systematically fully predictable.

2.1.3.5 Directed Evolution. Directed evolution consists in developing mutants of an initial wild type protein by random mutagenesis and (or) DNA shuffling in order to enhance some selected property(ies) of the protein such as activity and stability.[71,72,73,74] The mutants usually display diverse characteristics with efficiencies lower, higher, or equal to that of the wild type parent. Given the unpredictable effects of random mutation/DNA shuffling on the protein, the resulting variants further have to be screened for the targeted property(ies).[71] The mutant(s) exhibiting the greatest improvement is(are) isolated and serve as parent sequence(s) for a second round of random mutation.[71] Selection methods rely on the growth of a host organism under conditions (temperature, pressure, culture medium…) only viable for the mutants with the desired trait(s), and may be used as a pre-screening process.[75] Optimization is obtained by reiterating the process several times. Since this approach is based on random mutagenesis/DNA shuffling, only the protein primary structure needs to be known. Therefore, unlike site directed mutagenesis, extensive knowledge on the structural bases for biological functions is not necessary.

Directed evolution is a powerful tool to improve biological functions and guide protein evolution towards new properties, by mimicking to a certain extent the evolution *in vivo* of proteins. Moreover, it enables the development of biological properties that are not present in nature but of major interest for commercial applications. Directed evolution has, for example, largely contributed to the enhancement of protein thermostability. Unlike chemical modification and

immobilization techniques, increases in thermostability are obtained without reducing the biological activity.[72,75]

2.2 Immobilization of Agentases

2.2.1 Agentases

A number of enzymes exist which are capable of degrading a wide range of organophosphate (OP) compounds.[76,77] The first OP degrading enzyme was observed by Mazur, who reported the hydrolysis of DFP to hydrofluoric acid and diisopropylphosphoric acid by enzymes found in the tissues of humans and rabbits.[76,78] Since this report, a wide number of bacteria and eukaryotic organisms have been shown to possess the ability to degrade organophosphate compounds.[76,78] OP degrading enzymes have been isolated from a variety of sources, including microorganisms, insects, plants, mammals, birds, and squid.[78, 79, 80, 81, 82, 83, 84, 85] Bacteria with OP degrading capabilities have been identified in *Flavobacterium*, *Pseudomonas*., *Bacillus*., and *Anthrobacter*. In addition, OP degrading activity has been found in the fungi *Phanaerochaete chrysosporium* and *Trichoderma viride* and in algae and cyanobacteria.[77,76]

Considerable research has focused on the isolation of organophosphate hydrolyzing enzymes and the cloning and sequencing of the genes that code for them. This information has been successfully used for the introduction of these genes into

other organisms, for site-directed mutagenesis,[86,87,88,89,90,91] for directed evolution studies and for the development of protein:protein fusions.[92,9394,95] The enzymes responsible for organophosphate degradation are ideal for biocatalysis since they do not require expensive cofactors, are stable over a wide range of temperatures and pH, and generally have broad substrate specificity. The nomenclature and classification of phosphoric triester hydrolases can be rather bewildering and the reader is referred to a number of reviews that describe in more detail the many types of OP and CW degrading enzymes.[76,77,96,97] Nevertheless, these enzymes are very diverse and the exact physiological substrate is not known for most of them.[96] They have been classified somewhat sporadically as the phophotriester hydrolases (EC 3.1.8) which are further broken down into two basic categories based on their substrate specificity: 1) the aryldialkylphosphatases (EC 3.1.8.1) which cleave P-O, P-S, and P-N bonds and 2) the diisopropylfluorophosphatases (DFPases, EC 3.1.8.2) which cleave P-F and P-CN bonds.

The most thoroughly characterized enzyme is the organophosphohydrolase (OPH) from *Pseudomonas dismuta* MG.[79] Native OPH is a metalloenzyme, requiring zinc for catalytic activity, and has broad substrate specificity. OPH has been shown to degrade pesticides such as paraoxon, parathion, coumaphos and diazinon, as well as nerve agents such as sarin, soman, and VX.[86, 87] For some substrates, such as paroxon, OPH catalyzes the hydrolysis at a rate very close to the diffusion-controlled rate;[98] however, for substrates such as VX, hydrolysis may occur at 0.1% of this rate.[86] The

DFPase enzymes isolated from squid,[81,91,99,100,101] and the organophosphate anhydrolase (OPAA) have also gained much attention since they can efficiently catalyze the hydrolysis of DFP, soman, sarin, and tabun.[76,96]

2.2.2 Nerve-Agent Degrading Biomaterials

Since the discovery of OP degrading enzymes, there has been interest in the application of these enzymes not only for the decontamination of waste waters and nerve agent stockpiles, but also for the protection of farmers and military personnel. Significant research has gone towards the development of clothing for the protection of individuals against exposure to nerve agents or the preparation of coating materials for resistance to chemical agents. Current protective clothing relies on an adsorptive polyurethane layer impregnated with activated carbon for OP adsorption. This type of clothing must be carefully disposed of since it lacks the ability to detoxify itself; furthermore, the adsorptive layer adds extra weight to the clothing. Special chemical agent resistant coatings (CARC) that prevent the penetration of chemical agents through the coating polymer layer are also required for military vehicles.[102] The development of enzyme-containing polymeric materials will enable the preparation of a wide variety of self-decontaminating clothing and surfaces.

The preparation and purification of enzymes can be costly; therefore, it is imperative to immobilize an enzyme in order to maximize productivity. Effective immobilization methods allow for the preparation of an immobilized enzyme that

retains most of its native activity, maintains high operational stability in its working environment, and maintains high storage stability. Since the late-seventies, a number of processes have been investigated for immobilizing OP degrading enzymes. Many methods have been used for developing biomaterials for application in biosensors and bioelectronics.

Much attention has been focused on preparing materials for use in the decontamination of OP-contaminated aqueous waste streams and for the detoxification of chemical weapon stockpiles. The first report of an immobilized enzyme preparation was by Munnecke in 1977 and 1979.[103,104] In these experiments, a crude cell extract from a mixed culture, capable of degrading nine organophosphate insecticides, was bound to glass beads via an azide coupling method. The enzyme-bead preparations were then used in packed columns and fluidized beds. The beads maintained good stability (about 50% of initial activity during discontinuous use over 180 days. However, the enzyme preparation was susceptible to deactivation by solvents and unknown inhibitors in the aqueous waste stream.[104]

Caldwell and Raushel immobilized *Pseudomonas diminuta* OPH by adsorption onto trityl agarose and by covalent attachment using glutaraldehyde onto various nylon supports including filters, membranes, tubing and packings.[105,59] They found that the trityl agarose column was not practical due to enzyme leaching from the support.[59] On the other hand, covalent attachment of OPH to nylon membranes showed no leakage and no loss of activity after 4 weeks of operation. Havens and Rase investigated the

effect of support chemistry and configuration on the performance of immobilized OPH for OP detoxification.[106] The supports (of varying particle size and porosity) were packed into columns and compared for their ability to attach enzyme and maintain stability. The authors found that a N-hydroxysuccinimide (NHS) activated support had the highest activity and a carbonyl diimidazole support had the highest stability (66.9 day half-life). It was suggested that the differences seen between the different support materials were caused by variations in support charge, porosity, or spacer length.

Grimsley et al. also investigated the use of cellulose for the covalent immobilization of OPH using glutaraldehyde.[107] Cotton is a highly absorptive material, and in combination with nerve agent degrading enzymes, would be appropriate for use as decontaminating towelettes, gauze, swabs, bandages and wound dressings.[107] A cotton towelette was reported to degrade 0.12 mg paraoxon/min/cm^2 of fabric and should be able to degrade gram size quantities of nerve agent in a few minutes.[107] However, long-term stability may be a concern since a dry fabric with trehalose added as a stabilizer lost nearly 30% of its initial activity after 35 days.[107]

Recent advances in materials synthesis using enzymes have allowed the preparation of a variety of bioplastics and enzyme-polymer composites for use as reactive monoliths, foams, fibers, wipes and coatings.[66,108] These polymers involve the incorporation (usually covalent) of the biological material directly into the polymer. The enzyme may actually participate in the reaction, and via the reactive functionalities on the enzyme surface, form multiple covalent attachments with the polymer. This ensures

retention of the enzyme in the polymeric material. Furthermore, enzymes prepared in this way maintain considerable stability under normally denaturing conditions.[113] A number of methods have been used to prepare bioplastic or enzyme-polymer composite materials with OP degrading enzymes and these are discussed below.

Enzyme-containing polyurethanes are ideal matrices due to their ease of preparation, the large range of polymer properties that can be prepared, and the ability for multi-point covalent attachment of the enzyme to the polymer. These bioplastics are prepared by reacting a polyurethane prepolymer that contains multiple isocyanate functionalities with an aqueous solution containing the enzyme. Both foams and gels can be prepared depending on the reactivity of the isocyanate.[109] Amines react with the isocyanate to crosslink the polyurethane matrix. Any enzyme that is present in the aqueous solution can participate in the polymer synthesis via the lysine residues on the surface.[109,63] Havens and Rase were the first to investigate the incorporation of OPH into a polyurethane sponge.[110] This approach has also been studied extensively in our laboratory.[63, 111, 112,113] Le Jeune et al. also prepared polyurethane foams containing acetylcholinesterase (AChE), reporting that 90% of available enzyme activity was retained within the polymer during synthesis. The AChE-foams were highly active after storage for two full years.[113, 114]

Gill and Ballesteros have investigated *P. dimunita* organophosphate hydrolase immobilized in sol-gel polymers and enzyme-polymer composite materials.[115,116] They developed a sol-gel encapsulation technique which employs poly(glyceryl silicate)

(PGS) rather than the conventional poly(methyl silicate) (PMS). When they compared the efficiencies of OPH immobilized in sol-gel materials with OPH immobilized in polyurethane foam, they observed high activity retention in the PGS derived sol-gel (94%) and polyurethane foam (68%) while the sol-gel prepared using PMS had an activity retention of only 28%. All three preparations had good stability over 700 hrs at 40^{o}C with the PGS sol-gel performing best after long time periods.[115]

In a more recent work, Gill and Ballesteros investigated the properties of OPH-silicone biocomposites.[116] The biocomposites were first prepared by adsorption of the enzyme to poly(hydroxymethylsiloxane) or by covalent attachment of the enzyme to silica activated with 3-isocyanatopropyltriethoxysilane. These enzyme-powders were used as activated fillers in room-temperature vulcanizable (RTV) silicone polymers. These protein-silicone biocomposites can be prepared with a wide range of physical properties and can be formed into biocatalytic sheets, thick films, granulates, and solid foams.[117] The activity retention of OPH in OPH-silicones ranged from 49% at very high enzyme loading to 67% at low enzyme loadings. When used as packing in continuous reactors in the presence of 10% v/v isopropanol, the silicone polymers were, in general, able to handle larger OP fluxes than OPH-polyurethane. Furthermore, silicone composites had better physical stability (especially in the presence of high solvent concentrations) than polyurethanes, which swelled slightly and began to disintegrate after long-term operation.

2.3 Incorporation of Enzyme into Polyurethane Foams

A number of researchers have assessed the properties of enzyme-polyurethanes.[118,119,120] Prior research in our own laboratory has focused on the properties of organophosphorus hydrolase (OPH)-containing polyurethane polymers.[63,121,111] OPH is an effective catalyst for the degradation of organophosphorus nerve agents, which are often characterized by a low solubility in aqueous media. The polyurethane polymer represented an attractive support material, since its relative hydrophobicity facilitates the interaction between biocatalyst and hydrophobic substrates. The biopolyurethanes also exhibit attractive chemical and mechanical properties such as solvent resilience and structural flexibility. OPH was immobilized during polyurethane foam synthesis, which involves the reaction of water with the multiple isocyanate functionalities of foamable polyurethane prepolymers, Hypol.[109] Hypol prepolymers are either aliphatic or aromatic polyisocyanate-terminated polyethers. The reaction between isocyanate groups and water molecules results in the formation of unstable carbamic acid, which decomposes into primary amine and carbon dioxide (Figure 8a). This degradation initiates the foaming process with the carbon dioxide bubbling through the reacting system, providing the porosity of the polyurethane polymer. The primary amines produced during the first step of polymerization compete with water to further react with isocyanates, leading to the formation of a crosslinked polyurethane matrix.(Figure 8b) The protein participates in the foam synthesis via its lysine residues, enabling the production of a theoretical

enzyme-polymer network.(Figure 8c) The addition of surfactants during polymerization changes the surface tension between reacting polymer and released carbon dioxide, influencing the carbon dioxide evolution and hence affecting the physical properties of the foam matrix, such as density, surface area, porosity, and rate of wetting.

The covalent incorporation of OPH into sponge-like foams leads to more than 50% of activity retention with a 3-fold increase in K_M value. No internal or external diffusional limitations were detected during activity measurements in aqueous media. Interestingly, no essential change in the inhibition effect of chemicals like DMF, dioxane and phenol on OPH was observed as a result of immobilization process. These results, combined with the kinetic analysis, suggest that the immobilization process does not significantly alter OPH intrinsic reactivity. The thermostablity of OPH-containing bioplastics was examined at 25 and 50^{o}C in the absence and presence of 20% DMSO. OPH incorporation into polyurethane foams dramatically stabilized its half-life, which changed from days to years under ambient conditions in aqueous media. Interestingly, the addition of DMSO to aqueous media enhanced the thermostability of native and immobilized enzyme in a similar manner. Since hypochlorite bleach constitutes an important means of nerve agent decontamination, the effect of oxidizers on OPH-containing biopolymers was also examined in aqueous media. It was demonstrated that the immobilization process resulted in viable biopolymer in buffered bleach solutions whereas the native enzyme is immediately denatured. Similar results were obtained for stability against pH fluctuations.

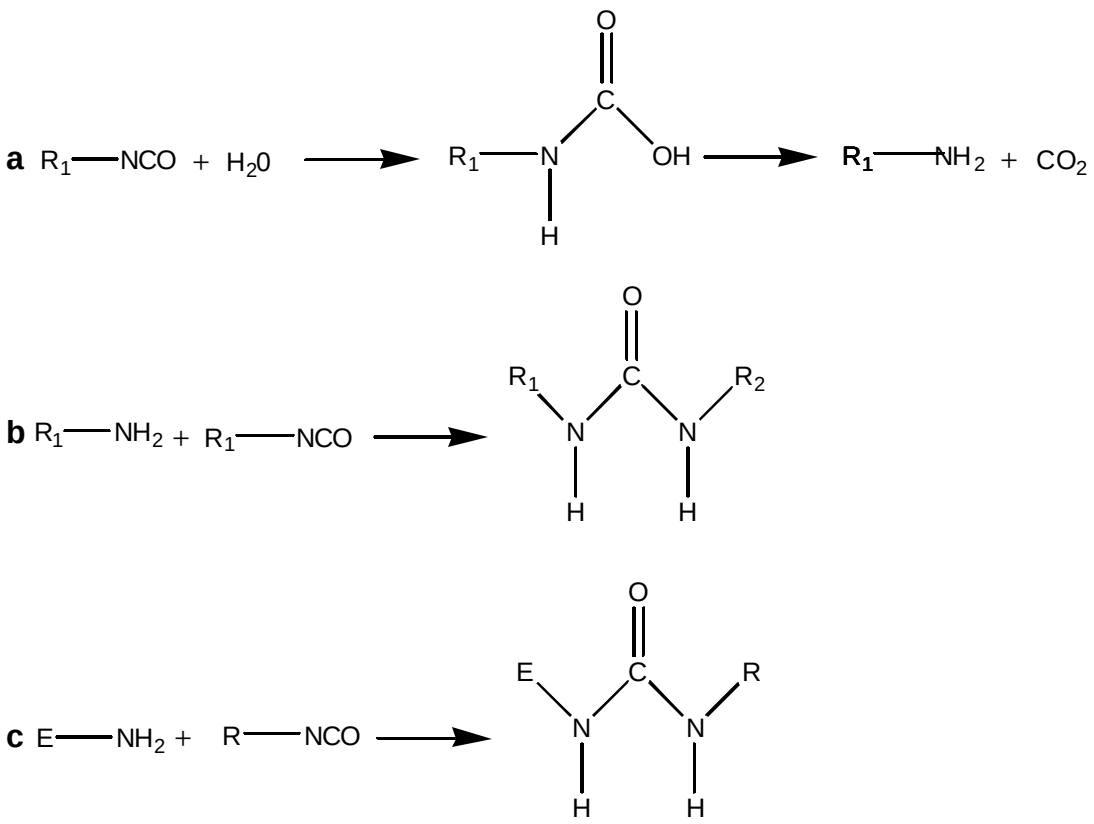

Figure 8 Reaction schematic of biopolymer synthesis

Incorporation into a PU polymer network through multi-point attachment was shown to be a rapid and effective strategy for enhancing the stability of OPH, while retaining its activity. Biocatalyst disadvantages such as short lifetime, limited solubility in organic solvents, and expensive separation of reactants and products were overcome. This immobilization method is particularly attractive for the biocatalytic decontamination and detection of nerve agents, and may serve as a leading tool for the protection of individuals. Consequently, investigating the potential of PU foams as matrices for the immobilization of other enzymes and especially agentases (nerve agent degrading enzymes) is of major interest.

2.4 Polymers Prepared Using ATRP

Atom transfer radical polymerization (ATRP) ensures the synthesis of polymers with controlled molecular weights and polydispersities.[122] This technique involves the radical polymerization of monomers in the presence of a halide initiator, the synthesis being catalyzed by a transition metal, often copper halide, complexed with a nitrogen-based ligand (Figure 9).[122] During polymerization, the initiator serves as a template for the polymer chain growth.[123] ATRP enables the synthesis of well-defined polymers in homogeneous organic and aqueous systems as well as in emulsions,[124] and is efficient at ambient temperature.[125] ATRP, performed in water and at room temperature, has been shown to be rapid for the polymerization of hydrophilic monomers such as glycerol monomethacrylate, methoxy-capped oligo(ethylene glycol) methacrylate, and

2-hydroxyethyl acrylate, and is characterized by high yields and relatively low polydispersities.[126,127,128,129] In the case of methacrylic monomers, the CuCl catalyst is often used in combination with a bromide-based initiator to achieve a better control of polymer growth, as recommended by Matyjaszewski et al.[130,131] CuCl solubilization in water phase relies on its complexion with unsubstituted bipyridine (bpy).[126] The use of polar co-solvents such as methanol has been reported for these waterborne systems.[132] The strategy for enzyme covalent incorporation into acrylic polymer consists in modifying the initiator with enzyme prior to polymerization,[133] and further performing ATRP at ambient temperature in aqueous system using the resulting bio-macroinitiator. This approach relies on the grafting of polymer chains from the bio-macroinitiator. ATRP have been successfully employed in waterborne systems with other types of macroinitiators and activated solid supports such as PEG beads and gold-coated wafers.[132,134,135]

2.5 Enzyme Immobilization into Coatings

The development of coatings or films with biocatalytic properties is of major interest for bioprocesses such as biocatalytic separation and filtration,[136,137] biochips,[138,139,140] and antifouling.[141,142] For example, the use of enzymes in the design of amperometric biosensors have been gaining importance for the last two decades. Biocatalytic thin films have been successfully prepared using bio-inspired methods including self-assembly technologies such as the Langmuir-Blodgett technique.[143] The Langmuir-Blodgett process involves the construction of organized mono- or multi-layer films

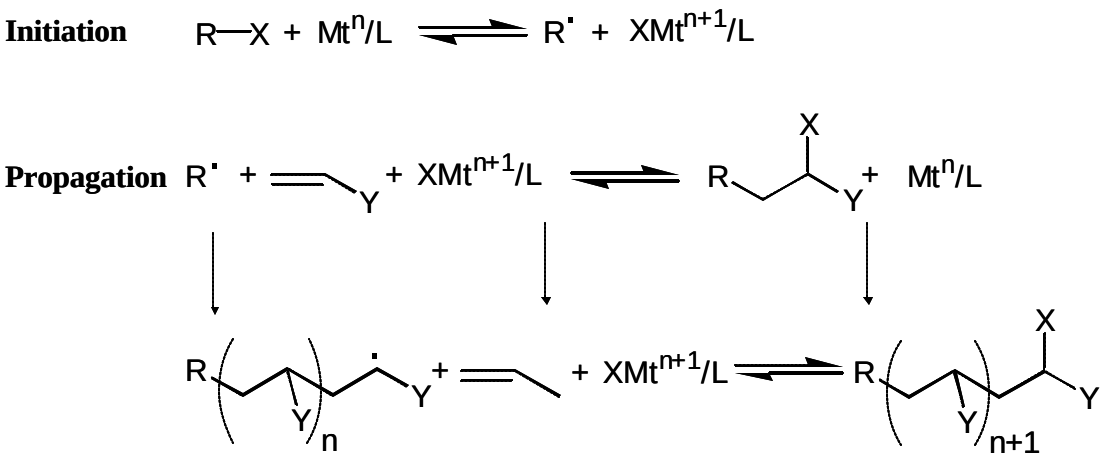

Figure 9 Principles for ATRP

From Matyjaszewski et al.[123]

starting from amphiphilic molecules including surfactants, lipids, fatty acids and membrane fragments. If present during the film construction, a membrane-associated enzyme is capable of spontaneous partial or total insertion into the self-assembled layer.[143] The resulting molecular bio-layer combines high packing density and elevated stability.[143] Other enzymes are nonamphiphilic when folded in their active conformation and do not tend to self-assembly into 2D crystals in the presence of amphiphilic molecules. Strategies have been developed to ensure their incoporation into bidimensional layers, and involve, for example, their chemical modification with lipids, or their fusion to amphiphilic proteins. The autoassembly of nonamphiphilic proteins has also been achieved by altering the enzyme-enzyme, enzyme-lipid and enzyme-substrate interactions via mutagenesis. [143] Another way to prepare biocatalytic self-assembled films is by immobilizing the enzyme onto the pre-formed layer by covalent or non-covalent coupling. [143]

Other strategies for the synthesis of bioactive films rely on combining enzymes to polymeric matrices. The biocatalyst is either immobilized onto the polymer surface or inserted within the bulk polymer. Physisorption is by far the simplest immobilization method. As the biocatalyst is linked to the coating surface by weak non-covalent bondings, it is likely to desorb and leach from the substrate. Schemes based on covalent attachment to the coating surface usually result in more stable interfaces, [144,145,146,147] although they may involve complicated chemistry and provoke significant enzyme deactivation. Encapsulation within the three-dimensional coating network is the most

popular immobilization means as it helps avoid, to a large extent, the problems encountered in covalent coupling and physisorption. One major advantage of physical entrapment is that it can occur in one-step during coating synthesis and is associated with a minimum risk of protein denaturation.

A large range of polymer films have been shown to be biocompatible and have been used for biocatalyst encapsulation or incorporation by mutli-point and covalent linkages. Examples of supports are hydrophilic membranes, hydrogels, hydrophobic matrices such as acrylic resins and sol-gel-derived inorganic-organic materials such as xerogels.[67148,149,150] Enzyme-containing hydrophilic films are often coated with an external water-resistant protective film to enhance their operational stability. [151,152,153] The preparation of biocatalytic films by crosslinking the enzyme with glutaraldehyde has also been reported.[154] Coatings formed electrochemically are being increasingly employed, especially in the fabrication of amperometric and miniaturized biosensors, as electropolymerization offers the major advantage of generating polymer layers with controlled thicknesses.[155,156,157] The main types of electrochemically deposited coatings used for biocatalyst immobilization are conducting polymers including polyaniline, polypyrrole, polyindole, and insulating polymers such as poly(o-phenyldiamine and polyphenols.[155]

The catalytic properties and thermostabilities of enzyme-containing polymeric coatings are summarized in Tables 1 and 2, respectively. A change in the Michaelis-Menten constant, K_M, upon enzyme immobilization is not systematic. For example,

glucose oxidase encapsulated into polypyrrole and polyindole films exhibited K_M's comparable to that of native enzyme (Table 1).[178,169,177,171] Similar observations were made for galactose oxidase physically entrapped into polyaniline, as well as glucose oxidase and pronase covalently inserted into polypyrole and polydimethylsiloxane, respectively (Table 1).[163,168,173,140] Dramatic increases in the K_M's of α-amylase, flavin reductase and pronase were observed when these enzymes were immobilized into acrylic resin, poly(pyrrole-flavin) and sol-gel derived film, respectively (Table 1).[153,140,162] A possible explanation for these observations is the low diffusion of substrates (or products) in the liquid phase within the bulk film. Higher K_M values may also be due to the unfavorable partitioning of the substrate between the liquid and the polymer phases. Another probable reason is a lowering in the affinity of the enzyme active site for the substrate, which results either from the alteration of the enzyme conformation or from the substrate-polymer interactions. Glucose oxidase physically entrapped into poly(aniline), *p*-phenyldiamine, and aniline copolymerized with *p*-phenyldiamine exhibited K_M's lower than that obtained for native enzyme (Table 1).[177] These results may be induced by the higher substrate affinity for the polymer phase as compared with the media. Cosnier and coworkers reported a 5-time decrease in the K_M of tyrosinase upon entrapment into a poly(amphiphilic-pyrrole) matrix (Table 1).[195,196] This unusual result was explained by a local increase in the substrate concentration as a result of the electrochemical regeneration of the enzymatically degraded substrate within the conductive coating.[195,196] Immobilization is often associated with a decrease in the k_{cat} value. Covalent processes are more likely to dramatically alter the biocatalyst

kinetics as they induce changes in the enzyme primary sequence and 3D structure. The effect of immobilization process on k_{cat} was only reported for the insertion of α-chymotrypsin into siloxane-based films.[140] As expected, the decrease in k_{cat} value induced by enzyme entrapment was not as severe as that resulting from enzyme multi-point and covalent immobilization (Table 1).[140] The lowering of k_{cat} value may be caused by diffusional limitations as well as the loss of flexibility undergone by the enzyme. The overall effect of the immobilization process on the enzyme kinetics is given by the activity retention, which corresponds to the ratio of the immobilized and native specificity constants ($\frac{k_{cat}}{K_M}$). The activity retention of biocatalytic coatings can significantly fluctuate depending on the enzyme and the polymer properties such as crosslinkage and hydrophilicity. The lowest activity retention was observed for the entrapment of flavin reductase into pyrrole-based coating (0.13 % AR), whereas lipase-containing poly(propylene glycol)-based coating exhibited the highest activity retention (81.6 % AR) (Table 1).[161,186] The process of immobilization into coatings resulted in most cases in the enhancement of enzyme thermostability (Table 2). As the immobilized enzyme is locked within the polymeric matrix, it is less flexible et hence less susceptible to denaturation.

The range of water-resistant matrices applied to the preparation of enzyme-containing coatings (or films) (ECC's) is still limited. Developing new strategies for the synthesis of ECC's with high catalytic efficiencies and good enzymatic stabilities would enlarge the use of enzymes in industrial applications.

Table 1

Kinetic properties of enzyme-containing coatings

Enzyme	Topics	Coating precursor/polymer	Method of immobilization	Media	S	Enzyme Activity	Enzyme characteristics					R
							Native		Immobilized			
							k_{cat} s^{-1}	K_M mM	k_{cat} s^{-1}	K_M mM	AR %	
a-**Amylase**	Biosensor	*p,p'*-Bisphenyl phenol A epoxide acrylic resin	Entrapment	Buffer	-	-	-	0.6 mg/ml	-	12.7 mg/ml	-	158
a-**CT**	Enzyme activity	Polydimethylsiloxane	Entrapment	Buffer	S_1	-	12	0.049	1.2	0.17	2.9	140
			Multi-point covalent incorporation	Buffer	S_1	-	12	0.049	1.0[b]	0.76[b]	0.5[b]	140

Enzyme	Topics	Coating precursor/polymer	Method of immobilization	Media	S	Enzyme Activity	Enzyme characteristics					R
							Native		Immobilized			
							k_{cat} s^{-1}	K_M mM	k_{cat} s^{-1}	K_M mM	AR %	
a-**CT**	Enzyme activity	Polydimethylsiloxane; Dimethyldimethoxy-silane; chlorinated rubber	Multi-point covalent incorporation	Buffer	S_1	-	12	0.049	0.65[b]	1.7[b]	0.2[b]	140
		Poly(vinyl acetate)	Entrapment	Buffer	S_1 (0.2 mM)	8.08±0.65 10^{-3}µM.s^{-1}.cm^{-2}	-	-	-	-	-	159
		Poly(methyl methacrylate)	Entrapment	Buffer	S_1 (0.2 mM)	8.10^{-3} µM.s^{-1}.cm^{-2}	-	-	-	-	-	159
		Polystyrene	Entrapment	Buffer	S_1 (0.2 mM)	$1.2.10^{-2}$ µM.s^{-1}.cm^{-2}	-	-	-	-	-	159
DAAO	Biosensor	Mercaptohydroquinone	Entrapment	Buffer	D-phe	-	-	-	-	4.83	-	160

Enzyme	Topics	Coating precursor/polymer	Method of immobilization	Media	S	Enzyme Activity	Enzyme characteristics					R
							Native		Immobilized			
							k_{cat} s^{-1}	K_M mM	k_{cat} s^{-1}	K_M mM	AR %	
DAAO	Biosensor	Mercaptohydroquinone	Entrapment	Buffer	D-ala	-	-	-	-	3.48	-	121
					D-val	-	-	-	-	2.50	-	160
					D-leu	-	-	-	-	1.08	-	160
Fre	Biosensor	[12-(Pyrrole-1-yl) dodecyl] triethylammonium tetrafluoroborate	Entrapment	Buffer	-	-	-	-	-	-	0.13	161
		Flavin-pyrrole conjugate; [12-(pyrrole-1-yl) dodecyl] triethylammonium tetrafluoroborate	Entrapment	Buffer	-	-	-	0.025	-	0.090	-	162

Enzyme	Topics	Coating precursor/polymer	Method of immobilization	Media	S	Enzyme Activi ty	Enzyme characteristics					R
							Native		Immobilized			
							k_{cat} s^{-1}	K_M mM	k_{cat} s^{-1}	K_M mM	AR %	
Galactose oxidase	Biosensor	Aniline	Entrapment	Buffer	-	-	-	$0.24.10^3$	-	$0.22.10^3$	-	163
GOD	Biosensor	Tetraethoxysilane; methyltriethoxysilane; 3-aminopropyl-trimethoxysilane	Entrapment	Buffer	Glucose	-	-	-	-	0.03[c]	-	164
		o-Aminophenol	Entrapment	Buffer	Glucose	-	-	-	-	16.4	-	165
		Polyaniline	Entrapment	Buffer	Glucose	-	-	-	-	12.4[c]	-	166
		o-Phenylenediamine	Entrapment	Buffer	Glucose	-	-	-	-	14.2	-	167

Enzyme	Topics	Coating precursor/polymer	Method of immobilization	Media	S	Enzyme Activity	Enzyme characteristics					R
							Native		Immobilized			
							k_{cat} s^{-1}	K_M mM	k_{cat} s^{-1}	K_M mM	AR %	
GOD	Biosensor	Pyrrole	Entrapment	Buffer	Glucose	-	-	17	-	19	-	168
								-	-	31	-	169
										78	-	170
		Pyrrole	Entrapment	Buffer	Glucose	-	-	-	-	1.5	-	171
					S_3	-	-	-		1.6	-	170
			Multi-point covalent incorporation	Buffer	S_2	-	-	-	-	13	-	172
								17	-	15[c]	-	168
								12.2	-	11.9	-	173

Enzyme	Topics	Coating precursor/polymer	Method of immobilization	Media	S	Enzyme Activity	Enzyme characteristics					R
							Native		Immobilized			
							k_{cat} s^{-1}	K_M mM	k_{cat} s^{-1}	K_M mM	AR %	
GOD	Biosensor	[12-(pyrrole-1-yl) dodecyl] triethylammonium tetrafluoroborate	Entrapment	Buffer	Glucose	-	-	-	-	0.4-0.5	-	174
		Indole	Entrapment	Buffer	Glucose	-	-	-	-	27.3	-	175
		Cellulose triacetate	Entrapment	Buffer	Glucose	-	-	2.3	-	2.4	-	176
	Enzyme activity	Aniline	Entrapment	Buffer	Glucose	-	-	33	-	21.8±5.4	-	177
		Aniline; *p*-phenylenediamine	Entrapment	Buffer	Glucose	-	-	33	-	23.5±0.8	-	177
		Indole	Entrapment	Buffer	Glucose	-	-	33	-	28.3±4.8		177

Enzyme	Topics	Coating precursor/polymer	Method of immobilization	Media	S	Enzyme Activity	Enzyme characteristics					R
							Native		Immobilized			
							k_{cat} s^{-1}	K_M mM	k_{cat} s^{-1}	K_M mM	AR %	
GOD	Enzyme activity	*o*-Phenylenediamine	Entrapment	Buffer	Glucose	-	-	33	-	22.0±2.0		177
		Pyrrole	Entrapment	Buffer	Glucose	-	-	33	-	16.0±1.8	-	177
								24	-	26	-	178
HRP	Biosensor	*o*-Phenylenediamine	Entrapment	Buffer	-	-	-	-	-	0.220	-	179
		Pyrrole	Entrapment	Buffer	-	-	-	-	-	0.04	-	180
		Polyaniline	Entrapment adsorption	Buffer	-	-	-	-	-	0.032	-	181
		Grafting polymer of poly(vinyl alcohol) and 4-vinylpyridine; tetraehtylorthosilicate	Entrapment	Buffer	-	-	-	-	-	1.5	-	182
										4.6	-	183

Enzyme	Topics	Coating precursor/polymer	Method of immobilization	Media	S	Enzyme Activity	Enzyme characteristics					R
							Native		Immobilized			
							k_{cat} s^{-1}	K_M mM	k_{cat} s^{-1}	K_M mM	AR %	
HRP	Biosensor	Grafting polymer of poly(vinyl alcohol) and 4-vinylpyridine; tetraehtylorthosilicate	Entrapment	Buffer	-	-	-	-	-	2.1	-	184
Lipase	Enzyme activity	3-Aminopropyl-triethoxysilane; methyltriethoxysilane	Entrapment	Buffer	*p*NPB (0.5 mM)	12±8 mol.min^{-1}.m^{-2}	-	-	-	-	-	185
		3-Mercaptopropyltri-methoxysilane; tetraethoxysilane	Entrapment	Buffer	*p*NPB (0.5 mM)	62 mol.min^{-1}.m^{-2}	-	-	-	-	-	185

Enzyme	Topics	Coating precursor/polymer	Method of immobilization	Media	S	Enzyme Activity	Enzyme characteristics					R
							Native		Immobilized			
							k_{cat} s^{-1}	K_M mM	k_{cat} s^{-1}	K_M mM	AR %	
Lipase	Enzyme activity	Tetraethoxysilane	Entrapment	Buffer	*p*NPB (0.5 mM)	6±3 $mol.min^{-1}.m^{-2}$	-	-				185
		Prepolymer based on poly(propylene glycol)	Entrapment	Benzene	S_4 S_5	0.78 $\mu mol.h^{1}mg_{enz}^{-1}$	-	-	-	-	23.9	186
				n-Hexane	S_4 S_5	7.50 $\mu mol.h^{1}mg_{enz}^{-1}$	-	-	-	-	63.6	186
				Isooctane	S_4 S_5	5.26 $\mu mol.h^{1}mg_{enz}^{-1}$	-	-	-	-	81.6	186
				Isopropyl ether	S_4 S_5	12.0[d] $\mu mol.h^{1}mg_{enz}^{-1}$	-	-	-	-	44.1[a]	186

Enzyme	Topics	Coating precursor/polymer	Method of immobilization	Media	S	Enzyme Activity	Enzyme characteristics					R
							Native		Immobilized			
							k_{cat} s^{-1}	K_M mM	k_{cat} s^{-1}	K_M mM	AR %	
LOD	Enzyme activity	2-Hydroxylethyl methacrylate	Entrapment	Buffer	-	-	-	-	-	-	20	187
NADPH oxidase	Enzyme activity	Gelatin	Entrapment	Buffer	-	-	-	-	-	-	60	188
OPH	Enzyme activity	Silanol-terminated poly(dimethylsiloxane); poly(diethyl silicate); poly(3-amino-propylethoxysiloxane)	Entrapment	Buffer	-	-	-	-	-	-	62[a]	189
PPO	Biosensor	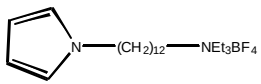	Entrapment	$CHCl_3$	-	-	-	-	-	0.02	-	190

Enzyme	Topics	Coating precursor/polymer	Method of immobilization	Media	S	Enzyme Activity	Enzyme characteristics					R
							Native		Immobilized			
							k_{cat} s^{-1}	K_M mM	k_{cat} s^{-1}	K_M mM	AR %	
PPO	Biosensor	Aniline	Entrapment	Buffer	*p*-cresol	-	-	-	-	0.035	-	191
					m-cresol	-	-	-	-	0.032	-	191
					catechol	-	-	-	-	0.065	-	191
Pronase	Enzyme activity	Polydimethylsiloxane	Entrapment	Buffer	-	-	-	0.62	-	1.9[b]		140
		Polydimethylsiloxane	Multi-point covalent incorporation	Buffer	-	-	-	0.62	-	0.85		140
		Polydimethylsiloxane; Dimethyldimethoxy-silane; chlorinated rubber	Multi-point covalent incorporation	Buffer	-	-	-	0.62	-	2.4		140

Enzyme	Topics	Coating precursor/polymer	Method of immobilization	Media	S	Enzyme Activity	Enzyme characteristics					R
							Native		Immobilized			
							k_{cat} s^{-1}	K_M mM	k_{cat} s^{-1}	K_M mM	AR %	
SBP	Biosensor	Grafting copolymer of poly(vinyl alcohol) and 4–vinylpyridine; tetraethyl orthosilicate	Entrapment	Buffer	-	-	-	-	-	5.12	-	192
Tyrosinase	Biosensor	Poly(hydroxy cellulose)	Entrapment	Buffer	catechol	-	-	-	-	0.07	22	193
					p-cresol	-	-	-	-	0.08	-	193
					phenol	-	-	-	-	0.12	-	193
					dopamine	-	-	-	-	0.61	-	193

Enzyme	Topics	Coating precursor/polymer	Method of immobilization	Media	S	Enzyme Activity	Enzyme characteristics					R
							Native		Immobilized			
							k_{cat} s^{-1}	K_M mM	k_{cat} s^{-1}	K_M mM	AR %	
Tyrosinase	Biosensor	Poly(vinyl alcohol); poly(hydroxy cellulose)	Entrapment	$CHCl_3$	catechol	-	-	-	-	0.06	-	194
					phenol	-	-	-	-	0.58	-	194
					p-cresol	-	-	-	-	3.5	-	194
		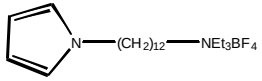	Entrapment	Buffer	catechol	-	-	0.24	-	0.05	9	195 196

[a]: highest reported activity retention
[b]: highest reported catalytic properties
[c]: lowest reported Michaelis-Menten constant
Abbreviations:
AR: activity retention, k_i: inactivation constant, *p*NBP: 4-nitrophenyl butyrate, R: reference, S: substrate, S_1: *N*-succinyl-L-ala-L-ala-L-pro-L-phe-*p*-nitroanilide, S_2: 4-aminoantipyridine, S_3: benzoquinone, S_4: isopropenyl acetate (2 mM), S_5: racemic sulcacol (2 mM)
Amino acid abbreviations:
D-prol: D-proline, D-phe: D-phenylalanine, D-ala: D-alanine, D-val: D-valine, D-leu: D-leucine
Enzyme abbreviations:
CA: creatinine amidohydrolase, CI: creatinine amidinohydrolase, DAAO: D-amino acid oxidase, Fre: flavin reductase, GOD: glucose oxidase, HRP: horseradish peroxidase, LOD: lacatate oxidase, OPH: phosphotriesterase from *Pseudomonas diminuta*
PPO: polyphenyl oxidase, α-CT: α-chymotrypsin, SBP: soybean peroxidase, SO: sarcosine oxidase

Table 2

Thermostability of enzyme-containing coating

Enzyme	Coating precursor/polymer	Method of immobilization	Thermostability	R
a-CT	Polydimethylsiloxane	Entrapment	Native enzyme: $t_{1/2} \approx 0.6$ hr at 55 ^{o}C; Immobilized enzyme: $t_{1/2} \approx 1$ hrs at 55 ^{o}C	140
		Multi-point covalent incorporation	Native enzyme: $t_{1/2} \approx 0.6$ hr at 55 ^{o}C; Immobilized enzyme: $t_{1/2} \approx 1.4$ hrs at 55 ^{o}C	140
	Polydimethylsiloxane; dimethyldimethoxy-silane; chlorinated rubber	Multi-point covalent incorporation	Native enzyme: $t_{1/2} \approx 0.6$ hr at 55 ^{o}C; Immobilized enzyme: $t_{1/2} \approx 1.4$ hrs at 55 ^{o}C	140
DAAO	Mercaptohydroquinone	Entrapment	The immobilized enzyme lost 20 % activity in 6 days of storage in buffer at 5 ^{o}C.	160

Enzyme	Coating precursor/polymer	Method of immobilization	Thermostability	R
Fre	[12-(Pyrrole-1-yl) dodecyl] triethylammonium tetrafluoroborate	Entrapment	No change in activity was observed after 6 days of storage in buffer at 6 ^{o}C.	161
GOD	Tetraethoxysilane; methyltriethoxysilane; 3-aminopropyl-trimethoxysilane	Entrapment	1 day < $t_{1/2}$ < 5 days (storage dry and in buffer at 8 ^{o}C)	164
	o-Aminophenol	Entrapment	$t_{1/2}$ = 10 months (storage in buffer at 4 ^{o}C)	165
	Polyaniline	Entrapment	$t_{1/2} \approx$ 22-23 days (storage in buffer at 6 ^{o}C)[d]	166
	o-Phenylenediamine	Entrapment	No loss of activity in 9 days of storage at 4 ^{o}C in buffer	167

Enzyme	Coating precursor/polymer	Method of immobilization	Thermostability	R
GOD	Pyrrole	Entrapment	$t_{1/2} \approx 60$ min at 60 ^{o}C in buffer	168
			$t_{1/2} > 22$ days (storage at 4 ^{o}C in buffer)	169
		Multi-point covalent incoporation	$k_i = 0.95.10^{-4}$ s^{-1} at 60 ^{o}C; The immobilization process led to a 2.5 fold increase in the enzyme thermostability.	172
			$t_{1/2} \approx 150$ min at 60 ^{o}C in buffer[d]	168
			$t_{1/2} \approx 150$ min at 60 ^{o}C in buffer[d]	168
	[12-(pyrrole-1-yl) dodecyl] triethylammonium tetrafluoroborate	Entrapment	The immobilized enzyme did not undergo any activity loss when stored dry at 4 ^{o}C for 7 days.	174
	Aniline	Entrapment	$t_{1/2} = 40$ min at 55 ^{o}C; $t_{1/2} = 4.2$ min at 60 ^{o}C; $t_{1/2} = 8.1$ min at 65 ^{o}C (immobilized GOD); $t_{1/2} = 9.8$ min at 55 ^{o}C; $t_{1/2} = 8.6$ min at 60 ^{o}C; $t_{1/2} = 2.2$ min at 65 ^{o}C (native GOD)	177
	Aniline: *p*-phenylenediamine	Entrapment	$t_{1/2} = 63$ min at 55 ^{o}C; $t_{1/2} = 21$ min at 60 ^{o}C; $t_{1/2} = 1.6$ min at 65 ^{o}C (immobilized GOD); $t_{1/2} = 9.8$ min at 55 ^{o}C; $t_{1/2} = 8.6$ min at 60 ^{o}C; $t_{1/2} = 2.2$ min at 65 ^{o}C (native GOD)	177

Enzyme	Coating precursor/polymer	Method of immobilization	Thermostability	R
GOD	Indole	Entrapment	$t_{1/2}$ = 8.4 min at 55 ^{o}C; $t_{1/2}$ = 3.9 min at 60 ^{o}C; $t_{1/2}$ = 1.8 min at 65 ^{o}C (immobilized GOD); $t_{1/2}$ = 9.8 min at 55 ^{o}C; $t_{1/2}$ = 8.6 min at 60 ^{o}C; $t_{1/2}$ = 2.2 min at 65 ^{o}C (native GOD)	177
	o-Phenylenediamine	Entrapment	$t_{1/2}$ = 80 min at 55 ^{o}C; $t_{1/2}$ = 24 min at 60 ^{o}C; $t_{1/2}$ = 6.4 min at 65 ^{o}C (immobilized GOD); $t_{1/2}$ = 9.8 min at 55 ^{o}C; $t_{1/2}$ = 8.6 min at 60 ^{o}C; $t_{1/2}$ = 2.2 min at 65 ^{o}C (native GOD)	177
	o-Phenylenediamine	Entrapment	$t_{1/2}$ = 80 min at 55 ^{o}C; $t_{1/2}$ = 24 min at 60 ^{o}C; $t_{1/2}$ = 6.4 min at 65 ^{o}C (immobilized GOD); $t_{1/2}$ = 9.8 min at 55 ^{o}C; $t_{1/2}$ = 8.6 min at 60 ^{o}C; $t_{1/2}$ = 2.2 min at 65 ^{o}C (native GOD)	177
	Pyrrole	Entrapment	$t_{1/2}$ = 24 min at 55 ^{o}C; $t_{1/2}$ = 22 min at 60 ^{o}C; $t_{1/2}$ = 9.0 min at 65 ^{o}C (immobilized GOD); $t_{1/2}$ = 9.8 min at 55 ^{o}C; $t_{1/2}$ = 8.6 min at 60 ^{o}C; $t_{1/2}$ = 2.2 min at 65 ^{o}C (native GOD)	177
			Good stability	178
HRP	*o*-Phenylenediamine	Entrapment	Good stability	179
	Pyrrole	Entrapment	Less than 40 % activity loss was observed after 2 weeks of storage at 4 ^{o}C.	180

Enzyme	Coating precursor/polymer	Method of immobilization	Thermostability	R
HRP	Grafting polymer of poly(vinyl alcohol) and 4-vinylpyridine; tetraehtylorthosilicate	Entrapment	A 6 % activity loss was observed after 30 days of storage at 4 ^{o}C in a drying state.	182
			A 8 % activity loss was observed after 110 days of storage at 4 ^{o}C in buffer.	183
			A 4 % activity loss was observed after 30 days of storage at 4 ^{o}C.	184
Lipase	3-Aminopropyl-triethoxysilane; methyltriethoxysilane	Entrapment	Less than 10 % activity loss after a 6 month- period of storage at 4 ^{o}C.	185
	3-Mercaptopropyltri-methoxysilane; tetraethoxysilane	Entrapment	Less than 10 % activity loss after a 6 month- period of storage at 4 ^{o}C.	185
Lipase	Tetraethoxysilane	Entrapment	Less than 10 % activity loss after a 6 month- period of storage at 4 ^{o}C.	185

Enzyme	Coating precursor/polymer	Method of immobilization	Thermostability	R
OPH	Silanol-terminated poly(dimethylsiloxane); poly(diethyl silicate); poly(3-amino-propylethoxysiloxane)	Entrapment	Less than 5% activity loss after 6 months of storage at 5 ^{o}C (dry, 100 % humidity, wet); Activity losses after a 6 month-storage period at 20 ^{o}C: 6±2 % (dry), 7±3 % (100 % humidity), 9±3 % (wet); Activity losses after a 6 month-storage period at 45 ^{o}C: 6±5 % (dry), 14±2 % (100 % humidity), 13±3 % (wet);	189
PPO	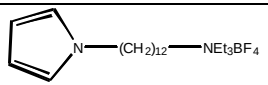	Entrapment	A 28 % activity loss was observed after a 1 week storage period at 4 ^{o}C in buffer.	190
	Aniline	Entrapment	No significant loss of activity was observed after 8 months of storage at 4 ^{o}C.	191
Pronase	Polydimethylsiloxane	Entrapment	Native enzyme: $t_{1/2} \approx 0.6$ hr at 75 ^{o}C; Immobilized enzyme: $t_{1/2} \approx 2$ hrs at 75 ^{o}C	140
		Multi-point covalent incorporation	Native enzyme: $t_{1/2} \approx 0.6$ hr at 75 ^{o}C; Immobilized enzyme: $t_{1/2} > 3$ hrs at 75 ^{o}C	140

Enzyme	Coating precursor/polymer	Method of immobilization	Thermostability	R
Pronase	Polydimethylsiloxane; Dimethyldimethoxy - silane; chlorinated rubber	Multi-point covalent incorporation	Native enzyme: $t_{1/2} \approx 0.6$ hr at 75 ^{o}C; Immobilized enzyme: $t_{1/2} > 3$ hrs at 75 ^{o}C	140
SBP	Grafting copolymer of poly(vinyl alcohol) and 4–vinylpyridine; tetraethyl orthosilicate	Entrapment	No apparent activity loss was observed after 90 days of storage at 4 ^{o}C.	192
Tyrosinase	Poly(hydroxy cellulose)	Entrapment	An activity loss of 2 % was observed after 3 months of storage at 4 ^{o}C in a dry state	193
	Poly(vinyl alcohol); poly(hydroxy cellulose)	Entrapment	An activity loss of 2 % was observed after 3 months of storage at 4 ^{o}C in a dry state.	194
	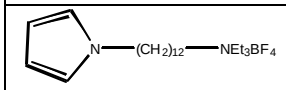	Entrapment	15 and 80 % activity losses were observed after 7 and 54 days of storage at 4 ^{o}C, respectively.	194

[d]: highest reported thermostability

Abbreviations:
k_i: inactivation constant, R: reference
Enzyme abbreviations:
CA: creatinine amidohydrolase, CI: creatinine amidinohydrolase, DAAO: D-amino acid oxidase, Fre: flavin reductase, GOD: glucose oxidase, HRP: horseradish peroxidase, LOD: lacatate oxidase, OPH: phosphotriesterase from *Pseudomonas diminuta*
PPO: polyphenyl oxidase, α-CT: α-chymotrypsin, SBP: soybean peroxidase, SO: sarcosine oxidase

2.5.1 Waterborne Two-Component (2K) Polyurethane (PU) Coatings as Support

Waterborne polyurethane (PU) coatings result from the polymerization of aqueous polyester-based polyol dispersions and water dispersible aliphatic polyisocyanates(*). As the film is cured at room temperature, water evaporates and cross-linking occurs through the condensation between hydroxyl groups and isocyanate functionalities (Figure 10). Cross-linking provides water resistance to the coatings. Two-component waterborne polyurethanes are increasingly used in industrial applications, and they exhibit properties similar to those of solvent borne polyurethane coatings.[197,198,199] Waterborne polyurethane coating represents a potentially ideal polymeric matrix for multipoint and covalent immobilization of enzymes. Given our depth of understanding of monolith polyurethane-enzyme composites,[121,63] we believe that an enzyme added to the aqueous phase of a two-component system prior to polymerization can act as a monomer during coating curing. The immobilization process would rely on the ability of amines at the enzyme surface to react with isocyanate functionalities at a faster rate than hydroxyl groups on the polyol (Figure 10). A similar approach has been used for the insertion of enzyme into hydrophobic acrylate polymer coatings.[200]

* Polyisocyanates correspond to polymers containing multiple isocyanate functionalities

2.5.2 Michael Adduct-Based Coating as Support

Michael adduct-derived latex coatings are of major interest for enzyme immobilization, as they exhibit interesting physical and chemical properties as well as low toxicity.[201] Michael adduct based-coatings result from the photocatalytical copolymerization of Michael adducts and commercially available di-and tri-acrylates.[201] Photocuring occurs at room temperature in the absence of solvent.[201] To prepare biocatalytically active Michael adduct based-coatings, standard immobilization procedures can be used.[202,203,204,205,206,207,208] For example, the coating surface can be activated by chemical pre-treatment or by glow-discharge, followed by covalent coupling of the enzyme. A more interesting strategy involves modifying the enzyme in such a way that it can be homogeneously inserted in the organic mixture composed of the Michael adducts, and the di-and tri-acrylate derivatives prior to curing. In this approach, a two-step procedure is required, where the native enzyme, solely soluble in aqueous media, needs first to be chemically modified with an amphiphilic polymer. The polymer forms a protecting shell around the enzyme and protects it against potential denaturation when the modified enzyme is further introduced in the organic phase.[209,210,211,212] After curing, the enzyme remains uniformly distributed within the coatings.

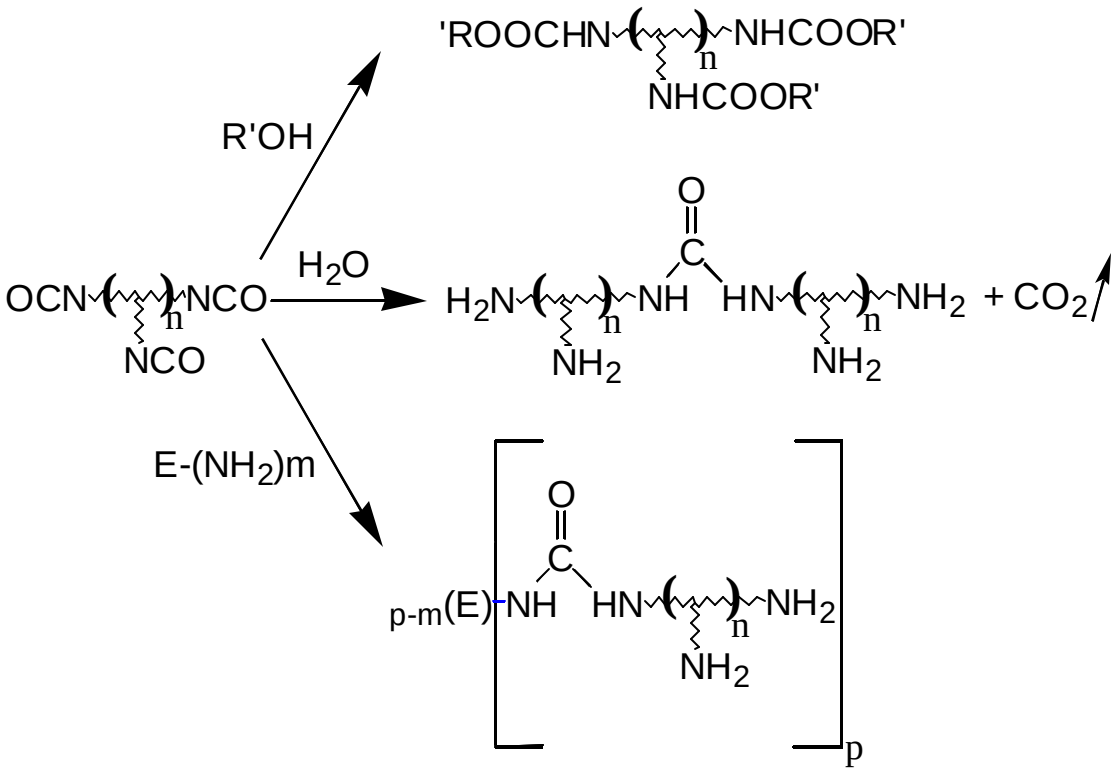

Figure 10 Irreversible immobilization of enzyme into waterborne 2K-PU coatings

3.0 SPECIFIC AIMS

The primary goal of this work was to incorporate enzymes into various plastics and study the enzyme behavior once inserted in these polymer matrices. Two different enzymes were used: the nerve agent-degrading enzyme, diispropylfluorophophatase (DFPase) and carbonic anhydrase (CA), which catalyzes the reversible hydration of carbon dioxide.

Aim 1: Synthesis and characterization of biocatalytic polyurethane (PU) foams

We postulated that enzyme would be irreversibly immobilized into PU foams, and would retain a high catalytic efficiency and be highly stable.

Polyurethane (PU) foam was used as a first type of polymer support since it offers various advantages such as chemical resilience and structural flexibility. Given its relative hydrophobicity, PU-foams should facilitate the interaction between the enzyme and hydrophobic substrates. The covalent immobilization into polyurethane foams relies on the reaction of enzyme surface exposed lysines with isocyanates during the foaming process. The reaction between protein primary amines and isocyanate functionalities is highly favorable. Characterization of the foams included determination of the degree of immobilization of DFPase; alteration of the polymer macro-and microstructures to modulate diffusional limitations on catalysis; and measurement of the intrinsic catalytic efficiency of the bioplastics. The effects of immobilization on the enzyme structure and mode of thermoinactivation were also determined. Immobilized enzyme was compared

to native and PEGylated enzymes, to determine the thermoinactivation of enzyme-polyurethanes.

Aim 2: Synthesis and characterization of enzyme-polymer prepared using atom transfer radical polymerization (ATRP)

We hypothesized that ATRP would take place using an enzyme-based halide initiator. As ATRP can be performed under mild conditions in aqueous media, we believed that the enzyme would remain active during the polymerization.

ATRP is a powerful technique for the synthesis of polymer with low dispersities and controlled molecular weight. It has been recently successfully conducted in water phase under mild temperature and pH. Since enzymes are usually stable under such conditions, it is interesting to determine whether ATRP is actually biocompatible. The objective was to determine whether ATRP could proceed using enzyme/initiator and whether the resulting bioplastics was active. CA was used as a model enzyme for the polymerization of styrene and acrylic based-polymers. The strategy involved the enzyme modification with the halide initiator prior to radical polymerization and the use of the resulting bio-macroinitiator for ATRP. CA-containing polymers were characterized by mass spectrometry and enzymatic assays.

Aim 3: Synthesis and characterization of enzyme-containing PU coatings

Our hypothesis was that enzyme could be incorporated covalently and homogeneously into PU coating in a one-step process. The coating characteristics led us to believe that the resulting bioplastics would be catalytically active and stable.

Two-component waterborne PU coatings are progressively replacing solvent borne PU coatings for a large range of applications. The coating curing occurs at room temperature and involves the reaction of hydroxyl groups on a polyol dispersion with isocyanates functionalitites of a water-dispersible polyisocyanate. The resulting films are highly crosslinked and water-resistant. Given their water-based chemistry, PU coatings constitute a potential matrix for enzyme immobilization. The enzyme can be solubilized in the polyol water dispersion. Once contacted with the polyisocyanate prepolymer the primary amines at the enzyme surface react with isocyanate functionalities at a faster rate than hydroxyl groups on the polyol. The biocompatibility of PU coatings was assessed with DFPase. The characterization of enzyme-containing coatings (ECC's) involved the determination of degree of immobilization of DFPase; the distribution of immobilized enzyme within the polyurethane coatings; the effect of coating relative hydrophobicity on catalysis; and the estimation of the intrinsic activity retention using a theoretical model which combines substrate diffusion and enzymatic degradation within the coatings. The immobilized enzyme was concentrated at the coating surface to facilitate its accessibility to substrate.

Aim 4: The synthesis and characterization of enzyme-containing NVF derived coatings

We postulated that enzyme could be uniformly inserted into Michael adduct-based coatings. Since enzymes have been shown to retain activity and have enhanced stability in hydrophobic media, we thought that enzyme-containing coating would be active and highly stable.

Michael adduct-derived latex coatings exhibit interesting physical and chemical properties as well as low toxicity. They are prepared by co-polymerizing photocatalytically Michael adducts and NVF with di-and tri-acrylates. An enzyme can be physically entrapped into NVF-derived coatings via a two-step process. The native enzyme, which is hydrophilic in nature, has first to be modified in such a way that it becomes soluble in the organic mixture used for casting the films. The enzyme encapsulation further takes place during the film curing. The application of NVF-derived coatings to enzyme immobilization was investigated using CA. Native CA was immobilized into a water-soluble NVF-based polymer (EP), which was soluble in the organic mixture and enabled the ECC synthesis. The activity and stability of EP and ECC were assessed.

4.0 IRREVERSIBLE IMMOBILIZATION OF DFPASE IN PU POLYMERS

4.1 Introduction

The existence of a stockpile of organophosphorus compounds across the globe, along with the threat of chemical warfare, leads to the necessity to develop strategies for the protection of individuals. Biocatalytic decontamination of nerve agents is now a leading tool in this growing list of potential responses to an accidental or intentional release. Biocatalytic decontamination is particularly attractive since it constitutes an environmentally benign approach with high specificity and efficiency under ambient conditions.

Native DFPase, which was isolated from the optic ganglion of the squid *Loligo vulgaris*, catalyzes the hydrolytic cleavage of the P-F or P-C bond from the organosphates sarin, tabun, soman, and cyclohexylsarin. Once hydrolyzed, these agents show relatively low toxicities. The recombinant DFPase has been produced at high yields using an *Escherichia coli* expression system (200 mg/l) and purified to homogeneity via ion metal affinity chromatography (Ni^{2+}-IMAC). [99] The primary sequence contains 314 amino acids, yielding a molecular weight of 35 kDa.[99] Native DFPase is associated with two Ca^{2+} ions. [213] One of the calcium ions displays low-affinity and exhibits a dissociation constant of 21±4 nM at low salt concentration, is present at the active site and plays an essential role in the catalytic activity.[213,214] It is

easily displaced by bivalent metal ions including Sr^{2+}, Mn^{2+}, Ni^{2+}, Co^{2+}, Zn^{2+}, and Cd^{2+}.[213] The second calcium ion is high-affinity and is characterized by a dissociation constant lower than 5.3 nM. It is located in a solvent inaccessible region of the protein and serves as a stabilizer of the protein structure.[213] Depletion of the high-affinity calcium ion leads to the irreversible denaturation of the enzyme.[213] The enzyme activity is temperature- and pH-dependent with the maximal rate of reaction being reached at 35 ^{o}C and pH 8.[91] The k_{cat} increases with pH and reaches a maximal value at pH's ranging between 8.0 and 9.0.[91] Unlike k_{cat}, K_M is not significantly affected by pH over the pH range 6.0-9.0.[99] Both k_{cat} and K_M depend on the medium ionic strength, the maximal catalytic efficiency being reached at 500 mM NaCl.[91] A reaction mechanism for DFPase was described by Scharff and coworkers (Figure 11).[215] In proposed mechanism, His287 intially interacts with Trp244 by H-bonding, while the low-affinity calcium is associated with a water molecule.[215] As the substrate enters the active site, it displaces the water molecule bound to the calcium and disrupts the H-bonding between His287 and Trp244.[215] One side chain of the substrate is likely to interact with Trp244 via non-polar forces. Simultaneously, the calcium ion polarizes the phosphorus atom of the substrate.[91,215] The His287 subsequently acts as a base and deprotonates a water molecule.[91,215] The resulting hydroxyl ion attacks the electrophilic phosphorus, while a polar interaction is formed between the protonated His287 and the negatively charged Glu 37.[91] The last step involves the product release and the His287 deprotonation. [215]

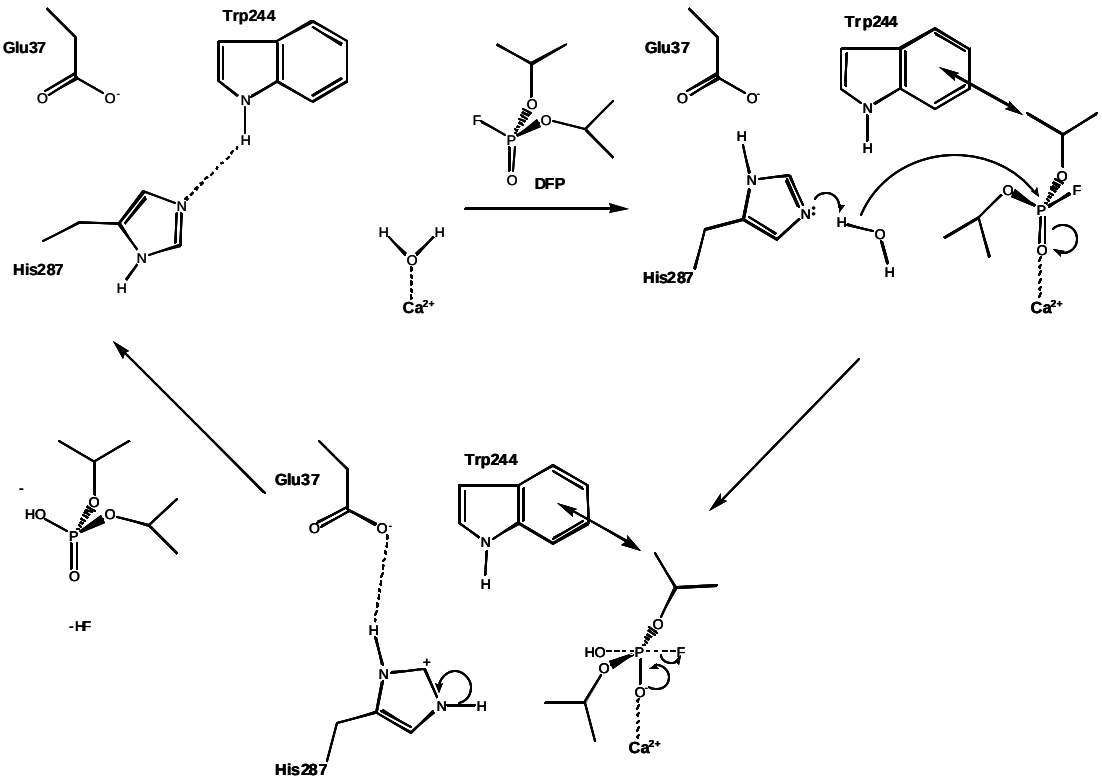

Figure 11: Model mechanism for the DFPase-catalyzed hydrolysis of DFP[215]

The immobilization of DFPase into PU foams is reported herein. Covalent and multi-point immobilization of DFPase into polymer matrices has been accomplished to enhance the catalytic stability, facilitate the biocatalyst use and maximize its reusability. Since alterations in foam morphology could influence the enzymatic activity retention, the immobilization process was performed in the presence and absence of Pluronic surfactants L62, P65 and F68 (from BASF). These non-ionic surfactants are copolymers of ethylene oxide and propylene oxide with hydroxyl termini. As the activity of soluble DFPase is dependent on ionic strength, the activity of the bioplastics was investigated in the absence and presence of salt (NaCl). In each case, the degree to which the enzyme was irreversibly attached to the support was determined. The influence of mass transfer on the activity of enzyme-polymers, as well as the effect of non-ionic surfactants on modified DFPase efficiency and diffusional phenomena, were also examined. The effect of DFPase-polyurethane synthesis on enzyme thermostability were further explored. Since immobilization may prevent denaturation and unfolding of enzyme, the structural basis of these effects was studied. The structural mechanisms involved in protein thermoinactivation can be monitored with classic tools such as circular dichroism (CD).[216,217,218] However, CD is not suitable for use with solid and opaque monoliths such as PU foam. Therefore, the polyurethane reaction was mimicked by studying the structure and activity of DFPase which had been modified using poly (ethylene glycol)-monoisocyanate (PEG-NCO) or poly (ethylene glycol)-diisocyanate (PEG-$(NCO)_2$). Both biopolymer synthesis and DFPase PEGylation involve the reaction of surface amino groups with isocyanate functionalities of PEG chains. Techniques such as

capillary electrophoresis, electrospray mass spectrometry and matrix-assisted laser desorption/ionization mass spectrometry (MALDI MS) have been used to measure the extent of PEG modification of proteins,[219,220,221,222,223]. In this study, the degree of modification of PEG conjugates was determined using MALDI and the CD spectra and kinetics of thermal deactivation of several PEG derivatives were examined. The effects of calcium metal ions such as calcium, cobalt, zinc, magnesium and copper on enzymatic activity and stability have been described many times.[224,225,226,227] Similarly, native DFPase properties are calcium-dependent. Therefore, the influence of calcium ions on the immobilized enzyme was evaluated.

4.2 Materials and Methods

4.2.1 Materials

Hypol prepolymer 3000 and Pluronic surfactants (L62, P65 and F68), used in synthesizing protein-containing polymers, were purchased from Hampshire Chemical Co. (Lexington, MA) and from BASF (Parsippany, NJ), respectively. Di-isopropylfluorophosphate (DFP), Bradford reagent, bovine serum albumin, optima grade hexane (99.9% pure), acetonitrile, trifluoroacetic acid (TFA), tris(hydroxymethyl)aminomethane (Tris), sodium chloride (NaCl), calcium chloride, bis-tris propane (BTP), sinapinic acid, and ethylene-glycol-bis(ß-aminoethyl ether) (EGTA) were purchased from Sigma-Aldrich Chemical Co. (St Louis, MO). PEG-NCO (M_w 5000) and PEG $(NCO)_2$ (M_w 3000) were obtained from Shearwater Polymers

Incorporation (Hunstville, AL). DFPase was received from Dr. Rüterjans, Johann Wolfgang Goethe-Universität, Institut für Biophysikalische Chemie, Frankfurt, Germany, after purification by Dr. Stefan Dierl.

DFP is a highly toxic organophosphorus-based agent, which targets the central nervous system. It should be stored in a tightly closed container in a cool area (4 ^{o}C). It should be handled only in a fume hood and maintained cool during use. Eyeglasses, goggles and nitrile gloves should be worn to prevent skin and eye exposure.

4.2.2 Methods

4.2.2.1 <u>Protein-Containing Polymer Synthesis.</u> DFPase-containing polyurethane foams were synthesized following the procedure we have published previously.[63] All polymers were prepared using buffered aqueous mixtures (50 mM BTP, pH 7.5, 5 mM $CaCl_2$). When studying the effects of salt on immobilized DFPase, the buffered medium was supplemented with NaCl (0.5 M). In the case of immobilization in presence of surfactant, the surfactant concentration reached a level of 1 % (w/w) in the aqueous media. The aqueous mixture (5 ml) was poured into a cylindrical vessel, and followed by the addition of enzyme (0.05-10 mg). Hypol 3000 (5 g), a prepolymer composed of a PEG chain functionalized by several isocyanate functionalities, was added to the DFPase solution, and the biphasic mixture was agitated for 30 s with a custom designed mixing head attached to a 2500 rpm hand held drill. After synthesis was completed, the foam was weighed and then allowed to dry for 14 hrs under ambient conditions and

weighed again. After drying, the foam may contain a residual amount of water. Since all foams are prepared in a similar manner, we think that the fluctuations in residual amount of water are non-significant.

4.2.2.2 <u>Activity of DFPase Polyurethanes.</u> Soluble enzyme was assayed in a 10 ml reactor in the presence of DFP (3 mM). The buffered medium in use contained 5 mM $CaCl_2$ and 50 mM Bis-Tris-Propane, pH 7.5. Some experiments were performed in a buffered solution supplemented with 0.5 M NaCl. As DFPase acts by binding and hydrolyzing DFP (see below), the activity was measured by following fluoride release with a fluoride ion electrode.

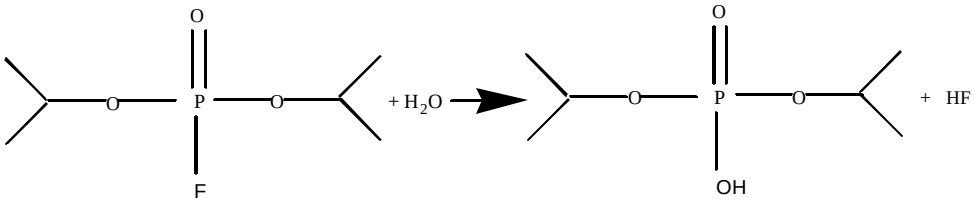

Immobilized enzyme was assayed in a similar manner, using blocks of DFPase-foam cut from bulk-synthesized sample and ranging in weight from 0.08 to 0.02 g. Typically, the cubes were then placed in 12ml of 3mM DFP buffered solution and agitated by magnetic stirring. Fluoride bulk solution concentration was measured every 20 s for 3 min.

In order to validate the sensor approach we also followed DFP consumption directly.[228] In a 10 ml reactor containing 3 mM DFP solution, samples of 0.1 ml were taken over time and added to 0.1 ml hexane. The biphasic mixtures were then equilibrated at room temperature with a constant shaking speed of 2500 rpm for 5 min and centrifuged to separate the organic and aqueous phases. The upper phase in each sample was analyzed with a Hewlett-Packard Model 5890 series II gas chromatograph system (Hewlett-Packard, Wilmington, DE) equipped with a Nitrogen-Phosphorus Detector (NDP). An Alltech EC-1 capillary column with a 30-m × 0.53-mm-i.d., 1.2-µm film thickness, composed of a 100 % polydimethylsiloxane phase was used. The temperature was programmed from a 50 ^{o}C initial temperature with a 1.5 min initial time to a 190 ^{o}C final temperature with a 7 min final time, applying a ramp rate of 20 ^{o}C/min, and leading to a total elapsed run time of 15.5 min. The injector and detector temperatures were held constant at 250 and 300 ^{o}C, respectively. Runs were performed using 0.5µl injection volumes, air and hydrogen gas flow rates of 100 and 3 ml/min, respectively, and a 21 pA baseline offset. Helium was used as both the carrier and makeup gas, with carrier and makeup gas flow rates of 11 and 19 ml/min, respectively.

4.2.2.3 <u>Product and Substrate Partitioning.</u> The product and substrate partitioning between the foam and the bulk solution need to be evaluated in order to determine the activity retention associated with the immobilization process and the kinetic characteristics of DFPase-containing bioplastics. Since the use of surfactants during the

bioplastic synthesis affects the structure and properties of polyurethanes, it is necessary to assess the dependence of partition coefficients on foam formulations.

The fluoride ion partitioning was estimated by following the enzymatic activity of soluble DFPase in the absence and the presence of foam blocks not containing enzyme. Additionally, various buffered solutions (50 mM bis-tris-propane, 5 mM $CaCl_2$, pH 7.5) of fluoride ion at both high and low salt concentrations (0.5 M NaCl) were prepared and examined with a fluoride ion electrode. Blank foam samples were then inserted into the fluoride ion solutions, and after 20 min of magnetic stirring at room temperature, the fluoride ion concentrations were re-measured. To determine the substrate partition coefficients ($\frac{[DFP]_{aqueous}}{[DFP]_{foam}}$), blank foam blocks were added to buffered solutions containing various DFP concentrations, and the resulting biphasic systems were magnetically agitated for a 20 min period. Samples of the final solutions were then used to assay the activities of fixed soluble DFPase amounts. Knowing the kinetic constants of native DFPase, the residual DFP concentrations were calculated and compared to the substrate concentrations obtained by following the same procedure in absence of foam blocks.

4.2.2.4 <u>Determination of Kinetic Constants.</u> The Michaelis-Menten Equation was applied as a kinetic model, and the kinetic constants for both soluble and immobilized DFPase were calculated using non-linear regression analysis and the algorithm of Marquardt-Levenberg (SigmaPlot Version 2.0). The observed reaction rates and

substrate concentrations were corrected using the substrate and product partitioning coefficients measured as described above.

4.2.2.5 Protein Concentration Determination. Protein concentrations were evaluated using the Bradford reagent.[229,230] The addition of the dye to protein solutions at room temperature resulted in the formation of a dye-protein complex within 15 min, with an absorption maximum at 596 nm. A calibration curve with an extinction coefficient of 0.0341 ml/(μg.cm) was obtained for protein concentrations ranging from 1 to 10 μg/ml.

4.2.2.6 PEGylation of DFPase. PEG-NCO was added at room temperature to a buffered solution (10 mM Tris, 5 mM $CaCl_2$, pH 7.5) containing DFPase (8 mg/ml), using a 1/100 protein to PEG-NCO molar ratio. The mixture was agitated vigorously for 10min by magnetic stirring. The PEG-modification involved the same reaction as those described for the synthesis of DFPase-containing polymer. Unreacted PEG-amine was separated from the modified enzyme by dialysis overnight at 6 ^{o}C against buffered medium (10 mM Tris-HCl, 5 mM $CaCl_2$, pH 7.5) using a 15 kD dialysis membrane. Conjugates of DFPase and PEG $(NCO)_2$ were prepared in a similar manner using protein to PEG- $(NCO)_2$ molar ratios of 1/20, 1/50 and 1/1000.

4.2.2.7 Characterization of DFPase Modification. MALDI-MS analyses were performed with a Perseptive Biosystems Voyager elite MALDI-TOF. The acceleration voltage was set to 20 kV in a linear mode. 1 μl of PEGylated enzyme solution (1-2 mg/ml) was mixed with 10 μl of matrix solution (0.4 ml water, 0.3 ml acetonitrile, 1 μl

TFA and 16 mg sinapinic acid), and 2 µl of the final solution was spotted on the plate target. Spectra were recorded after evaporation of the solvent mixture, and were calibrated externally with protonated ion monomer and dimer of BSA.

4.2.2.8 Preparation of apo-DFPase. DFPase (2 mg/ml) was incubated 1 hr at 6 ^{o}C in a buffered solution (50 mM BTP, 0.5 M NaCl, pH 7.5) containing 30 mM EGTA. EGTA-calcium complexes and unreacted EGTA were then removed by dialysis overnight against buffered medium (10 mM Tris-HCl, pH 7.5).

4.2.2.9 Thermostability of Native DFPase. DFPase was added to a buffered medium (50 mM BTP, 0.5 M NaCl, pH 7.5) containing a range of calcium concentrations (1, 5, 50 or 100 mM) and incubated at 50 or 65 ^{o}C. The activity of DFPase was followed over time at room temperature in buffered media (50 mM BTP, 5 mM $CaCl_2$, pH 7.5) as described above. The thermoinactivation of enzyme at 6 ^{o}C was determined in a similar manner with a 5 mM calcium concentration. To enable a direct comparison of results for the thermal deactivation of native and immobilized DFPase, a range of native enzyme concentration varying from 0.03 to 0.05 mg/ml was used.

4.2.2.10 Thermostability of Native DFPase in Presence of PEG-Amine. To ensure the full conversion of isocyanates into amines PEG-NCO was mixed vigorously with water at room temperature for 2hrs. The PEG-amine solution (10% w/v) was then added to buffered medium (50mM BTP, 0.5M NaCl, 5mM $CaCl_2$, pH 7.5) and preheated at 65^{o}C. The thermoinactivation of native enzyme was followed as described previously.

4.2.2.11 **Thermostability of PEG-Modified DFPase.** The thermoinactivation of PEG-DFPase was measured at 65 ^{o}C in the presence of calcium chloride (5 mM) as described for native DFPase.

4.2.2.12 **Thermostability of Immobilized DFPase.** Bioplastic samples (0.1 g) were cut in small pieces and added to buffer (50 mM BTP, 0.5 M NaCl, pH 7.5) supplemented with calcium chloride (1, 5 or 50 mM) and incubated at 50 or 65 ^{o}C. Samples were removed over time, and assayed for enzymatic activity at room temperature in buffered media (50 mM BTP, 5 mM $CaCl_2$, pH 7.5) as described above. The same procedure was followed for thermal deactivation in the presence of EGTA (30 mM), in the presence of a 5 mM calcium concentration at both 6 ^{o}C and at 65 ^{o}C and in the presence of PEG-amine (10 % w/v).

4.2.2.13 **CD Spectroscopy.** CD spectra were recorded at 25 ^{o}C with an Aviv model 202CD spectrometer using quartz cells of 1-mm path length. Spectra were collected for protein (0.3 mg/ml) in buffer (10 mM Tris-HCl, pH 7.5). Each spectrum was accumulated from ten scans between 195 and 300 nm and was corrected for residual protein concentration from the A_{270} value. During thermal deactivation experiments, the relative ellipticity represented the ratio of signal values for deactivated and non-deactivated enzyme. The secondary structure of DFPase was determined using the Lincomb program and the data set yang.dat 231.

4.3 Results and Discussion

4.3.1 Reversibility of DFPase Attachment

The extent to which DFPase is irreversibly (covalently) attached to the polymer was determined using the Bradford reagent. Foam blocks cut from DFPase-containing polymers with a protein content of approximately 0.3 % (by weight) were extensively rinsed with distilled water. Less than 1 % (w/w) of the protein amount present within the blocks was detected in the rinsates, indicating that the immobilization efficiency approached 100 %.

4.3.2 Substrate and Product Partitioning

The enzymatic activity of soluble DFPase was not influenced by the presence of blank foams. The product (fluoride ions) partition coefficient was determined to be 1, and was independent of the type of polyurethane polymer formulation.

DFP is hydrophobic enough to become concentrated in the foam, with an equilibrium partitioning coefficient of 1.3 (Table 3). In the presence of salt in the aqueous media, the use of surfactant L62 further accentuates this partition, increasing the partition coefficient to 1.5.

4.3.3 Activity in Absence of Surfactant

To assess the enzyme dispersion within the polyurethane, the different regions of DFPase-containing polymer were assayed for enzymatic activity. The activity did not fluctuate significantly from one region to another, implying that DFPase was homogeneously distributed in the foam.

As shown in Figure 12, the effect of enzyme concentration on DFPase polyurethane activity is non-linear, with saturation occurring above 0.5 mg_{DFPase}/g_{foam}. Below approximately 0.1 mg_{DFPase}/g_{foam}, the enzymatic activity is directly proportional to enzyme loading. To further investigate DFPase-polyurethane polymer properties we determined the DFPase concentration dependence of apparent K_M and k_{cat} for polymers containing 0.02 to 0.64 mg/g_{foam} (Table 4, Experiments 3 and 4). A 6-fold increase in enzyme loading provoked a consequent decrease in apparent k_{cat}, coupled with an increase in the apparent K_M, which are a strong indication of the presence of diffusional limitations. We further investigated mass transfer limitations by determining the effect of particle size on activity and kinetics. The polyurethane blocks were ground into particles with a diameter ranging from 0.1 to 0.3 mm, and apparent K_M and k_{cat} were measured once again for particles containing 0.02 to 0.64 mg/g_{foam}. Experiments 5 and 6 (Table 4) demonstrate that for the small particles neither apparent K_M, nor k_{cat}, were sharply dependent on DFPase concentration in the polymer. Clearly, it indicates that the activities of the polyurethanes at high enzyme loading were limited by internal diffusion. At low DFPase loading the direct proportionality between apparent activity

and enzyme concentration implied the absence of mass transfer limitations. Additionally, at low loading we observed that the activities for block foams and crushed foams were identical, and that no change in the kinetic constants was found by varying the agitation type and speed. Therefore, we concluded that polyurethanes with low enzyme loading were not diffusionally limited

4.3.4 Activity with Surfactants.

Bioplastics synthesized in the presence of non-ionic surfactants L62, P65 and F68 display greater apparent activity retention than those prepared without surfactant (Figure 13). L62-containing polyurethanes displayed the highest activity retention, and in this case, an increase in enzyme loading from 0.02 and 1.66 mg/g_{foam} resulted in only a 4-fold decrease in catalytic efficiency (the degree to which rate is reduced relative to that predicted from solution kinetics) (Table 4, Experiments 7 and 8). Clearly, there are less severe diffusional limitations in the presence of the surfactant.

We investigated the role of external mass transfer by measuring the agitation dependence of the kinetic constants (Table 4, Experiments 9, 10 and 11). As expected, the K_M and k_{cat} values do not significantly vary with agitation speed. Moreover, they are similar to those obtained using magnetic stirring at a 0.02 mg/g_{foam} immobilized DFPase loading (Table 4, Experiments 3, 4 and 7).

Table 3

DFP partitioning into bioplastics

	Surfactant	Degree of Swellability (DS)	DFP Partitioning Coefficient (PC)
Salt	-	5.9	1.3 ± 0.4
Salt	L62	10.5	1.5 ± 0.3
No salt	-	6.2	1.3 ± 0.3
No salt	L62	11.4	1.3 ± 0.2

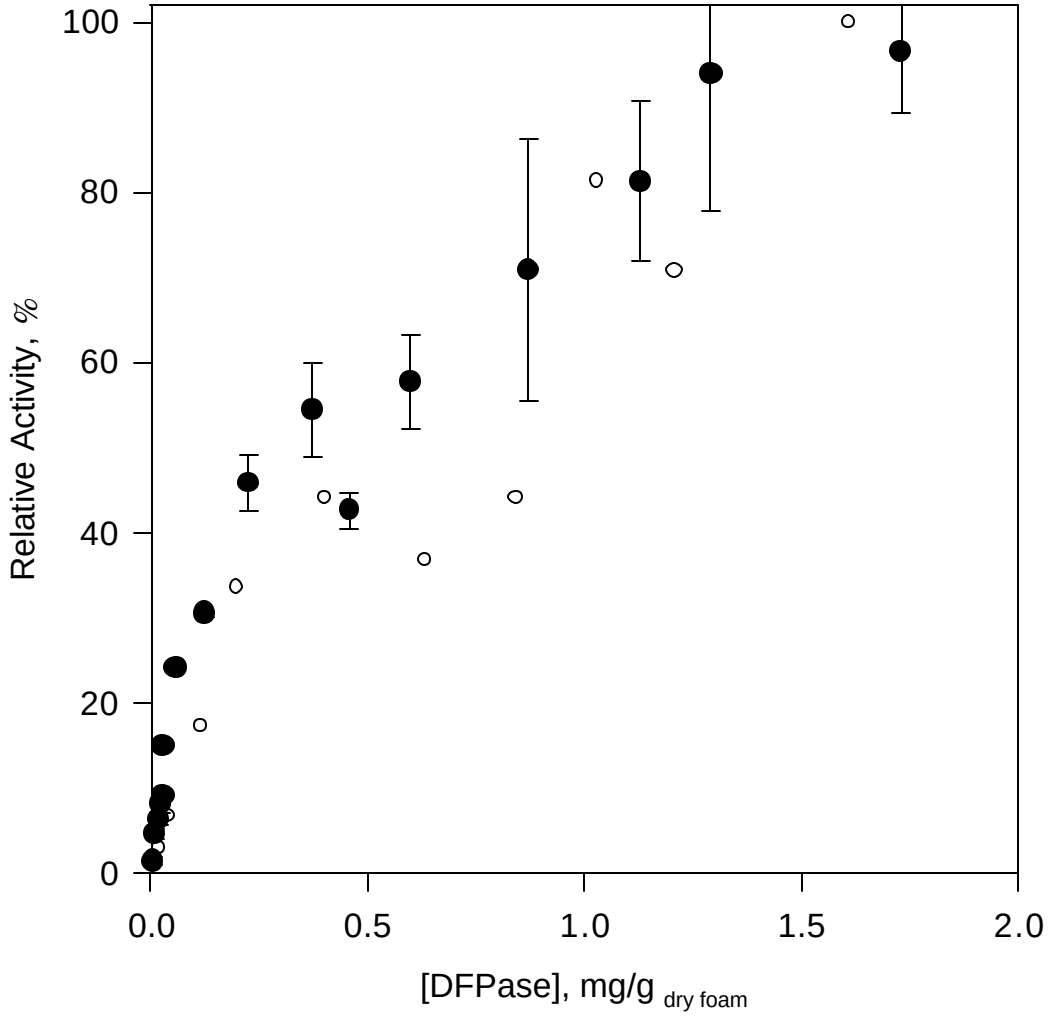

Figure 12 Effect of DFPase concentration on DFPase-containing polymer efficiency

Enzymatic activity measured using NPD-GC (opened circles) and fluoride sensor (closed circles). The activity of the bioplastic is reported at a 3 mM DFP concentration.

Table 4

Kinetic parameters for DFPase-containing polymers and soluble DFPase

Exp.	Salt loading (M)	Surfactant	Agitation (rpm)	DFPase concentration (mg/g_{foam})	Apparent K_M (mM)	Apparent $k_{cat,app.}$ (s^{-1})	Apparent k_{cat}/K_M ($s^{-1}_{(}mM^{-1}_{)}$)
1[a]	0.5	-	magnetic	-	0.53 ± 0.04	219 ± 5	413 ± 41
2[a]	-	-	magnetic	-	0.79 ± 0.02	232 ± 2	294 ± 10
3	0.5	-	magnetic	0.02	1.2 ± 0.1	49 ± 3	41 ± 6
4	0.5	-	magnetic	0.64	2.9 ± 0.4	14 ± 1	5± 1
5[c]	0.5	-	magnetic	0.02	0.7 ± 0.1	46± 4	66 ± 15
6[d]	0.5	-	magnetic	0.64	1.1 ± 0.1	43 ± 2	39 ± 5
7	0.5	L62	magnetic	0.02	0.46 ± 0.04	113 ± 3	249 ± 28
8	0.5	L62	magnetic	1.66	1.6 ± 0.2	83 ± 3	52 ± 8
9	0.5	L62	mechanic 600	0.03	0.30 ± 0.06	87 ± 3	290 ± 68

Exp.	Salt loading (M)	Surfactant	Agitation (rpm)	DFPase concentration (mg/g_{foam})	Apparent K_M (mM)	Apparent $k_{cat,app.}$ (s^{-1})	Apparent k_{cat}/K_M ($s^{-1} mM^{-1}$)
10	0.5	L62	mechanic 800	0.03	0.34 ± 0.05	103 ± 4	303 ± 56
11	0.5	L62	mechanic 1000	0.03	0.36 ± 0.04	94 ± 3	261 ± 37
12[e]	-	-	magnetic	0.04	1.6 ± 0.2	54 ± 3	34 ± 6
13[f]	-	-	magnetic	1.27	1.3 ± 0.2	45 ± 3	35 ± 8

a,b: native DFPase

c,d,e,f: polyurethane blocks ground into particles

The errors on specific constants were calculated as follows:

$$\Delta\left(\frac{k_{cat}}{K_M}\right)=\left(\frac{k_{cat}}{K_M}\right)\cdot\left[\frac{\Delta k_{cat}}{k_{cat}}+\frac{\Delta K_M}{K_M}\right]$$

4.3.5 Effect of Surfactant on Polymer Morphology

Our interest in the underlying reasons for why the activity of the L62-containing materials were less dependent on loading led us to study the morphological effects of the surfactant with electron microscopy (Figure 14). Depending on the type of surfactant used, polyurethane foams display both macro- and microporosity.[121,232] The use of L62 resulted in a significant enlargement of the micropores (Figure 14 a and c) and also changed the surface contours within the micropores (Figure 14b and d). The increased micropore diameter may therefore explain the reduction in mass transfer limitation, by facilitating the substrate and product diffusion within the foam.

4.3.6 Effect of Salt removal on Enzyme Activity

Soluble DFPase promotes a turnover number of 232±2 s^{-1} and a K_M of 0.79± 0.02 mM in buffered media (50 mM bis-tris-propane, 5 mM $CaCl_2$) at pH 7.5, under ambient conditions (Table 4, Experiment 2). Given the known effect of salt on the activity of soluble DFPase, we investigated the effect of salt (0.5 M NaCl) on activity retention and transport effects in the biopolyurethane.

The loading dependence of activity, and its elimination upon crushing, is not affected by the additional of salt (Figure 15; Table 4, Experiments 12 and 13). Once again, the addition of L62 during synthesis considerably reduces the diffusional limitations as shown by the increase in apparent activity.

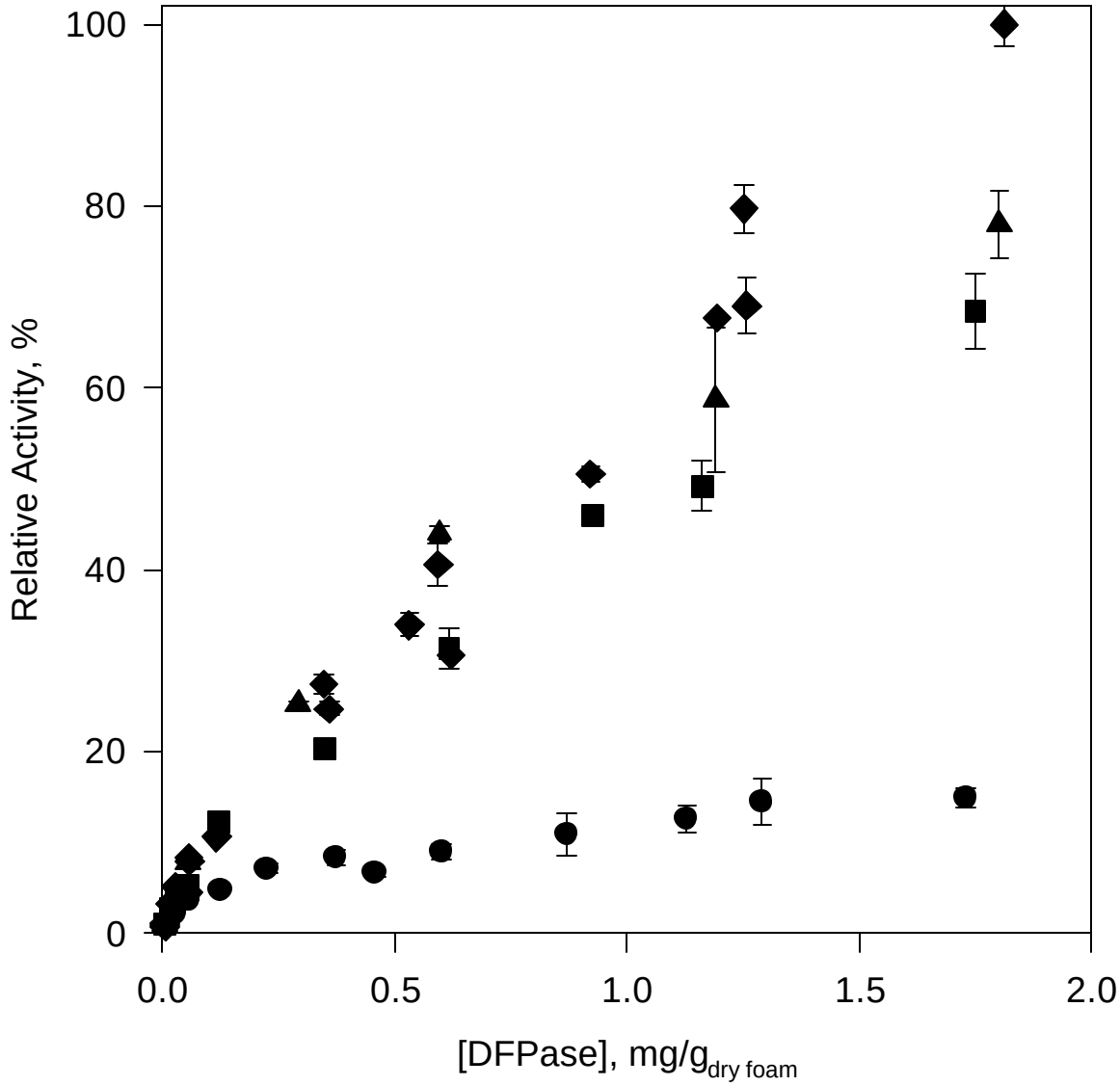

Figure 13 Effect of surfactant on DFPase-polymer efficiency

Foams were synthesized without surfactant (closed circles), and containing P65 (closed squares), F68 (closed triangles), and L62 (closed diamond) in buffered solutions (50 mM bis-tris-propane, 5 mM $CaCl_2$, 0.5 M NaCl) at pH 7.5. The activity of the bioplastic is reported at a 3 mM DFP concentration.

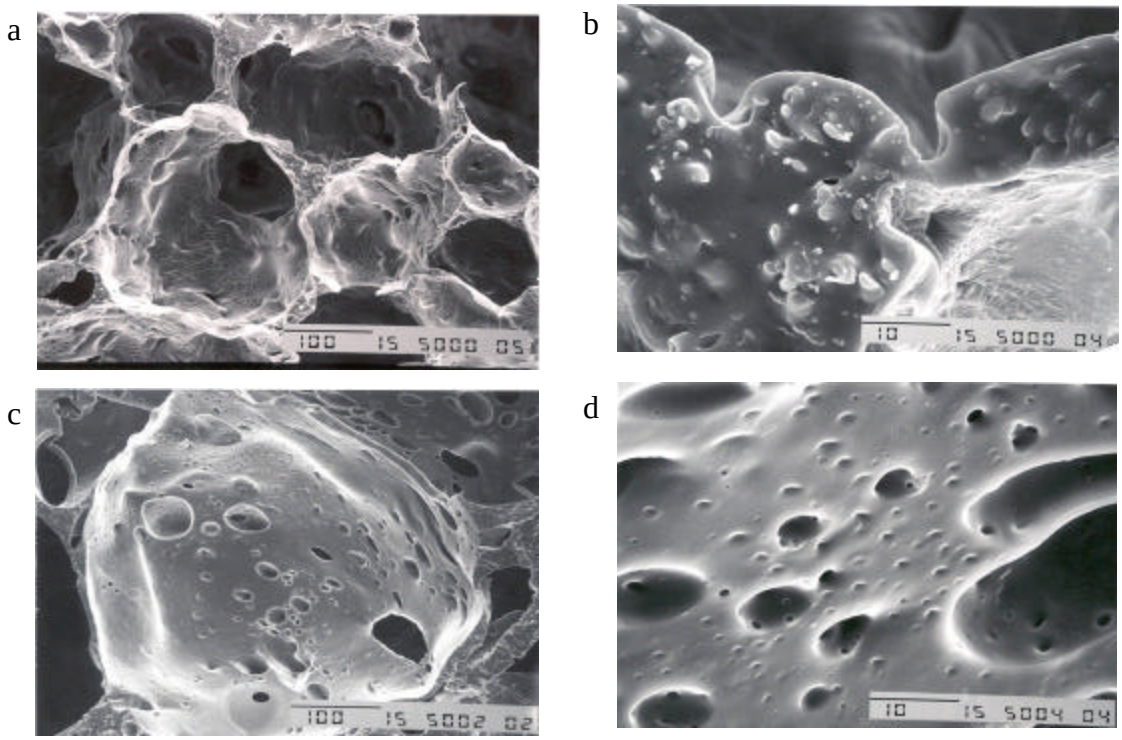

Figure 14 Scanning electron micrographs of polymers prepared without surfactant (a and b) and with L62 (c and d)

Since the DFPase-containing polymers were under kinetic control at low loading, their intrinsic kinetic characteristics were evaluated. The retention of 67 % activity under these conditions is characteristic of other multi-point immobilization techniques.[121,233,234,63] At high enzyme loading, recovery of the activity predicted from the intrinsic kinetic data could only be achieved after crushing.

4.3.7 Thermoinactivation of Native DFPase

As shown in Table 5, native DFPase is highly stable at 6 ^{o}C with no loss of activity after 41 weeks of incubation. At a temperature of 50 ^{o}C, the enzyme is still highly stable with a half-life of 3.4 days. This compares very well to other agentases such as phosphotriesterase (half life of 1.5 hr at 50 ^{o}C) and organophosphorus acid anhydrolase (half life of 100 min at 37 ^{o}C).[235] DFPase temperature-induced inactivation begins to be a concern at temperatures above 60 ^{o}C, where the half-life drops precipitously to approximately 6 min (at 65 ^{o}C) (Table 5). Addition of PEG (10 % w/v) to the incubation medium did not affect the stability of enzyme at 65 ^{o}C (data not shown). To determine whether DFPase thermoinactivation is due to unfolding, the enzyme deactivation was monitored at 65 ^{o}C using CD (Figure 16). As can be seen, the ellipticity value at 208 nm drastically decreased as the remaining enzymatic activity decreased, but the overall shape of the spectrum remained roughly constant with a minimum at 208 nm. As implied by the clear changes in the intensity of CD spectrum during thermoinactivation, the major mechanism involved in the thermoinactivation of

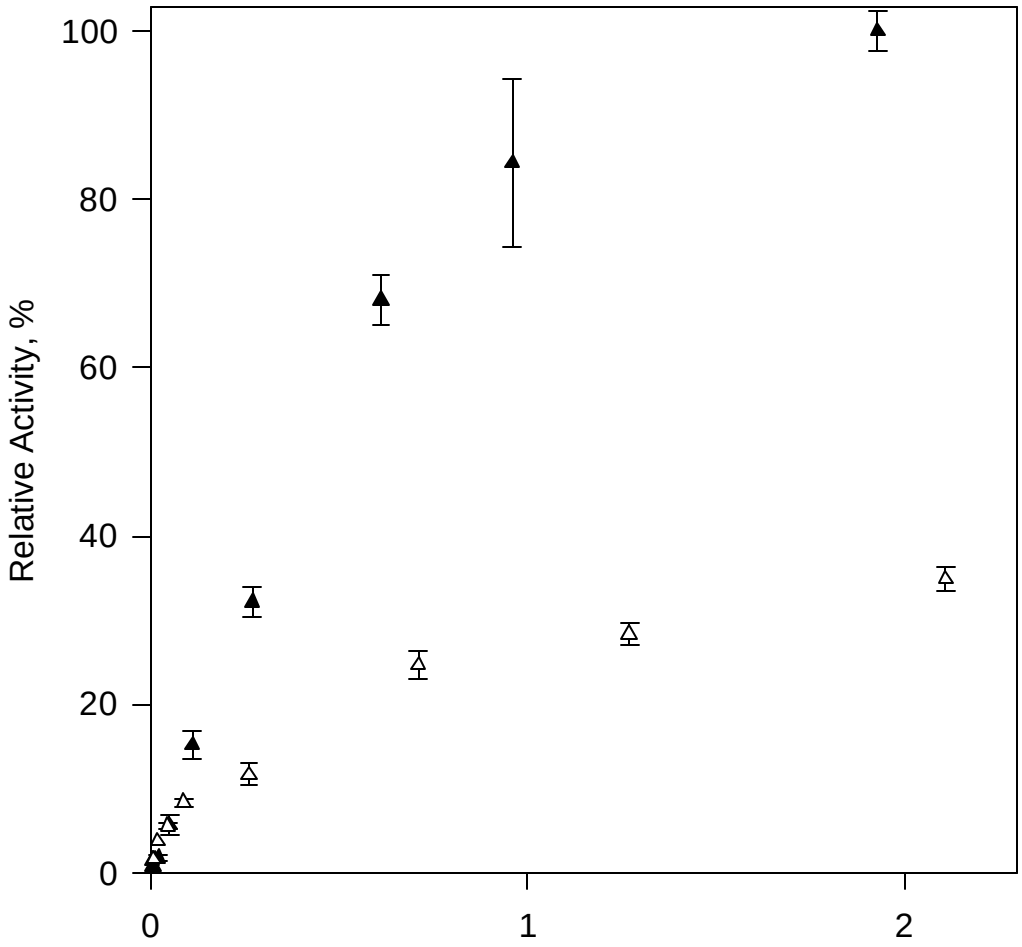

Figure 15 Effect of DFPase loading on DFPase-containing polyurethane efficiency in the absence of salt

Foams not containing surfactant (open triangles) and containing L62 (closed triangles) in buffered solutions (50 mM bis-tris-propane, 5 mM $CaCl_2$) at pH 7.5. The activity of the bioplastic is reported at a 3 mM DFP concentration.

DFPase at 65 ^{o}C is likely to result from a rapid unfolding of the enzyme and a reduction in b-sheet content (Figure 16).

4.3.8 Thermostability of DFPase-Containing Polyurethane

DFPase-containing polyurethanes present an opportunity to investigate whether the multi-point covalent attachment strategy we employed will indeed stabilize the protein. Our hope was that we would essentially lock the enzyme in an active conformation once polymerized, thereby increasing activity retention at elevated temperatures. In Table 6 it is clear that the strategy we followed is successful, to a point. The DFPase-containing polyurethane did not significantly deactivate after 41 weeks of incubation at 6 ^{o}C. Immobilized DFPase exhibited a higher stability at 50 ^{o}C than at 65 ^{o}C. At both temperatures, the thermoinactivation followed a non-first order profile characterized by a rapid deactivation phase followed by a remarkably stable phase (Table 6). After 45 min of incubation at 65 ^{o}C, immobilized DFPase retained approximately 10 % of its initial activity for more than 380 min, while the soluble DFPase was totally deactivated. It is possible that immobilized protein is hyperstable, but the initial loss of activity is a result of leaching of non-immobilized protein. No protein was detected in the incubation media after incubating samples of bioplastic prepared with a 1.6 mg/g_{foam} enzyme loading for 1 hr at 65 ^{o}C. Therefore detachment of enzyme from the polyurethane was not responsible for the biphasic behavior. The immobilization-induced transition from first order to biphasic inactivation kinetics has

Table 5

Kinetic parameters for thermoinactivation of native DFPase

Temperature (^oC)	$[Ca^{2+}]$ (mM)	Half-life	k_1	Time to 93 % inactivation
65	-	<0 min	-	-
65	1	1 min	0.63±0.05 min^{-1}	4 min
65	5	6 min	0.117±0.004 min^{-1}	23 min
65	50	16 min	0.043±0.003 min^{-1}	62 min
65	100	18 min	0.039±0.001 min^{-1}	68 min
50	5	3.4 day	0.202±0.008 day^{-1}	13 day
6	5	> 41 week	-	-

Deactivation of native DFPase was conducted in buffered solution (50 mM BTP, 0.5 M NaCl, pH 7.5). The remaining enzymatic activity was measured over time at room temperature in buffered media (50 mM BTP, 0.5 M NaCl, 5 mM $CaCl_2$, pH 7.5) using DFP (3 mM) as a substrate. The kinetic constant, k_1, was determined using a first order deactivation model:

$$E \rightarrow E_d \; ; \; a = a_0 \, exp(-k_1 t)$$

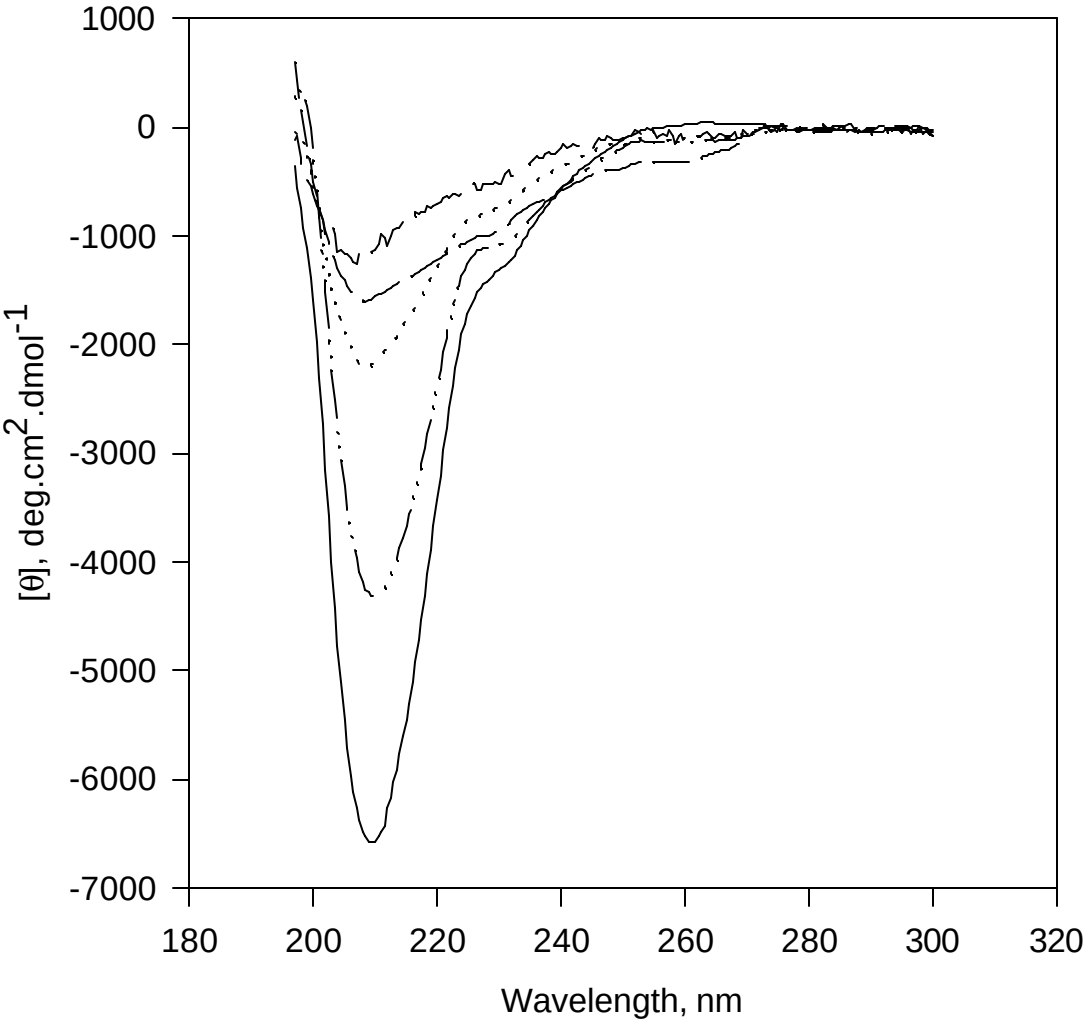

Figure 16 Conformation of native DFPase at various remaining enzymatic activities during thermoinactivation

The experiment was performed at 65 ^{o}C in buffer (10 mM Tris-HCl, pH 7.5) supplemented with 50 mM $CaCl_2$. CD spectra were recorded in 0.1-mm quartz cell at 25 ^{o}C for native DFPase (solid line), 38 % deactivated DFPase (dash-dot-dot line), 64 % deactivated DFPase (dotted line), 90 % deactivated DFPase (long dash line), 93 % deactivated DFPase (short dash line).

been observed previously, but never explained. For example, the immobilization of b-amylase on both organic and inorganic supports resulted in a transition from mono- to biphasic inactivation kinetics.[236] For amylase inactivation, the authors suggest that the enzyme denatures via a partially active intermediate, and given that this approach fits our data well we report equivalent results in Table 6. The model assumes the scheme described in the section 1.1.2.1:[5,237]

$$E \xrightarrow{k_1} \overset{a_1}{E_1} \xrightarrow{k_2} \overset{a_2}{E_2}$$

For the data presented herein, E would have stability similar to the native enzyme (with somewhat reduced activity) and E_1 would be 23 % activity but hyperstable. The enzymatic activity (a) is expressed as follows:

$$a = \left(1 + \left(\frac{a_1 k_1 - a_2 k_2}{k_2 - k_1}\right)\right)\exp(-k_1 t) + \left(\frac{k_1 (a_2 - a_1)}{k_2 - k_1}\right)\exp(-k_2 t) + a_2$$

Where *t* is the time of thermoinactivation. Table 4 presents the fit of the data to the above equation.

The thermostability of bioplastics was not affected by the presence of PEG (10 % w/v), as observed for native DFPase (data not shown).

4.3.9 Effect of Calcium on the Thermostability of Native and Immobilized DFPase

Calcium ions form a complex with native DFPase. Since the bioplastics synthesis may alter the binding of calcium to the enzyme, we measured the impact of calcium ion concentration on activity and stability.

First, we explored the effect of calcium on the conformation of the native enzyme in the presence or absence of the strong chelator EGTA, using CD (Table 7). The secondary structure of native enzyme varied slightly with the calcium concentration. Addition of EGTA (1 mM) resulted in a significant decrease in the α-helix and β-turn content along with an increase in the proportion of β-sheet. Clearly removal of the calcium ions significantly alters secondary structure. A 20 % loss of activity was recorded during the treatment of DFPase with EGTA. As shown in Table 5, the thermostability of native DFPase was also affected by the free calcium concentration. The enzyme half-life at 65 ^{o}C increased from 1 min in calcium chloride (1 mM) to 16 min at 50 mM. DFPase treated with EGTA had no activity when placed in buffer at 65 ^{o}C. After re-introduction of calcium ions, the original thermostability of DFPase was regenerated. Native DFPase denatured upon heating, the thermostability being dependent on the free calcium concentration. Similar results have been found for

Table 6

Kinetic parameters for thermoinactivation of PEG-modified and immobilized DFPase

System	T (^oC)	$[Ca^{2+}]$ (mM)	$t_{1/2}$	α_1	α_2	k_1	k_2	93 % inactivation
PEG-DFPase r=1/100; PEG-NCO	65	5	2 min	0.47±0.03	0.018±0.003	0.8±0.1 min^{-1}	0.100±0.007 min^{-1}	23 min
PEG-DFPase r=1/20; PEG-$(NCO)_2$	65	5	6 min	0.30±0.06	0	0.21±0.04 min^{-1}	0.029±0.006 min^{-1}	55 min
PEG-DFPase r=1/1000; PEG-$(NCO)_2$	65	5	3 min	0.28±0.02	0.020±0.002	0.37±0.02 min^{-1}	0.042±0.003 min^{-1}	42 min

System	T (^oC)	[Ca^{2+}] (mM)	$t_{1/2}$	α_1	α_2	k_1	k_2	93 % inactivation
Immobilized DFPase	65	5	1 min	0.23±0.02	0.071±0.005	0.91±0.05 min^{-1}	0.041±0.009 min^{-1}	311 min
Immobilized DFPase	65	50	2 min	0.40±0.02	0.095±0.009	1.0±0.1 min^{-1}	0.019±0.003 min^{-1}	-
Immobilized DFPase	50	5	0.5 day	0.60±0.02	0.07±0.02	122±3 day^{-1}	0.45±0.07 day^{-1}	33 days
Immobilized DFPase	6	5	>41 week	-	-	-	-	-
Immobilized PEG - DFPase r=1/100; PEG-NCO	65	5	3 min	0.24±0.02	0.013±0.003	0.36±0.03 min^{-1}	0.024±0.003 min^{-1}	60 min

System	T (^oC)	$[Ca^{2+}]$ (mM)	$t_{1/2}$	α_1	α_2	k_1	k_2	93 % inactivation
Immobilized PEG-DFPase r=1/20; PEG $(NCO)_2$	65	5	2 min	0.23±0.02	0.015±0.002	0.23±0.01 min^{-1}	0.022±0.002 min^{-1}	66 min

r represents the molar ratio between PEG-isocyanate and DFPase during the PEGylation. Deactivation of PEGylated and immobilized DFPase was conducted in buffered solution (50 mM BTP, 0.5 M NaCl, 5 mM $Cacl_2$, pH 7.5). The remaining enzymatic activity was measured over time at room temperature in buffered media (50 mM BTP, 0.5 M NaCl, 5 mM $CaCl_2$, pH 7.5) using DFP (3 mM) as a substrate. The biphasic behavior was described with a four parameter model, and the kinetic constants α_1, α_2, k_1 and k_2, were determined using the algorithm of Marquardt-Levenberg (SigmaPlot Version 2.0).

a subsequent number of other metalloenzymes.[238,239] For proteinases, changing the added calcium concentration may also affect the period of occupancy of metal-binding site and thus modify the stability of enzyme.[240,241,242]

Deactivation at 65 ^{o}C in the absence or presence of calcium (50 mM) resulted in changes in secondary structure as determined by CD. Decreases in the ellipticity values at 208 nm were similar over two different time scales (Figure 16, Figure 17). Clearly, calcium ions help maintain the enzyme conformation and prevent denaturation upon heating.

The removal of calcium ions from the enzyme prior to immobilization lead to inactive bioplastics in buffer at 65 ^{o}C, as observed with soluble enzyme. When incubated in the presence of EGTA at 65 ^{o}C, immobilized DFPase fully deactivated within 6 min. Therefore, the fast phase of thermoinactivation ($E \rightarrow E_1$) is calcium-dependent. Bioplastics were also deactivated for a 200 min period in the presence of calcium, and further treated with EGTA at 65 ^{o}C. EGTA destabilized the deactivated enzyme, which lost its residual activity in ~110 min. Thus, the second phase of thermoinactivation ($E_1 \rightarrow E_2$) for immobilized DFPase is also calcium-dependent. Increasing the free calcium concentration in the incubation medium from 5 to 50mM slightly affected the thermoinactivation of immobilized DFPase at 65 ^{o}C (Table 7). The stabilization of DFPase in polyurethanes is not derived from removing the necessity for calcium binding.

Table 7

Secondary structure of native and modified DFPase in the presence of EGTA and different free calcium concentrations

System	$[Ca^{2+}]_{added}$ (mM)	[EGTA] (mM)	Composition (%)			
			α-helix	β-sheet	β-turn	Random
Native DFPase	-	-	6.7	45.3	18.9	29.0
Native DFPase	1	-	7.8	43.2	19.8	29.3
Native DFPase	5	-	10.8	38.9	22.8	27.5
Native DFPase	50	-	7.5	45.0	18.3	29.2
Native DFPase	-	1	2.7	53.4	12.5	31.4
PEG-DFPase	50	-	9.3	43.3	19.8	27.7
PEG-NCO; r=1/100*						

System	$[Ca^{2+}]_{added}$ (mM)	[EGTA] (mM)	Composition (%)			
			α-helix	β-sheet	β-turn	Random
PEG-DFPase	50	-	20.4	27.6	40.5	11.6
PEG-$(NCO)_2$; r=1/1000*						

r represents the molar ratio between PEG-isocyanate and DFPase during the PEGylation. The conformation of enzyme was monitored at 25 ^{o}C by CD. Each spectrum was averaged from ten scans between 300 and 195 nm. The composition of secondary structure was determined using the Lincomb program and the data set yang.dat.

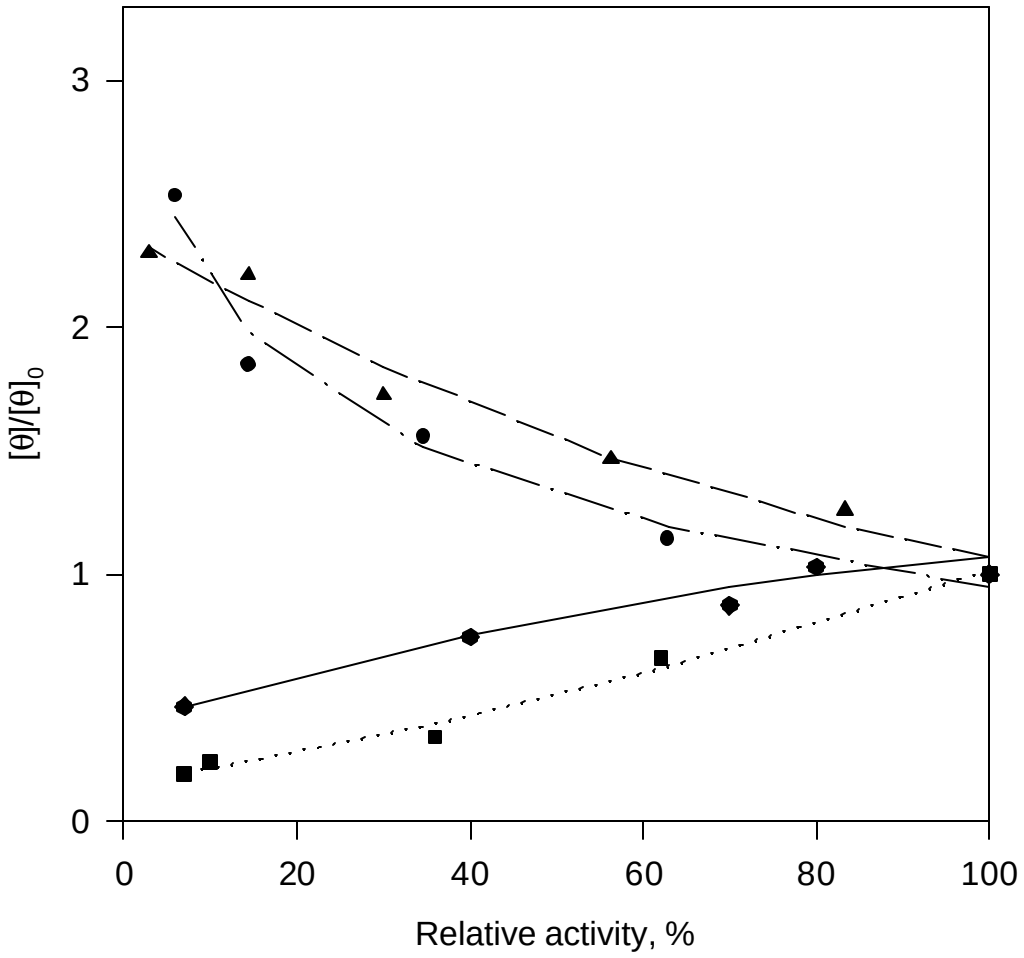

Figure 17 Effect of calcium on DFPase secondary structure

Relative CD signal at the minimum ellipticity during thermoinactivation was studied in the absence (closed diamonds) and presence of added calcium (50 mM) (closed squares) for native enzyme, PEG-DFPase (protein to PEG-NCO molar ratio 1/100 (closed circles)) and PEG-DFPase (protein to PEG-$(NCO)_2$ molar ratio 1/1000 (closed triangles)) in the presence of added calcium (50 mM) at 65 ^{o}C. The CD spectra were recorded at 25 ^{o}C for various remaining enzymatic activities.

4.3.10 Thermostability of PEG-Modified DFPase

DFPase was chemically modified via a non-specific reaction of polyethylene glycol-isocyanate (PEG-NCO or PEG-$(NCO)_2$) with the Lysine residues on the protein surface. DFPase contains 24 theoretically modifiable residues. Figure 18 is a MALDI spectrum of the PEG-DFPase obtained from a 1/100 DFPase to PEG-NCO mole ratio during synthesis. The peaks are labeled with the corresponding number of PEG chains attached to the enzyme, and the difference between two subsequent peaks is approximately 5000, which is the average molecular weight of the PEG used. The degree of PEG-modification was 100 % (No native protein remains) with two to seven PEG chains attached per molecule of enzyme. The width and overlap of peaks is explained by the polydispersity of PEG chains. Examples of proteins highly modified with polymer chains via their ε-amino groups have been previously reported in the literature. The degree of modification of DFPase is represented in Figure 19, which also gives the effect of PEG-isocyanate to enzyme molar ratio on modification efficiency. When using PEG-NCO_2, DFPase was surrounded by up to 14 PEG chains. This greater extent of PEGylation could also be explained by the ability of PEG–$(NCO)_2$ to react with both the enzyme and another PEG chain. We were unable to characterize the conjugates obtained with a 1/1000 enzyme to PEG-$(NCO)_2$ ratio since the high PEG content appeared to prevent the ionization of modified DFPase in the MALDI instrument.

Unlike native DFPase, PEGylated enzyme displayed a biphasic thermoinactivation profile at 65 ^{o}C. After a first phase of fast deactivation, the remaining activity was significantly stabilized by a high extent of modification (Table 6). The thermoinactivation patterns followed the two-step deactivation model proposed earlier. Table 6 contains a compilation of the kinetic parameters calculated for the PEG-DFPase at various protein to PEG ratios. By increasing the protein to PEG-$(NCO)_2$ molar ratio from 1/20 to 1/1000, the extent of PEG modification increased and PEG-DFPase showed higher thermostability after the first phase of fast deactivation with a profile identical to that observed for immobilized DFPase. By increasing the protein to PEG-$(NCO)_2$ molar ratio, k_1, the relative activity of final enzyme state a_2 and k_2 all increased, while the relative activity of intermediate enzyme state a1 slightly decreased.

The secondary structure of PEG-DFPase (1/100) appears identical to that of native DFPase (Table 8). The far-UV CD spectrum of PEG-DFPase possessed a minimum ellipticity value at 210 nm instead of 208 nm for the native enzyme. As the PEG-modified DFPase was irreversibly deactivated upon heating at 65 ^{o}C, the strength of CD signal at the minimum ellipticity value increased significantly (Figure 17). Interestingly, this is the complete reverse of the observations made with native enzyme. When using PEG-$(NCO)_2$ (1/1000), DFPase was modified to a higher extent and its secondary structure was significantly altered (Table 8). Mabrouk reported similar observations for equine cyotochrome C.[243] For deactivation at 65 ^{o}C, the CD signal for the relative minimum ellipticity increased linearly (Figure 17).

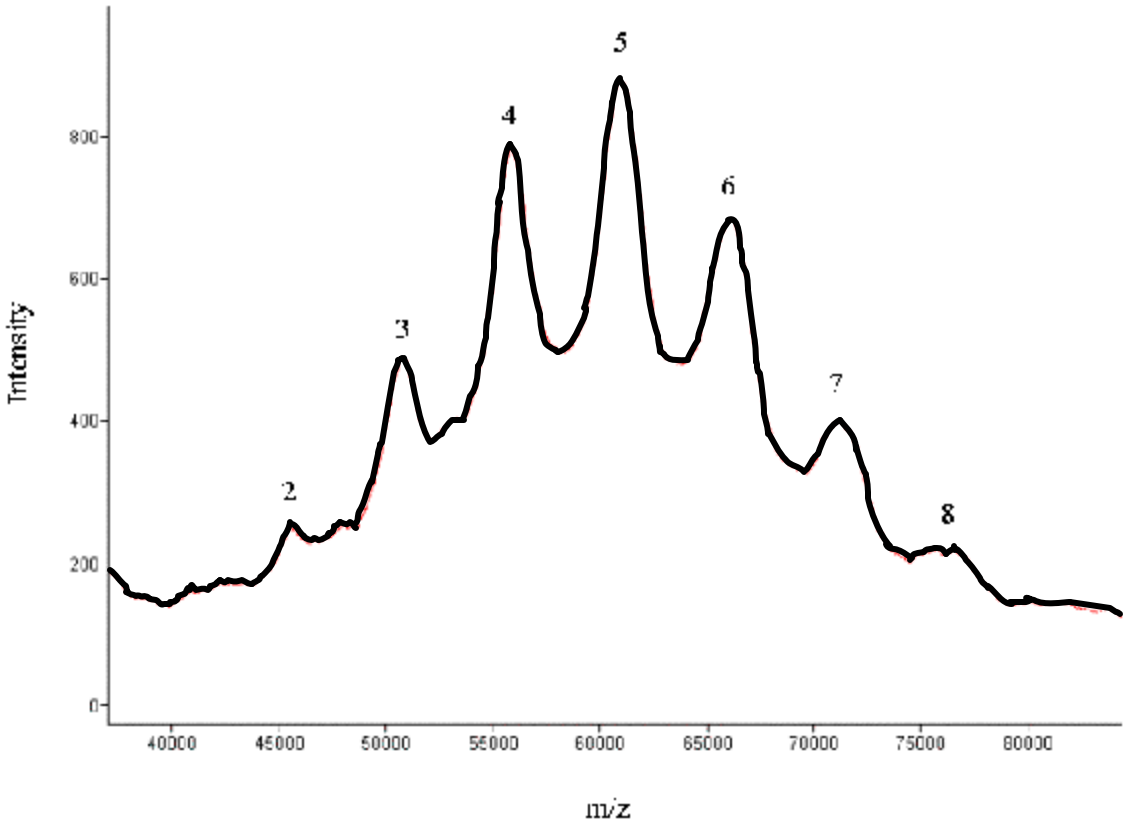

Figure 18 MALDI spectra of PEG-DFPase prepared with a 1/100 protein to PEG-NCO molar ratio

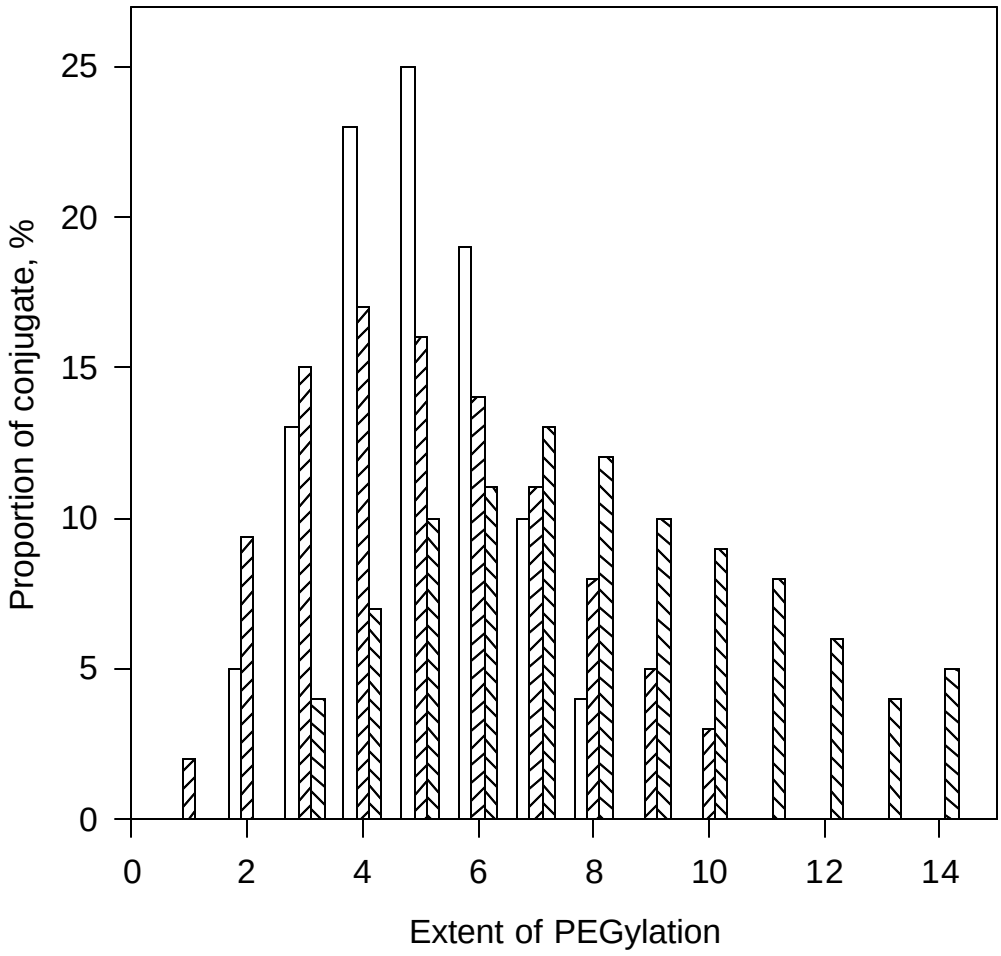

Figure 19 PEGylation of DFPase

The extent of PEG-modification was obtained with a 1/100 protein to PEG-NCO molar ratio (▭), a 1/20 protein to PEG-$(NCO)_2$ molar ratio (▨) and a 1/50 protein to PEG-$(NCO)_2$ molar ratio (▩).

Table 8

Secondary structure of native and modified DFPase during denaturation at 65 ^{o}C

System	$[Ca^{2+}]$ (mM)	Activity loss (%)	Composition (%)			
			α-helix	β-sheet	β-turn	Random coil
Native DFPase	0	0	6.7	45.3	18.9	29.0
		20	5.9	44.8	17.4	31.9
		30	5.2	42.6	19.8	32.5
		60	4.6	41.0	21.2	33.2
Native DFPase	50	0	7.5	45.0	18.3	29.2
		38	6.7	44.6	22.7	26.0
		64	7.5	32.8	35.2	24.5
PEG- DFPase	50	0	9.3	43.3	19.8	27.7
		17.6	8.5	46.4	13.1	32.1
(PEG-NCO ; r=1/100)		43.7	6.3	47.1	7.9	38.6
PEG- DFPase	50	0	20.4	27.6	40.5	11.6
		37.1	19.3	43.4	33.8	3.5
$(PEG-(NCO)_2$;		65.4	12.4	52.5	15.2	20.0

r represents the molar ratio between PEG-isocyanate and DFPase during the PEGylation. The conformation of enzyme was monitored at 25 ^{o}C by CD spectroscopy in buffered media (10 mM Tris, pH 7.5). Each spectrum was averaged from ten scans between 300 and 195 nm. The composition of secondary structure was determined using Lincomb program and the data set yang.dat.

4.3.11 Structural Basis for Deactivation

The PEGylation and immobilization of DFPase both involve the reaction between amino-groups on the protein surface and isocyanate functionalities on the PEG-based polymer. Indeed, the only difference is the number of isocyanate per chain. When using PEG-$(NCO)_2$, PEG can self polymerize after attachment to the protein, mimicking closely the immobilization, but yielding a non-crosslinked soluble product. The length of polymer branches attached to the enzyme surface increased with the protein to PEG ratio during the modification process. PEG–DFPase, as a model for DFPase-polyurethane, is useful because we can study the inactivation of the protein, determine whether it mirrors that of native or immobilized enzyme, and then most importantly study the spectroscopic changes which are associated with the activity loss. Once again, in order to perform experiments on a reasonable time scale we used an elevated temperature of 65 ^{o}C to inactivate the enzyme. Table 8 shows the composition of secondary structure for native DFPase during deactivation in the presence or absence of added calcium. In the absence of added calcium, a 30 % activity loss lead to a small decrease in β-sheet to β-turn ratio (2.4 to 2.2) and little change in the α-helix to β-sheet ratio (0.2 to 0.1). In the presence of 50 mM calcium, the β-sheet to β-turn ratio decreased from 2.5 to 2.0 for a 60 % active enzyme. The same activity reduction did not change the α-helix to β-sheet ratio (0.2 to 0.2). Interestingly, the same level of activity loss (40 %) for PEG-DFPase (1/1000) in the presence of calcium (50 mM) exhibited a 3.1-fold increase in the β-sheet to β-turn ratio and a 0.5-fold decrease in the α-helix to

β-sheet ratio (Table 8). By extrapolation, a 40 % activity loss for PEG-DFPase (1/100) in the presence of calcium (50 mM) would result in a 2.2-fold increase in the β-sheet to β-turn ratio and a 0.6-fold decrease in the α-helix to β-sheet ratio (Table 8). As the PEGylated enzyme inactivates the structure changes significantly, and most importantly in a way which is different than the native enzyme. The study shows that the modified enzyme increases the amount of β-sheet in the hyperstable form of the protein.

4.4 CONCLUSION

Covalent incorporation of DFPase into polyurethane foams has been performed in a single step protein-polymer synthesis using a foamable prepolymer (Hypol 3000). The results show that the activity of DFPase-containing bioplastics is limited by internal diffusion. The addition of non-ionic Pluronic surfactants during the immobilization process changes the foam macro- and microstructure, leading to an enhancement of apparent and intrinsic catalytic efficiency. When synthesized with L62, the efficiency of DFPase-foam was 67 % of that of the soluble enzyme.

Native DFPase inactivates as a result of conformational changes. DFPase–containing polyurethanes lose 90 % of their activity quickly, but then become hyper-stable at elevated temperature. The stabilization is not a result of altered interactions between the enzyme and bound metal ions. The known propensity for multi-point covalent incorporation of proteins into a growing polymer chain to prevent protein unfolding, led to a study of the effect of PEGylation and immobilization on protein

stability. PEGylation results in a noticeable change in secondary structure, reducing the level of randomness and enhancing the amount of ordered structure. This compact active form of the enzyme now undergoes a two-stage inactivation. As is the case for DFPase–polyurethanes, the partially active form is extremely stable relative to the native enzyme (which inactivates completely in a single-step). Since the kinetics of unfolding for the immobilized enzyme mimic the PEGylated form, we expect that the polymerized form of the enzyme is immobilized in a state similar to the structure of the PEG-DFPase.

5.0 IMMOBILIZATION OF CA IN POLYMERS USING ATRP

5.1 Introduction

ATRP is an attractive method for the controlled radical polymerization of a broad range of functionalized monomers. It is compatible with a large variety of solvents and results in the preparation of polymers with relatively low polydispersities. It has also been employed to graft polymer chains from polymeric macroinitiators and solid supports in a controlled way.[135,134] It would be interested to determine whether ATRP is compatible with biological systems and can be used for the incorporation of biocatalysts into polymer matrices.

In this chapter, we focused on the polymerization of two ionic monomers, sodium sulfonate styrene and 2-(N,N,N-trimethylammonio)ethyl methacrylate trifluoromethanesulfonate, at room temperature in homogeneous water phase using carbonic anhydrase (CA, EC 4.2.1.1) functionalized with bromo-intitiators. Native CA is a zinc-containing enzyme catalyzing the reversible hydration of carbon dioxide. Although the physiological function of CA is to catalyze the interconversion between carbon dioxide and bicarbonate, the enzyme is known to have a low specificity and to catalyze, for example, the reversible hydration of various aldehydes and the hydrolysis of several esters such as p-nitrophenyl esters.[244,245] It is found in humans, all animals, photosynthesizing organisms and some non-photosynthetic bacteria. The CA isozyme II is purified from red cells and exhibits the highest CO_2 hydration turnover number. The

zinc ion is at the enzyme active site and plays a catalytic function. In the classic mechanism, the zinc is bound to a hydroxyl ion, which acts as the reactive specie and attacks carbon dioxide to form HCO_3^-.[246,247] The waterborne controlled radical polymerization of these specific monomers was successfully performed with the conventional initiators 2-bromopropionate and 2-bromoisobutyrate esters of poly(ethylene oxide) monomethyl ether by Tsarevsky et al.[248] The effects of reagents for ATRP on the enzyme activity were determined. CA chemical modification with bromoinitiators, as well as biopolymers were characterized by mass spectrometry and activity assays.

5.2 Materials and Methods

5.2.1 Materials

2-bromopropionyl chloride, CA from bovine erythrocytes (CA II), boric acid, bromoisobutyric acid, dicyclohexyl carbodiimide, pyridine, p-nitrophenyl propionate, acetonitrile, bipyridine (bpy), copper(I) and (II), sodium 4-styrenesulfonate (NaSS), neurotensin, , phosphate sodium, and N-hydrosuccinimide (NHS) were purchased from Sigma-Aldrich Corporation (St Louis, MO). 2-(N,N,N-trimethylammonio)ethyl methacrylate trifluoromethanesulfonate (TMATf) was prepared by Nicolay V. Tsarevsky.[248]

5.2.2 Activity Assay

The esterase activity of CA was assayed using *p*-nitrophenyl propionate according to the procedure developed by Pocker Y and coworkers.[244] Typically, soluble CA was assayed in a 1.5 ml disposable cuvet in the presence of *p*-nitrophenyl propionate (0.4 mM) and 1 % (v/v) acetonitrile at room temperature. The medium in use contained 50 mM phosphate buffer, pH 7.5. During the substrate hydrolysis, *p*-nitrophenol was released and its formation was followed spectrophotometrically at 405 nm using an extinction coefficient of 12.55 $cm^{-1}mM^{-1}$. Substantial hydrolysis was observed in the absence of CA; hence, the background hydrolysis was systematically subtracted from the rates of reaction measured in the presence of enzyme.

5.2.3 CA Stability in the Presence of Reagents for ATRP

The enzyme (6 mg/ml) was incubated under ambient conditions in buffer (50 mM phosphate sodium, pH 7.5) and in various buffered mixtures of pyridine, copper bromide, monomer, and bpy.

To determine the stability of CA towards freezing-melting process, the enzyme solution (50 mM phosphate, pH 7.5) was frozen with liquid N_2 and further molten with a water bath at room temperature. The biocatalyst activity was measured before and after each freezing-melting cycle as described above.

5.2.4 Chemical Modification with 2-Bromo-Propionyl Chloride

The chemical modification was performed following the procedure described by Lynn et al.(Figure 20)[249]

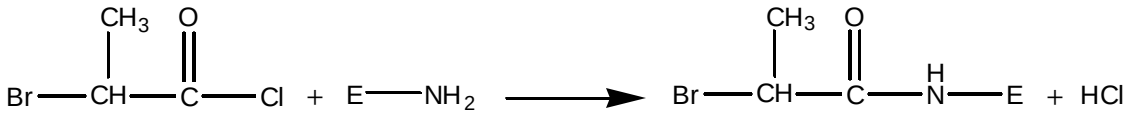

Figure 20 Enzyme coupling to 2-bromo-propionic chloride

The enzyme (or neurotensin peptide) was added to buffered media (0.5 M borate, pH 8.5). 2-bromopropionyl chloride is further introduced into the mixture, and the reaction was carried at room temperature for 1hr under vigorous mixing. The molar ratio between enzyme (or neurotensin peptide) and reagent was maintained at 500. The modified enzyme (or peptide) was purified and concentrated by centrifugation at 6 ^{o}C and 4,000 ×g using a centrifugal filter with a 10,000 membrane nominal molecular weight. The effect of coupling 2-bromopropionyl chloride to CA on the enzyme kinetics was determined by assaying the biocatalyst activity before and after modification as described in the section 5.2.2.

5.2.5 Chemical Modification with Bromoisobutyric Acid

Bromoisobutyric acid was reacted with NHS in anhydrous dioxane in the presence of dicyclohexyl carbodiimide at room temperature under magnetic mixing as reported by Yoshimoto et al. and Šuškovic et al. (Figure 21).[250,251] Activated bromoisobutyric acid was reacted with the enzyme (or neurotensin peptide) in buffered media (0.1 M borate, pH 8.5) at room temperature for the first hour and then at 6 ^{o}C overnight. The modified enzyme (or peptide) was purified and concentrated by centrifugation at 6 ^{o}C and 4,000× g using a centrifugal filter with a 10,000 membrane nominal molecular weight. The effect of coupling 2-bromopropionyl chloride to CA on the enzyme kinetics was determined by assaying the biocatalyst activity before and after modification as described in the section 5.2.2.

5.2.6 Characterization of Bio-Macroinitiator

MALDI-MS analyses were performed with a Perseptive Biosystems Voyager elite MALDI-TOF. CA modifications were analyzed by following the procedure described in the sections 4.2.2.7.

The chemical modifications of neurotensin were analyzed with MALDI-MS (Perseptive Biosystems Voyager elite MALDI-TOF). The acceleration voltage was set to 20 kV in a linear mode. The peptide solution (1-2 mg/ml) was mixed with an equal volume of the matrix solution (0.5 ml water, 0.5ml acetonitrile, 2 µl TFA and 8 mg α- cyano-4-

hydroxycinnamic acid), and 2 µl of the final solution was spotted on the plate target. Spectra were recorded after evaporation of the solvent mixture, and were calibrated externally with ACTH and FP.

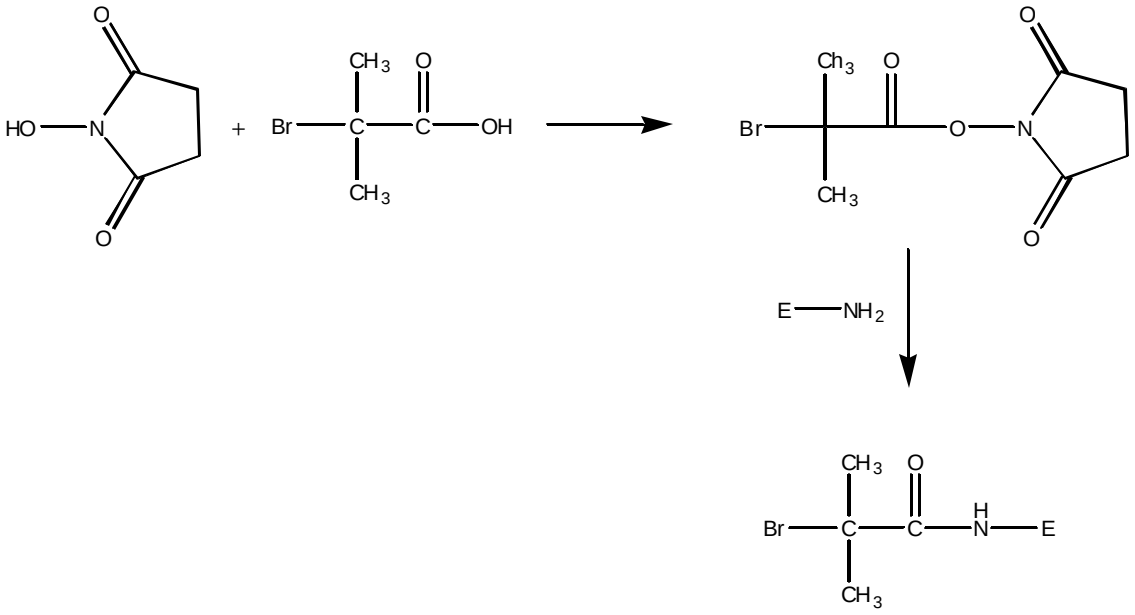

Figure 21 Coupling of CA to bromoisobutyric acid

5.2.7 ATRP Polymerization

ATRP was performed as described by Tsarevsky et al. using 4-styrenesulfonic acid sodium and 2-trimethylammonioethyl methacrylate trifluoromethanesulfonate as monomers.[248]

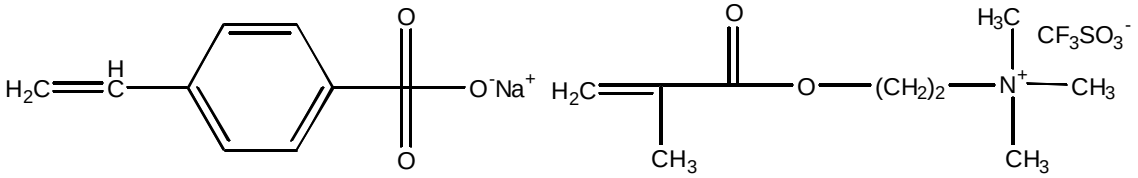

sodium 4-styrenesulfonate

2-(N,N,N-trimethylammonio)ethyl
methacrylate trifluoromethanesulfonate

Polymerization of the monomer 4-styrenesulfonic acid sodium was performed using the bio-macroinitiator prepared with 2-bromo propionyl chloride. The bio-macroinitiator (60 mg), monomer (1.030 g), buffer (3.6 ml, 50 mM Tris-HCl, pH 7.5), and pyridine (0.4 ml) were mixed together in a 10ml-reactor. The mixture was placed under vacuum for 45 min while kept cold with an ice bath, and further frozen in liquid N_2. bpy (0.0314 g), CuBr (0.0087 g) and $CuBr_2$ (0.0085 g) were introduced in the system, which was then degassed and sealed for 5 min. The reaction solution was liquid at room temperature. Polymerization was conducted at room temperature for 23 hr.

Polymerization of the monomer 2-trimethylammonioethyl methacrylate trifluoromethanesulfonate was performed using the bio-macroinitiator prepared with bromoisobutyric acid (Figure 21). The bio-macroinitiator (26 mg), monomer (1.6 g), buffer (3.1 ml, 50 mM Tris-HCl, pH 7.5), and pyridine (1.2 ml) were mixed together in a 10 ml-reactor. The mixture was placed under vacuum for 45 min while kept cold with

an ice bath, and further frozen in liquid N_2. The freezing-melting process did not affect significantly the enzyme activity. bpy (0.0314 g), CuBr (0.0086 g) and $CuBr_2$ (0.0085 g) were introduced in the system, which was then degassed and sealed for 5 min. The reaction solution was molten at room temperature. Polymerization was conducted at room temperature for 5 hr.

For each polymerization, the biocatalyst activity was measured before and after each freezing-melting cycle as described above.

5.2.8 Biopolymer Characterization

Various techniques are available to determine of the chemical modification of biocatalysts including GPC (or HPLC), MALDI, and electrophoresis.[252,253,256] In this study, these methods failed to give reliable results, and the characterization was performed with analytic ultracentrifugation.

Lyophilized native and immobilized CA were suspended in buffer (0.02 M phosphate, 0.3 M NaCl, pH 7.4). Analytical ultracentrifugation was performed in a Beckman-Coulter XL-A ultracentrifuge equipped with absorption scanner optics. For a qualitative analysis of the heterogeneity of the samples lyophilized native CA and EP were redissolved in buffer (0.02 M phosphate, 0.3 M NaCl, pH 7.4) and the sedimentation behavior was observed at 45000 rpm in aluminum filled epon double sector centerpieces. For the determination of average molecular weights the samples were spun in the same buffer at 14000 rpm until sedimentation diffusion equilibrium was

attained. From the observed concentration distribution the molecular weight was estimated according to

$$c_x = c_0 \exp\left(\frac{M(1-\bar{v}r)}{2RT} w^2 \left(x^2 - x_0^2\right)\right)$$

where $c_x(c_0)$: concentration at distance $x(x_0)$ *from rotor center*, M: molar mass of solute, *T:* absolute temperature, w: angular velocity of the rotor, r: density of the solution, and $\bar{v}$: partial specific volume of the solute. For estimation of $\bar{v}$ samples were dissolved in solutions of different densities r H_2O, D_2O, and a (50/50%) mixture of H_2O/D_2O. For heterogeneous samples this procedure yields approximately weight averaged molar masses.

5.3 Results and Discussion

5.3.1 Synthesis of Bio-Macroinitiator

The amino acid sequence for CA contains 18 lysines. Most of them are present at the enzyme surface and, hence, susceptible to react with the bromo-initiators. Given the low molecular weights of bromo-initiators, as compared with that of enzyme, only the overall extent of enzyme modification and the reaction yield can be determined by

mass spectrometry. To verify that the coupling between the bromo-initiators and the primary amines occured as expected (Figures 20 and 21), the reactions were performed with a low molecular weight peptide, called neurotensin, which contains only one lysine residue. For each reaction, the observed change in peptide molecular weight was calculated from MALDI spectra and compared to the predicted one. As expected, the reaction of neurotensin with 2-bromo propionyl chloride provoked a mass increase of 135 g/mol (Figure 22). Similarly, the coupling of neurotensin to bromoisobutyric acid was successful and induced an increase in the peptide mass of 149 g/mol (Figure 23). MALDI spectra for native and modified CA are presented in Figure 24. Both reactions led to full conversion of enzyme (No native enzyme is left). Each molecule of CA modified with 2-bromopropionyl chloride and bromoisobutyric acid is attached to an average of 5 and 12 initiator chains, respectively (Figure 24). Unlike native enzyme, the populations of modified CA's are highly heterogeneous, as indicated by the broad MALDI peaks. The chemical modifications did not induce any enzymatic deactivation.

5.3.2 CA Stability in the Presence of Reagents for ATRP

When used as a co-solvent (10 vol.%), pyridine destabilizes CA, as shown by the resulting 1.6-time increase in the deactivation constant (Table 9; Experiment 1 and 2). As reported for other hydrophilic solvents, pyridine may interact with the essential water molecules present at the enzyme surface, leading to the enzyme partial unfolding

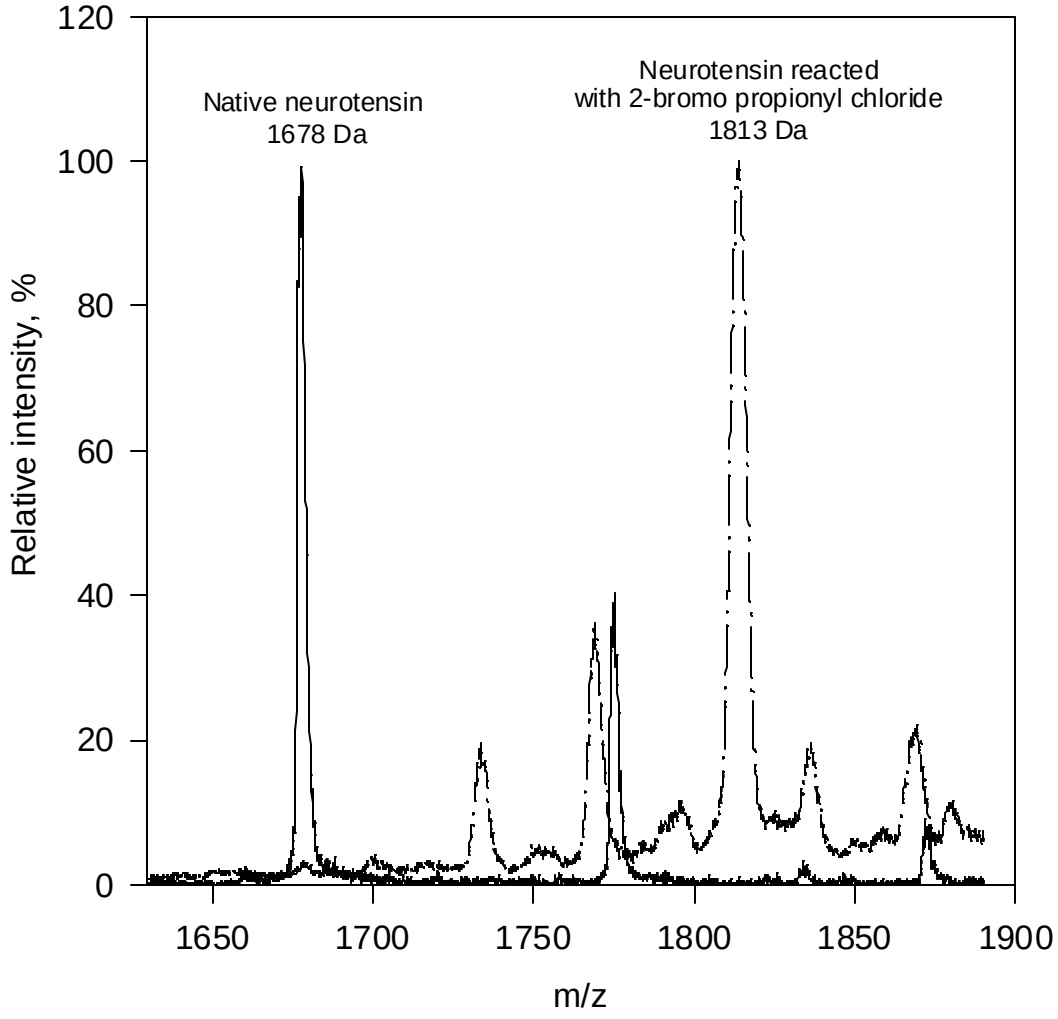

Figure 22 Coupling of neurotensin with 2-bromo propionyl chloride

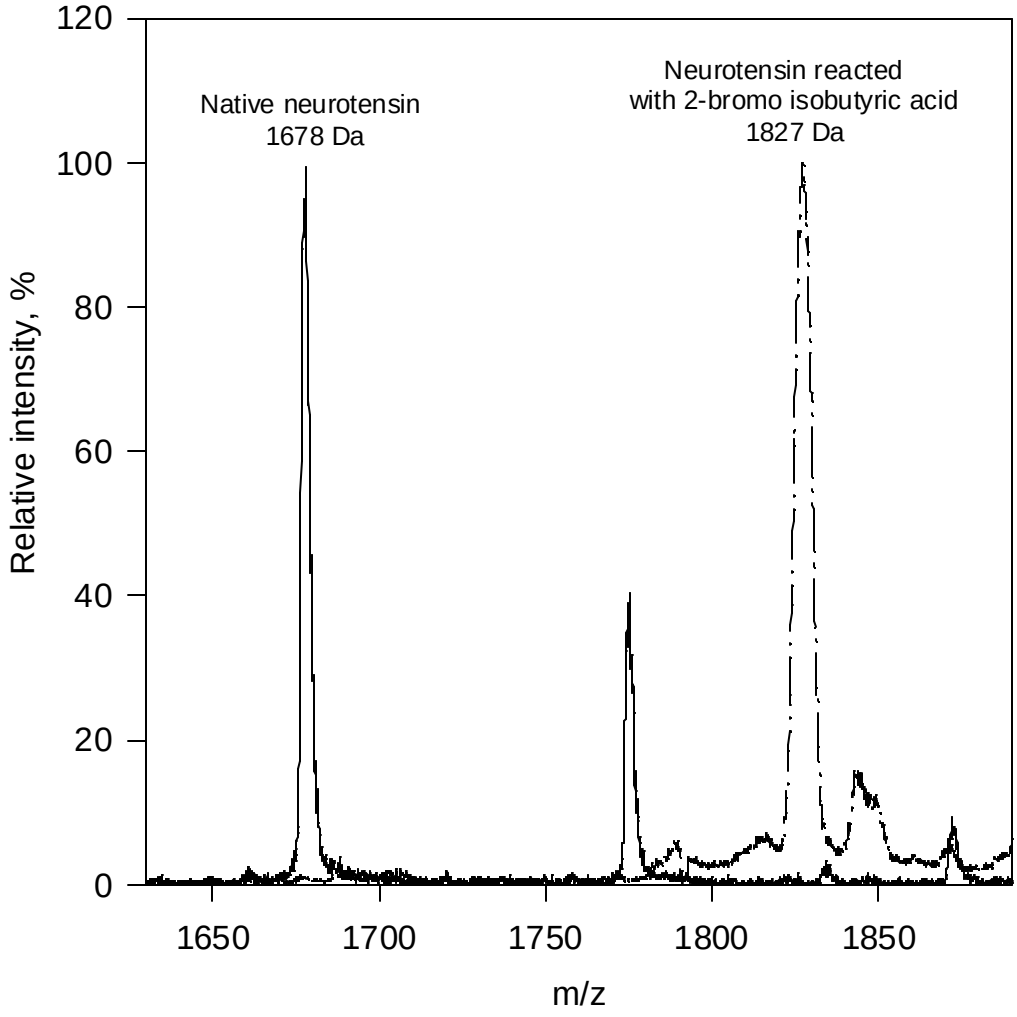

Figure 23 Coupling of neurotensin with 2-bromo isobutyric acid

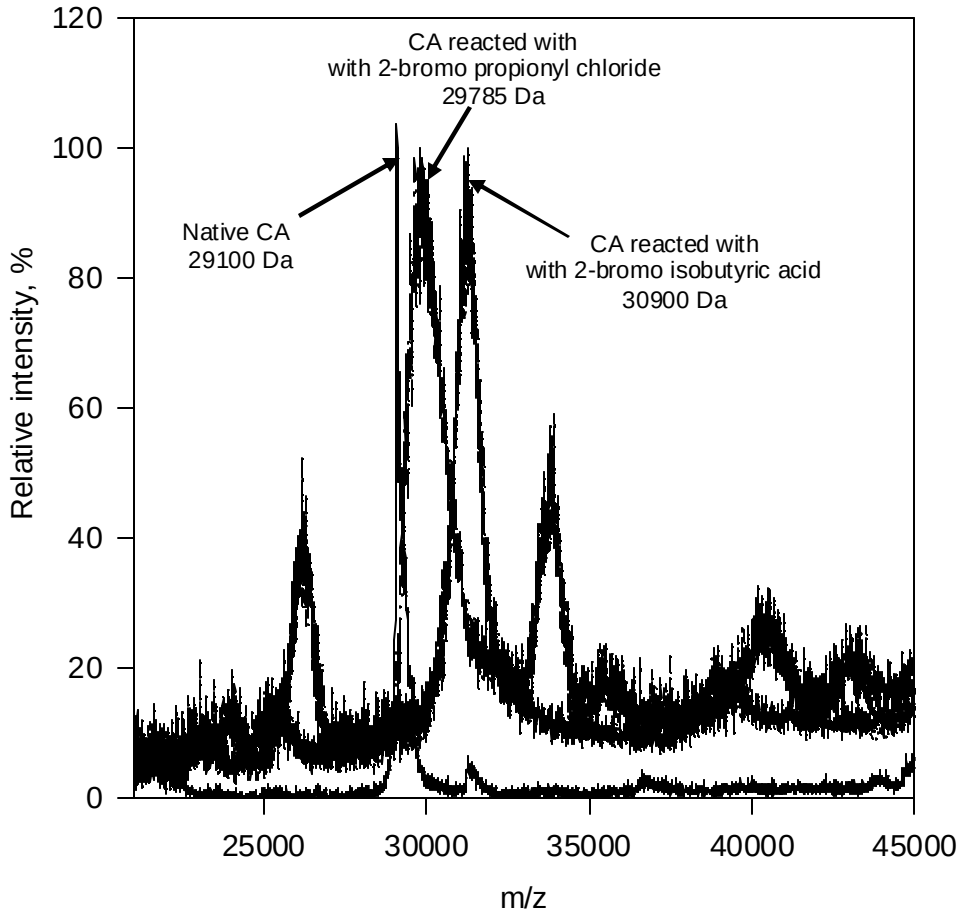

Figure 24 Coupling of CA with bromo-initiators

and inactivation (section 2.1.2.4). Conversely, NaSS tends to stabilize the enzyme, the effect being more pronounced at a 0.4 M monomer concentration (Table 9, Experiment 5). Stabilization was also observed in the presence of 0.4 mM $CuBr_2$ (Table 9, Experiment 4). Bpy did not seem to affect the enzyme stability (Table 9, Experiment 3). Clearly, among the reagents for ATRP, pyridine is of major concern since it provokes enzyme destabilization. However, the presence of this co-solvent is vital during the polymerization of NaSS and TMATf in homogeneous aqueous phase as it prevents the catalyst disproportionation by stabilizing the lowest oxidation state of copper.[248] Since the disproportionation of Cu^I in the absence of pyridine leads to low polymerization yields, it was decided to perform ATRP with the bio-macroinitiator in the presence of pyridine. [248]

5.3.3 Enzyme Immobilization

Both the polymerization of NaSS and TMATf occured in the presence of the bio-macroinitiator. For each reaction the bpy/(CuBr, $CuBr_2$), and bio-macrointiator/(CuBr, $CuBr_2$)/monomer molar ratios were fixed at 2/1 and 1/10/500, respectively. Given the high heterogeneity of bio-macrointiaitor populations, the biopolymers were expected to exhibit high polydispersities. No unreacted bio-macroinitiator was present after reaction, as shown by SDS gel electrophoresis. The characterization of biopolymers was performed by analytic ultracentrifugation. A molecular weight of 380 ± 76 kDa was found for bio-poly(TMATf). Bio-poly(NaSS)

was composed of two polymer species with molecular weights of 290 ± 58 and 45 ± 15 kDa, respectively. In both reactions, a high monomer to macroinitiator molar ratio was used. Given the extents of modification of CA with the halide initiators and the monomer and macoinitiator initial concentrations, the full consumption of monomers would give rise to polymer chains whith average molecular weights larger than 100 kDa. The observed polymer-enzyme final molecular weights are significantly smaller than what would be expected for full monomer conversion. The analysis with analytic ultracentrifugation confirmed that biopolymers were heterogeneous. Although the polymerization was successful, it led to the complete inactivation of the enzymic systems.

5.4 Conclusion

ATRP was applied to enzymatic macro-initiators, enabling the covalent and multi-point immobilization of enzyme within polymer matrices. The strategy followed was only partially successful, as no activity retention was obtained after polymerization.

Clearly, the reaction conditions during ATRP were not viable for enzymes, and need to be modified in order to prepare biopolymers with good catalytic efficiencies. The use of polar co-solvents is of major concern.

It has been reported that ATRP of amide-based monomers is often uncontrolled.[254] An explanation for the failure of ATRP with this category of monomers is the catalyst complexation with the amide functionalities.[255] Since

polypeptide chains contain numerous amide linkages, the enzyme primary structure may constitute a significant limitation for controlled living radical polymerization. The bio-macroinitiator was heterogeneous, and led to polydispersed biopolymers. Consequently, we could not address this problem and did not determine whether the polymerization was controlled.

Further study on the immobilization of enzymes via ATRP should include the optimization of the enzymatic activity reaction for the two selected polymerizations. The polymerization relies on the following independent parameters: the catalyst concentration, the macroinitiator concentration, the monomer concentration, the proportion of cosolvent, the reaction time and the reaction temperature. In order to optimize the immobilization process, the influence of each of these parameters on the polymerization and the enzyme activity retention should be determined using a two-level experimental design. The use of ATRP for enzyme immobilization could also be futher explored using non-ionic water-soluble monomers, which can be polymerized in aqueous buffer and under ambient conditions.

Table 9

Stability of CA in the presence of reagents for ATRP

Experiment	Pyridine (vol.%)	[bpy] (mM)	[$CuBr_2$] (mM)	[NaSS] (M)	$t_{0.75}$ (min)	k (min^{-1})
1	-	-	-	-	221	0.0013±0.0002
2	10	-	-	-	137	0.0021±0.0003
3	10	4.5	-	-	143	0.0020±0.0002
4	10	-	0.4		360	0.0008±0.0001
			4.8		125	0.0023±0.0006
5	10	-	-	0.4	719	0.0004±0.0001
				1.3	320	0.0009±0.0001

6.0 IMMOBILIZATION OF DFPASE INTO WATERBORNE 2K-PU-COATING

6.1 Introduction

Enzyme immobilization has been widely employed to enable and enlarge the use of enzymes as catalysts in industrial processes. Polymers such as polystyrene, polyacrylate, polymethacrylate, and polyurethanes have been shown to be viable matrices for the irreversible and multi-point immobilization of enzymes.[256,257] Biocoatings, prepared by following a similar strategy, could represent a powerful tool for the development of devices such as biosensors and biochips.

In this chapter, the immobilization of DFPase into waterborne polyurethane coatings was investigated. Since alterations in enzyme-containing coating (ECC) hydrophilicity could influence the activity retention and stability, the immobilization process was performed using polyisocyanates* with various hydrophilicities. The degree to which the enzyme was irreversibly attached to the support was determined. The enzyme distribution within the coating was observed by means of gold-labeling. A major concern was the influence of mass transfer on the activity of enzyme-coatings. Therefore, the mass transfers within coatings were examined using a diffusion cell apparatus, and the extent of internal diffusional limitations was evaluated. True and

* Polyisocyanates refer to polymers containing multiple isocyanate functionalities

apparent coating activity retention could be compared, and a non-conventional strategy could be developed to enhance the coating catalytic efficiency. The enhancement of DFPase thermostability via immobilization is also reported.

6.2 Material and Methods

6.2.1 Material

BAYHYDUR polyisocyanates XP-7063, XP-7007, XP-7148, BAYHYDROL polyol XP-7093, and Desmodur N3400 as well as thermoplastic polyolefin (TPO) panels, used in the synthesis and curing of protein-containing coatings were kindly provided by Bayer Corp. (Pittsburgh, PA). The surfactant BYK-345 was obtained from BYK-Chemie (Wallingford, CT). DFP, Bradford reagent, bovine serum albumin (BSA), BTP, Tris(hydroxymethyl)amino methane-HCl (Tris-HCl), $CaCl_2$, NaCl, K_2CO_3 and isopropanol were purchased from Sigma-Aldrich Chemical Co. (St Louis, MO). DFPase was purchased from BioCatalytics, Inc. (Pasadena, CA). Polybed 812 embedding resin was obtained from Polysciences (Warrington, PA)

6.2.2 ECC Synthesis

ECC's were prepared using buffered aqueous mixtures (10 mM BTP buffer, pH 7.5, 5mM $CaCl_2$). Waterborne two-component polyurethanes were synthesized using water-dispersible aliphatic polyisocyanates based on hexamethylene diisocyanate (HDI) BAYHYDUR and the polyol dispersion coreactants BAYHYDROL. During ECC

synthesis, a ratio between isocyanate and hydroxyl functionalities of 2 was used. Typically, BAYHYDROL XP-7093 (2.5 g) (water content of 70 w.%), BYK-345 surfactant (0.01 g) and buffered medium (1.2 g) were poured into a cylindrical vessel, and followed by the addition of enzyme (0.02-9 mg). The aqueous solution was further stirred mechanically (300 rpm) for 1 min. The amounts of BAYHYDUR XP-7063, XP-7007, XP-7148 required for ECC synthesis were calculated knowing the polyisocyanate equivalent molecular weights. When using XP-7007, the polyisocyanate (1 g) was added to the aqueous solution, and the biphasic mixture was agitated for 20 s with a custom designed head attached to a 2500 rpm hand held drill. After mixing, a white emulsion with a 63 w% water content was obtained, and applied (0.45 g) on thermoplastic polyolefin (TPO) panels previously cleaned with isopropanol and dried under ambient conditions. The ECC was then allowed to cure for 12 hrs under ambient conditions and weighed again (0.24 g).

BTP contains hydroxyl groups and secondary amines, which might react with the isocyanates during the coating synthesis. The amount of buffer salt added to the reaction mixture was negligible as compared with the reactive functionalities of the polyisocyanate and polyol dispersion, and, hence, did not affect the properties of the resulting two-component waterborne polyurethanes.

6.2.3 Protein Concentration Determination

Protein concentrations were evaluated using the Bradford reagent as described in the section 4.2.2.5.

6.2.4 Synthesis of Enzyme/Gold Conjugates

Gold colloids with diameters ranging from 25 to 30nm were prepared as previously described,[258] and conjugated to DFPase in aqueous medium.[259] During conjugation the pH was adjusted slightly above the enzyme isoelectric point (pI 5.8) with K_2CO_3. The pH was measured with litmus paper. Typically, an enzyme weight of 0.12 g was needed to stabilize 30 ml of gold colloid solution (gold concentration: 0.01 %). After addition of DFPase, the enzyme-gold solution was gently agitated, and bovine serum albumin solution (10 % (w/v)) was added to a final concentration of 0.1 % (w/v). BSA blocked areas of the colloidal surface that were not coated with the enzyme. The resulting solution was centrifuged for 1 hr at 100,000 rpm, and the enzyme-gold conjugate was recovered in the precipitate, which was resolubilized in buffered medium (10 mM Tris-HCl, pH 7.5). Centrifugation lead, to a certain extent, to the formation of gold clusters. The largest clusters were found in dense areas of the precipitate, which were discarded. Smaller clusters were still present among the colloidal gold conjugates. Coatings were further prepared with BAYHYDUR XP-7007 as described above using two different concentrations of colloidal gold conjugated to enzyme (0.001 $mg_{gold}/g_{coating}$ and 0.012 $mg_{gold}/g_{coating}$).

6.2.5 Localization of Gold-DFPase Conjugate in Coating

To embed the films for transmission electron microscopy (TEM), small strips were washed several times in 100 % ethanol then incubated in several 1 hr changes of Polybed 812 embedding resin. Films were cut into 1 mm x 2 mm strips, placed in embedding molds and embedded in Polybed 812. Blocks were cured overnight at 37 ^{o}C, then cured for two days at 65 ^{o}C. Ultrathin cross sections (60 nm) of the films were obtained on a Riechart Ultracut E microtome. Sections were viewed on a JEOL JEM 1210 or 100CX transmission electron microscope at 80 KV.

6.2.6 Activity of ECC's

ECC was assayed using pieces of peeled DFPase-film ranging in weight from 0.009 to 0.012 g. Typically, the pieces were placed in 10 ml of 3 mM DFP buffered solution (5 mM $CaCl_2$ and 10mM BTP, pH 7.5) and agitated by magnetic stirring. As DFPase acts by binding and hydrolyzing DFP, the activity was measured by following fluoride release with a fluoride ion electrode at room temperature. Fluoride bulk solution concentration was measured every 20 s for 5 min.

The enzyme concentration in the coatings were varied between 0 and 2 $mg/g_{coating}$. The ECC's with higher enzyme concentrations were too active for the initial velocities to be determined.

6.2.7 Determination of Kinetic Constants

The kinetic constants were determined by means of a fluoride sensor as described in the previous section. The substrate concentrations varied from 0 to 20 mM. The data were fit to the Michaelis–Menten equation using a non – linear regression (Sigma Plot Version 2).

6.2.8 Diffusion Cell Experiments

The diffusion apparatus is composed of a donor and a receptor compartment, each of them being equipped with a water jacket. The diffusion system was previously described in detail.[260] The ECC was mounted between the two compartments, and the experiments were conducted at room temperature (22 °C).

6.2.8.1 <u>Determination of Susbtrate Effective Diffusion Coefficient, D_{eff}.</u> The substrate effective diffusion coefficient, D_{eff} (m^2/min), was estimated by following the procedure developed by Page et al.[261] Urease was immobilized into the coating (3.6 $mg/g_{coating}$) to mimic the presence of DFPase. Initially, a 3 ml volume of buffered medium (5 mM $CaCl_2$, 10 mM BTP, pH 7.5) supplemented with DFP (4 mM) was placed in the donor cell, while the receptor cell was filled with buffered medium (3 ml). Each cell was well mixed by magnetic stirring. After a fixed period of time (5-300 min), the contents were removed and diluted 4 times with buffer medium (5 mM $CaCl_2$, 10 mM BTP, pH 7.5). The DFP concentration of each sample was then determined by an

activity assay with soluble DFPase. D_{eff} was based on the total area of the wetted coating (liquid and solid areas) and was calculated at quasi-steady state:[261]

$$[DFP]_R = \frac{D_{eff} A [DFP]_D}{V_{cell} d'} (t - t_0)$$

$[DFP]_D$ and $[DFP]_R$ are the DFP concentrations in the donor and receptor cell, respectively (mol/m^3). V_{cell} (3.10^{-6} m^3) and A ($6.36.10^{-5}$ m^2) are the cell volume and diffusion cross-section area, respectively. Assuming that the swelling of polyurethane film occurs predominantly in thickness, the thickness of wetted ECC, d', was estimated as follows:

$$d' = \frac{1}{1-e} d$$

The dry coating thickness, d (10 µm), was determined using scanning electron microscopy. ε (0.7) is the fraction of the total volume occupied by the liquid phase in the wetted coating.

6.2.8.2 <u>Activity Measurements.</u> The cells were filled with buffer (5 mM $CaCl_2$, 10 mM BTP, pH 7.5). The donor cell was initially supplemented with DFP (4 mM). The initial

DFP concentration in receptor cell was either 0 or 4 mM. The experiments were conducted using a fixed DFPase-ECC concentration (3.6 $mg/g_{coating}$), for which the substrate complete degradation occured on a reasonable time scale. Each cell was well mixed by magnetic stirring. After a fixed period of time (5-120 min), the contents were removed and diluted 4 times with buffer (5 mM $CaCl_2$, 10 mM BTP, pH 7.5). The DFP concentration of each sample was then determined by an activity assay with soluble DFPase.

Figure 25 is a schematic of the DFP concentration profile in the case of simultaneous diffusion and enzymatic reaction in the DFPase-containing coating when the receptor cell does not contain DFP at t=0 sec. If the diffusional resistance of boundary layer is neglected, the concentration profiles of DFP in the DFPase-ECC at unsteady state are given by the following equation. An outstanding derivation of these principles for the liquid phase was performed by Gray[262] and gives the following equation:[263, 264]

$$\frac{d[DFP]_{lc}}{dt} = \frac{D_{eff}}{e}\frac{d^2[DFP]_{lc}}{d^2x} - \frac{k_{cat,\text{int}}[DFPase]_{lc}[DFP]_{lc}}{K_{M,\text{int}} + [DFP]_{lc}}$$

$[DFP]_{lc}$ (mol/m^3) is the DFP concentration in the liquid phase in the coating. $k_{cat,int}$ (s^{-1}) and $K_{M,int}$ (mol/m^3) are the intrinsic kinetic constants for the ECC.

$\frac{D_{eff}}{e}$ represents the effective diffusivity of the substrate relative to the surface area of the liquid phase on the coating.

The initial conditions are as follows:

$$x = 0 \; and \; t = 0, \quad [DFP]_{lc} = 4$$
$$x \; (x \neq 0) \; and \; t = 0, \quad [DFP]_{lc} = 0$$

At the interface between the ECC and the donor cell we have:

$$\frac{d[DFP]_0}{dt} = \frac{AD_{eff}}{V_{cell}} \frac{d[DFP]}{dx}\Big|_0 - (V_{Surface} + V_{\mathrm{Re}\,lease})$$

Where $[DFP]_0$ represents the DFP concentration in the liquid phase at the surface of the ECC (x=0). $V_{Surface}$ (mol/(m^3.s)) represents the rate of DFP hydrolysis at the coating surface (x=0):

$$V_{Surface} = \frac{k_{cat,\mathrm{int}}[DFPase]_{Surface}[DFP]_0}{K_{M,\mathrm{int}} + [DFP]_0}$$

Where $[DFPase]_{Surface}$ (mol/m^3) is the number of moles of enzyme at the coating surface per unit volume of donor cell.

$V_{Release}$ (mol/(m^3.s)) corresponds to the rate of reaction catalyzed by the enzyme not covalently immobilized during the ECC synthesis and released in the donor cell :

$$V_{Release} = \frac{k_{cat,native}[DFPase]_{Release}[DFP]_0}{K_{M,native} + [DFP]_0}$$

Where $[DFPase]_{Release}$ (mol/m^3) is calculated with respect to the donor cell volume. $k_{cat,native}$ and $K_{M,native}$ are given in Table 10 (Experiment 1^{a*}).

Given the experimental DFP concentration profiles in donor and receptor cells the equation of diffusion was solved numerically using the boundary and initial conditions with Athena Visual Version 7.1.1. The intrinsic kinetic constants of the ECC, $K_{M,int}$ and $k_{cat,int}$ were then calculated.

6.2.9 Enzyme Modification with Desmodur N3400

DFPase-containing solution (1 ml)(50 mM MOPS, 5 mM $CaCl_2$, pH 7.5) was added to Desmodur N3400 (1 g), which is composed of the dimer and trimer of HDI.

The biphasic mixture was stirred at room temperature. The activity of modified enzyme was determined by means of a fluoride sensor as described previously.

Since the degree of DFPase modification could not be determined directly, the reaction of Desmodur N3400 and enzyme Lysine residues was mimicked using Bradykinin potentiator B, a low molecular weight peptide (1182.4 Da) containing one Lysine residue. The extent of Lysine modification was determined using MALDI-TOF for various reaction time (15 min to 17 hr) as described in sections 4.2.2.7 and 5.2.6.

DFPase modified with Desmodur N3400 was further immobilized into polyurethane coatings as described previously.

6.2.10 ECC Thermostability

Native and immobilized DFPase were added to buffer (10 mM BTP, 5 mM $CaCl_2$, pH 7.5) incubated at 65 ^{o}C, and assayed at room temperature in buffered media (10 mM BTP, 5 mM $CaCl_2$, pH 7.5) as described above.

The thermostability of dry ECC's was determined at room temperature. After fixed periods of storage under ambient conditions, the ECC samples were assayed for activity at room temperature in buffered media (10 mM BTP, 5 mM $CaCl_2$, pH 7.5) as described above.

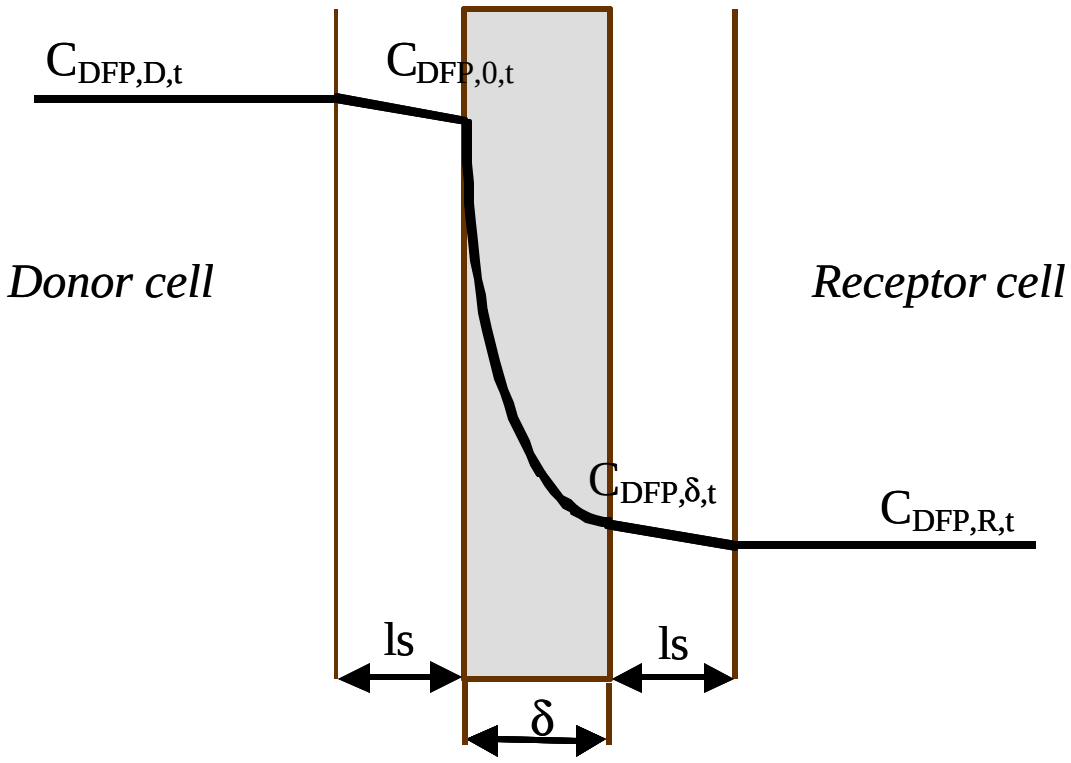

Figure 25 Schematic of the DFP concentration profile in the case of simultaneous diffusion and enzymatic reaction in the DFPase-containing polyurethane coating

ls, d' are the stagnant solution layer and the wetted coating thickness, respectively. $[DFP]_{D,t}$, $[DFP]_{R,t}$ are the bulk DFP concentrations at a time t in the donor and receptor cell, respectively. $[DFP]_{0,t}$, $[DFP]_{d,t}$ are the DFP concentration in the liquid phase of coating at the surfaces and at a time t.

6.3 Results and Discussion

6.3.1 Reversibility of DFPase Attachment to ECC's

The extent to which DFPase is irreversibly attached to the polymer was determined using the Bradford reagent. DFPase-containing polyurethane coatings were peeled from panels, cut into small pieces, and extensively rinsed with distilled water. Less than 4 % (w/w) of the protein loaded to the ECC was detected in the rinsates, indicating that the immobilization efficiency approached 100 %.

6.3.2 Enzyme Distribution in ECC's

When enzymes are incorporated into films, a key issue is whether the enzyme is equally distributed in the film. Gold labeling has been used to localize immobilized enzyme in polyurethane monolith foams.[265] Therefore, we decided to localize DFPase in ECC's via conjugation to colloidal gold particles. Figures 26A and 26B are micrographs of gold/DFPase conjugate-containing coatings obtained by dark field microscopy (0.001 $mg_{gold}/g_{coating}$) and inverse image light microscopy (0.012 $mg_{gold}/g_{coating}$), respectively. Gold/DFPase-containing coatings are analyzed using dark field microscopy (A; 0.0007 $mg_{gold}/g_{coating}$) and inverse (negative) images taken using light microscopy (B; 0.0116 $mg_{gold}/g_{coating}$). Cross sections of the coatings were obtained using Transmission Electron Microscopy (C and D). The arrows with filled heads show some of the gold/enzyme particles, while the arrows with emptied heads show some of the gold/enzyme conjugate clusters. The arrowheads indicate the extremities of coating

samples within the embedded resin. The stars designate some unfocussed areas as a result of high gold particle concentration and uneven surface. Bubbles in the coating are indicated by the letter h. As the concentration of immobilized colloidal gold/enzyme conjugate is increased by 12-fold it becomes apparent that the immobilized gold/enzyme complexes are uniformly distributed within the coating. The TEM's of the cross section of gold/enzyme-containing coating (0.012 $mg_{gold}/g_{coating}$) are given in Figure 26C (originally 2500-fold enlargement) and 25D (10,000-fold magnification). Similarly to light microscopy, TEM shows that the gold/enzyme particles and clusters are randomly distributed at the microscale level. This implies that the synthesis of gold/DFPase conjugate-containing coating leads to the homogeneous immobilization of gold/DFPase complexes in the polymeric matrix. By extrapolation one can predict that the DFPase local concentration in a film should not be location dependent.

6.3.3 Activity of ECC's

ECC's were prepared using the polyisocyanates XP-7007, XP-7148 and XP-7063. Figure 27 shows the activity of each ECC as a function of initial DFPase loading. The activity is directly proportional to the enzyme concentration, which implies that there is no significant mass transfer limitation. Since Figure 26 indicates that the films are non-porous, this result implies (as we will discuss in detail later) that only enzyme in a thin external layer of the film is accessible to substrate.

The hydrophilicity of polyisocyanate decreases in the order XP-7148>XP-7063>XP-7007. Interestingly, the apparent activity retention of ECC's increases as the

hydrophilicity of polyisocyanate decreases (Figure 27). Studies of enzyme activity in dehydrated organic solvents demonstrate that enzymes prefer hydrophobic environments. It may not be coincidental that less hydrophilic polyisocyanates are superior ECC materials.

The use of polyisocyanate XP-7007 generates ECC's with the highest levels of apparent activity retention, and thus subsequent experiments were performed with XP 7007-containing-ECC's.

The apparent kinetic characteristics calculated by assuming all the loaded enzyme is available (Table 10, Experiment 1^{b*}) lead to an observable activity retention (11 %) rather than intrinsic retention.

6.3.4 Effective Diffusivity of DFP in ECC, D_{eff}

Clearly, to understand activity retention in ECC's we must assess the diffusivity of the substrate in the film. D_{eff} was found to be $(5\pm 1)\times10^{-10}$ m^2/min (Figure 27). D_{eff} is two to three orders of magnitude lower than the diffusion coefficients of gases into liquids or organic solutes into hydrogels (**Error! Bookmark not defined.**266). Similarly, Buenfeld(267) observed high resistance of two-component waterborne polyurethane coatings to diffusion of chloride ions. The accessibility of enzyme located within the coating to substrate is clearly limited by the low coating permeability. Once again, this result indicates that the degree of penetration of DFP into coating should be taken into account in order to determine the activity retention of ECC's.

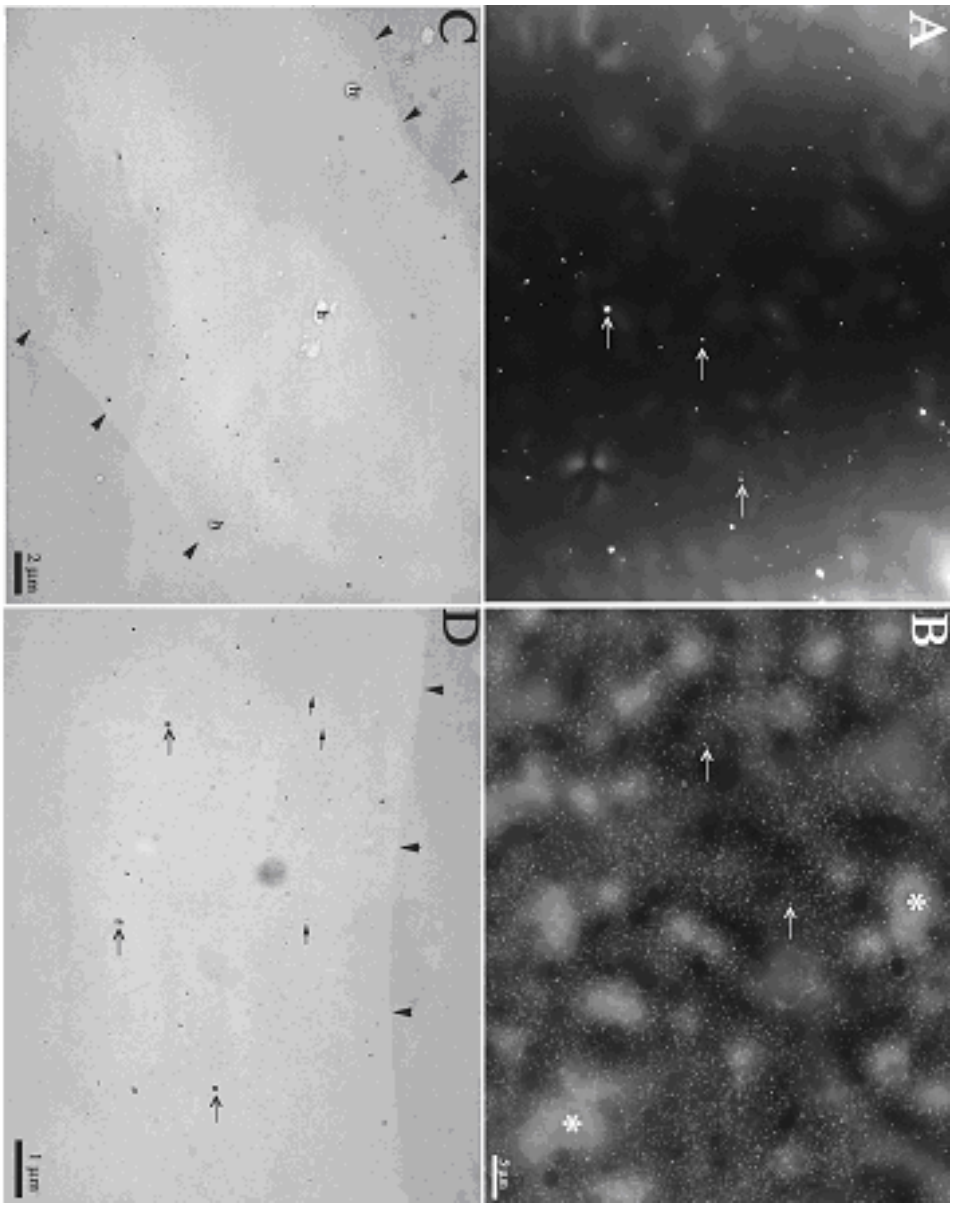

Figure 26 Enzyme distribution in polyurethane coating

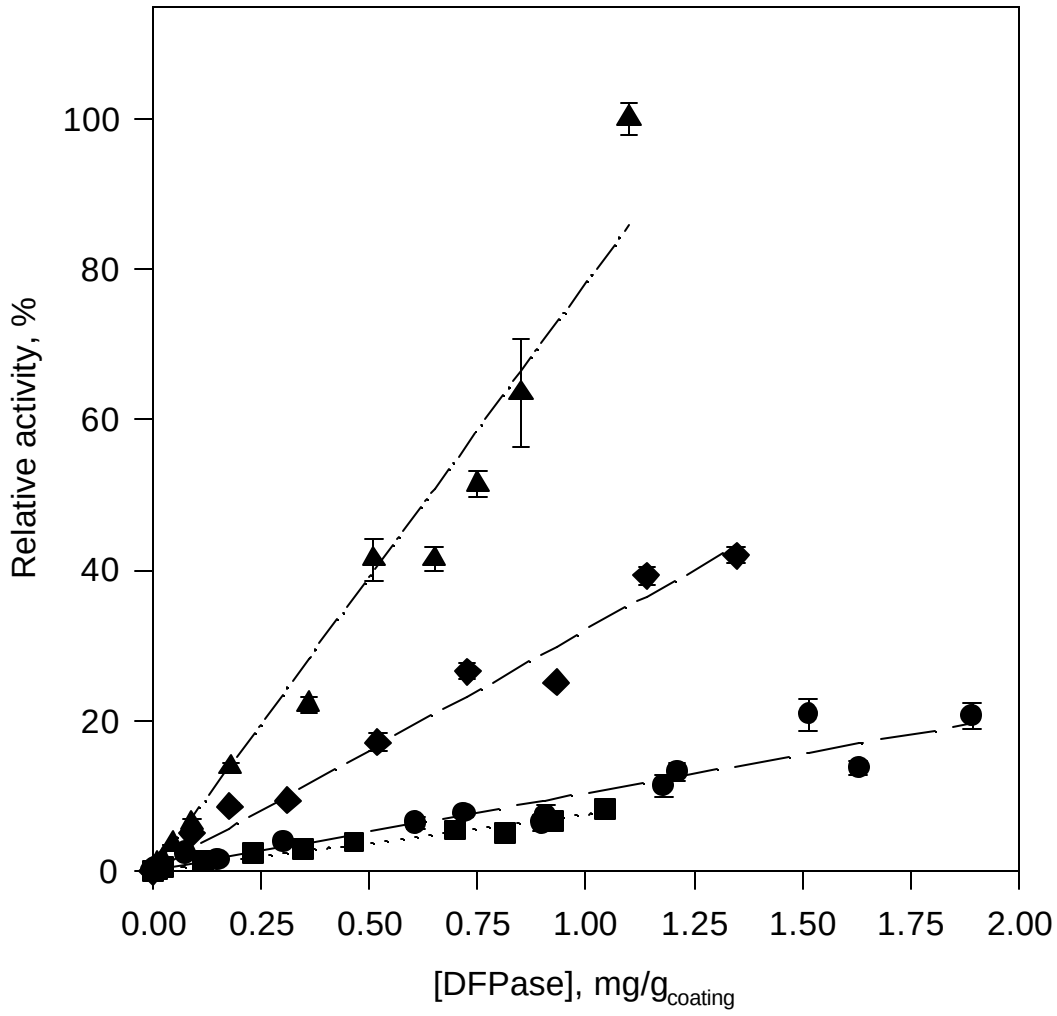

Figure 27 Effect of DFPase concentration on DFPase-containing coating efficiency

Coatings were synthesized with polyol XP-7093 and polyisocyanates XP-7007 (closed diamond), XP-7063 (closed circles) and XP-7148 (closed squares). The closed triangles correspond to the apparent activity of coatings synthesized starting from DFPase modified with Desmodur N3400, XP-7093 and XP-7007.

Figure 29 shows the profile for DFP concentration in donor and receptor cell over time when using a DFPase-ECC (3.6 $mg/g_{coating}$), and an initial concentration of 4 mM DFP in both cells. The profiles for the decrease in DFP concentration in donor and receptor cells follow similar trends. Assuming immobilized DFPase is homogeneously distributed in the coating (as implied in Figure 27), the enzymatic activity retention is therefore almost the same on both sides of coating. During curing, the ECC upper and lower surfaces are in contact with the TPO panel and exposed to air, respectively. As given by the little difference in activity retention of the ECC's external surfaces, the air interface and the polymeric/hydrophobic environment do not influence the ECC activity retention.

DFP concentration profiles in the donor and receptor cells were also measured for a DFPase-ECC (3.6 $mg/g_{coating}$) with no DFP in the receptor cell (Figure 30). The diffusion model describes well the experimental results (Figure 30a). The estimated intrinsic Michaelis constant of immobilized DFPase, $K_{M,int}$ (Table 10, Experiment 2^{b**}), is similar to that obtained without the diffusion apparatus (Table 10, Experiment 1^{b*}). Interestingly, by taking into account the coating resistance to substrate diffusion, $k_{cat,int}$ (Table 10, Experiment 2^{b**}) was found to be 2.4 times higher than the apparent $k_{cat,app}$ measured without the diffusion apparatus (Table 10, Experiment 1^{b*}). As shown by the simulated substrate profiles within the coating at different experimental times (Figure 30b), the substrate penetrates a third of the coating over the time course of the experiment. Clearly, the estimation of apparent kinetic parameters involves solely the

degradation of DFP in a layer of immobilized enzyme at the coating surface. Consequently, the apparent enzymatic efficiency of DFPase-ECC's is based on the activity retention of this external layer of immobilized DFPase. As given by the intrinsic kinetic constants of DFPase-ECC, the intrinsic activity retention within this layer is 38 %. The ratio of apparent to intrinsic k_{cat}, $R = \frac{k_{cat,app}}{k_{cat,\mathrm{int}}} = 0.4$, gives the proportion of immobilized DFPase in ECC's reachable by the substrate during activity measurements without the diffusion apparatus.

6.3.5 Desmodur N3400-Modified ECC's

The vigorous mixing of Bradykinin potentiator B-containing aqueous solution with Desmodur N3400 ensured the chemical modification of the peptide Lysine residue with the dimer of HDI, as observed using MALDI-TOF. A reaction yield fluctuating between 70 and 90 % was reached for a 15 min reaction time, and was not increased by further mixing of the peptide solution with the Desmodur N3400 phase.

Polyisocyanate Desmodur N3400 is based on the uretdione of HDI which is known to migrate from the bulk to the polymer/air interface during coating curing due to its low viscosity. By modifying DFPase with Desmodur N3400 prior to its immobilization into coatings, we expected the immobilized enzyme to be mainly concentrated within an external layer at the coating surface. Consequently, immobilized

Table 10

Kinetic parameters for DFPase-containing coatings and soluble DFPase

Experiment	K_M (mM)	k_{cat} (s^{-1})	k_{cat}/K_M ($s^{-1}.mM^{-1}$)
1[a*]; intrinsic native DFPase	0.79 ±0.02	232 ±2	293 ±3
1[b*]; apparent ECC	1.3±0.2	43±3	33±7
1[b#*]; apparent ECC	1.3±0.2	70±6	54±13
2[b**]; intrinsic ECC	0.96±0.01	102±1	106±2

The errors on specific constants were calculated as follows:

$$\Delta\left(\frac{k_{cat}}{K_M}\right)=\left(\frac{k_{cat}}{K_M}\right)\cdot\left[\frac{\Delta k_{cat}}{k_{cat}}+\frac{\Delta K_M}{K_M}\right]$$

[a]: native DFPase
[b]: polyurethane coatings
[*]: The kinetic parameters were evaluated by applying the Michaelis-Menten equation as a model and using a non-linear regression (SigmaPlot Version 2).
[#]: DFPase was modified with Desmodur N3400 prior to immobilization into polyurethane coatings.
[**]: The kinetic parameters were evaluated at room temperature in buffered media using the diffusion cell apparatus.

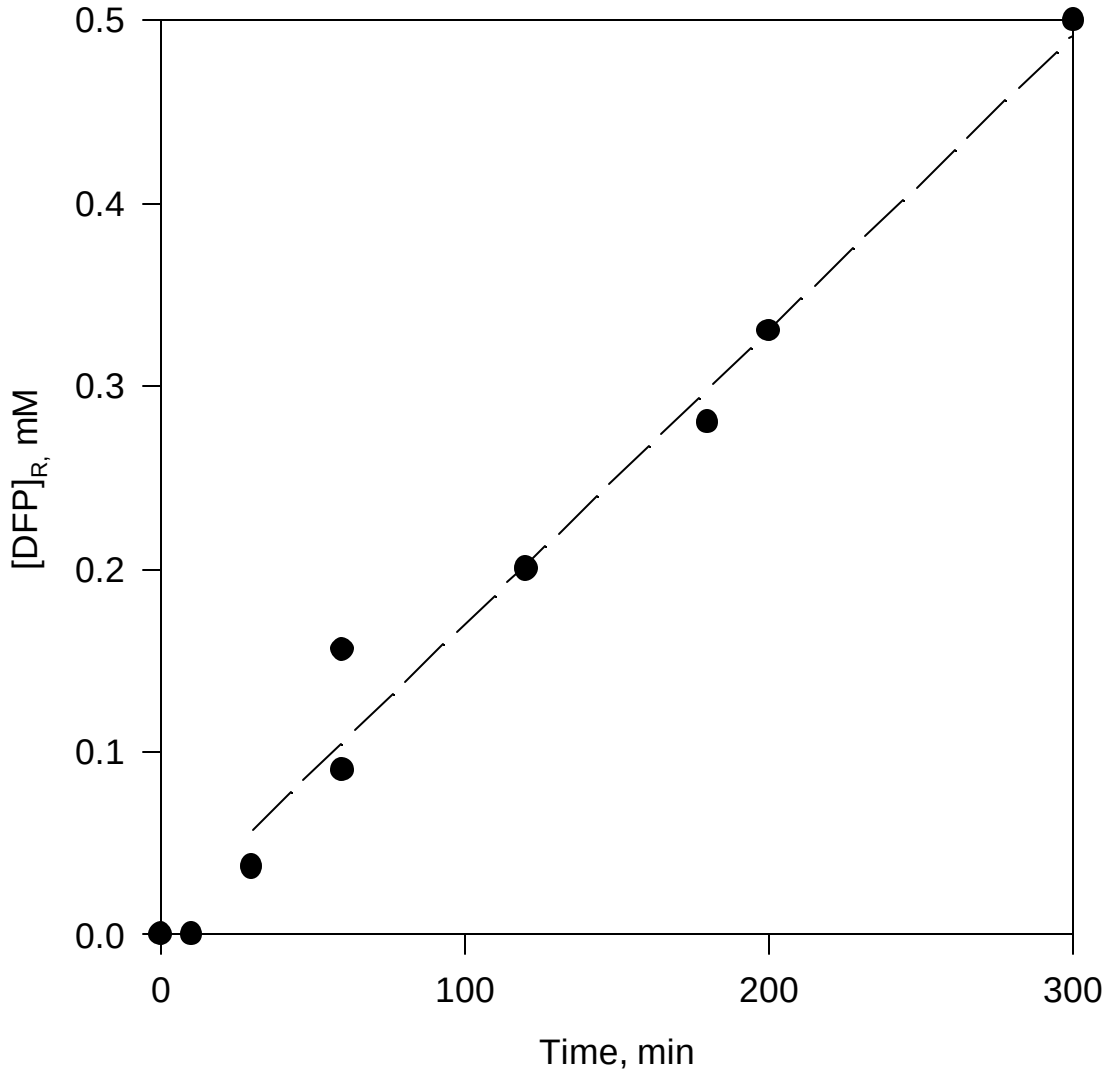

Figure 28 Effective diffusion of DFP through coatings

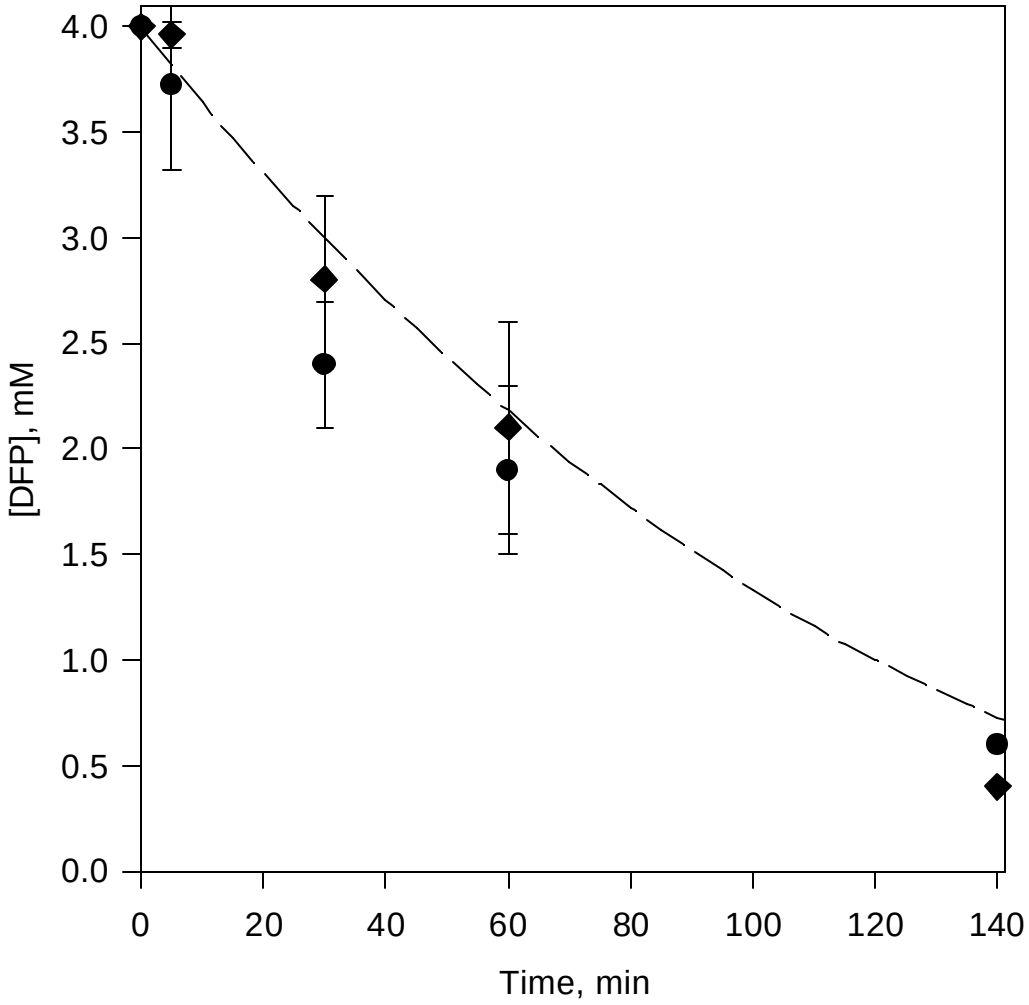

Figure 29 Profiles for DFP consumption in diffusion cells

The experiments were conducted using an initial DFP concentration of 4 mM in both donor and receptor cells. The DFP concentrations in donor (closed diamonds) and receptor (closed circles) cells were determined over time and compared to the simulated profile (dashed line).

DFPase would be well accessible to substrate, leading to an increased apparent activity retention. Given the fast favorable reaction between isocyanates of the dimer of HDI and the Lysine residue of Bradykinin potentiator B, DFPase was reacted with Desmodur N3400 for 15 min. No loss of enzymatic activity was observed. As shown in Figure 27 and Table 10 (Experiment 1b$^{\#*}$), the pre-treatment of DFPase with Desmodur N3400 produced a 64 % increase in apparent efficiency of ECC's. The increase in apparent efficiency may also result from the ability of the dimer of HDI to act as a surfactant. Therefore, the enzyme pre-modified with Desmodur N400 may be better dispersed into the coating than native enzyme and, hence, exhibit a higher activity retention.

6.3.6 Thermostability of ECC's

As explained in the previous section, not all the immobilized enzyme is seen by the substrate during activity measurement. Since the inaccessible enzyme does not interfere with rate determinations the thermal stability of the film can be determined without special consideration of diffusion resistances.

Unlike native DFPase, immobilized DFPase has a biphasic thermoinactivation profile at 65 °C (Figure 31). An elevated temperature of 65 ^{o}C was used to inactivate the enzyme in order to perform experiments on a reasonable time scale. For this range of incubation periods, the two-component polyurethane coatings did not dissolve significantly into the aqueous phase. Initially, the ECC follows a deactivation trend similar to that for native enzyme. This initial rapid deactivation leads, however, to the

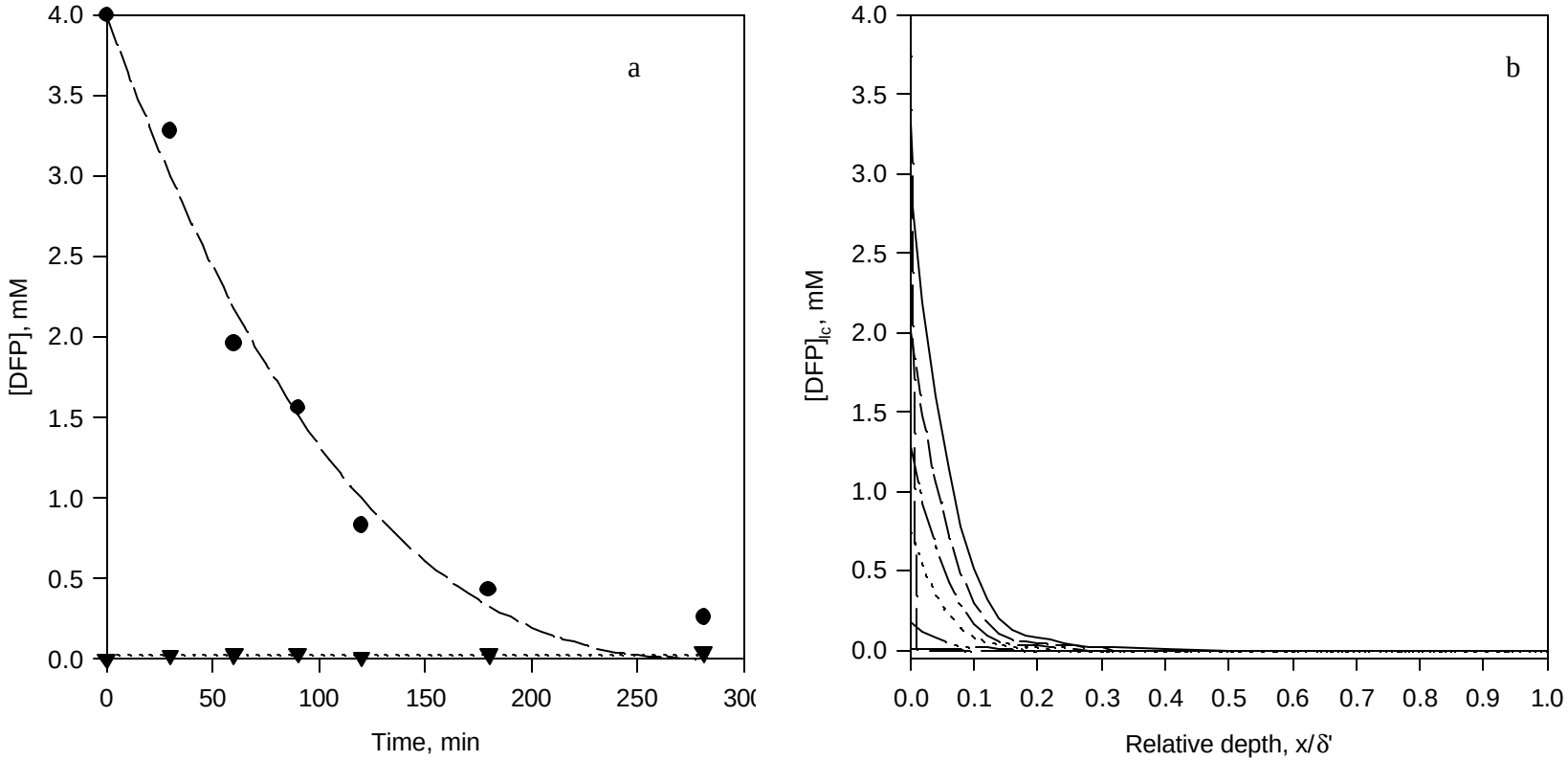

Figure 30 Profiles for DFP consumption in diffusion cells

a: DFP concentrations were measured over time ($[DFP]_{t_0 donor} = 4\ mM; [DFP]_{t_0\ receptor} = 0\ mM$) and simulated (donor cell: closed circles, dashed line; receptor cell: closed triangles, dotted line). b: The substrate profile in the ECC's was calculated at 0 (medium dashed line), 30 (solid line), 60 (small dashed line), 90 (dashed-dotted line), 120 (dotted line), 180 (dashed-dotted-dotted line) and 280 min (long dash line).

formation of a stable and active form of immobilized enzyme with a 6-7 % residual activity. No significant change in the activity of the highly stable form of the DFPase-ECC is observed over 350 min. The biphasic deactivation kinetics of the ECC can be modeled by the four-parameter model described in the sections 2.1.2.1 and 4.3.8, which assumes the following deactivation scheme :[5]

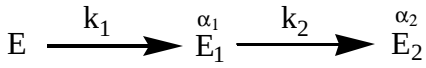

Another kinetic model assuming the existence of two different forms of DFPase in ECC's with different deactivation pathways, and requiring only four physical parameters did not adequately describe the experimental data. Further more complex mechanisms were not considered as they involved five or more parameters.[5]

The immobilization of DFPase in polyurethane foam and PEGylation also induced a transition from first order to biphasic inactivation kinetics. We believe that thermoinactivation of the DFPase-ECC results from structural changes similar to those described previously for the thermoinactivation of DFPase-containing polyurethane foam monoliths.

DFPase-ECC's exhibit a higher stability at room temperature than at 65 ^{o}C. Indeed, DFPase-ECC's lose only 40 % activity after 100 days of storage at room

temperature (Figure 32). Given the high stability of ECC's maintained dry under ambient conditions, the resulting catalyst should be an effective decontaminant for a variety of applications.

6.4 Conclusion

Covalent incorporation of DFPase into waterborne polyurethane coatings has been performed in a single step protein-polymer synthesis using polyol and polyisocyanates. The use of polyisocyanate XP-7007 and enzyme modified with Desmodur N3400 during the immobilization process leads to the highest intrinsic catalytic efficiency (with 18 to 38 % activity retention). At high temperature, DFPase-ECC's lose 93 % of their activity quickly, but then become hyper-stable.

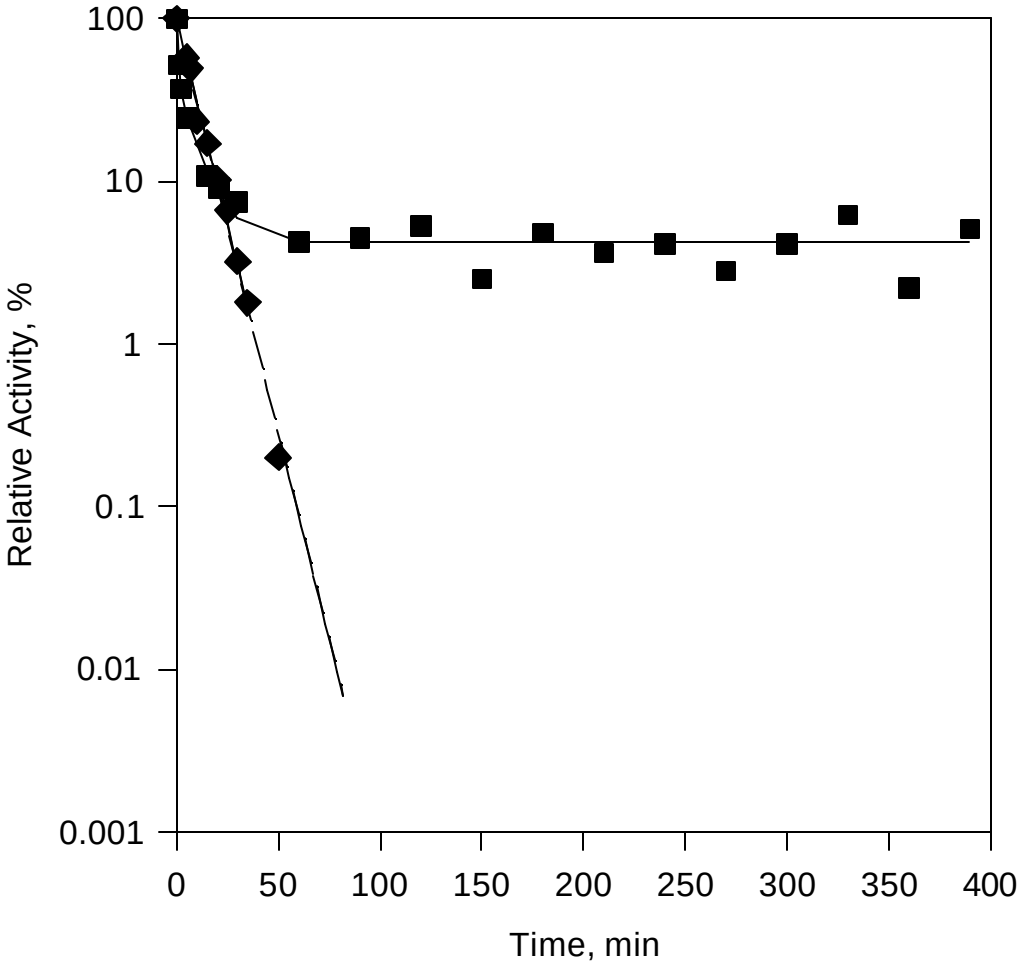

Figure 31 Thermoinactivation of DFPase-containing coating

Deactivation of immobilized DFPase (closed squares) and native DFPase (closed diamonds) was conducted at 65 ^{o}C. The biphasic behavior was described with a four parameter model (α_1 (0.34±0.03), α_2 (0.10±0.01), k_1 (1.3±0.1) and k_2 (0.042±0.003)).

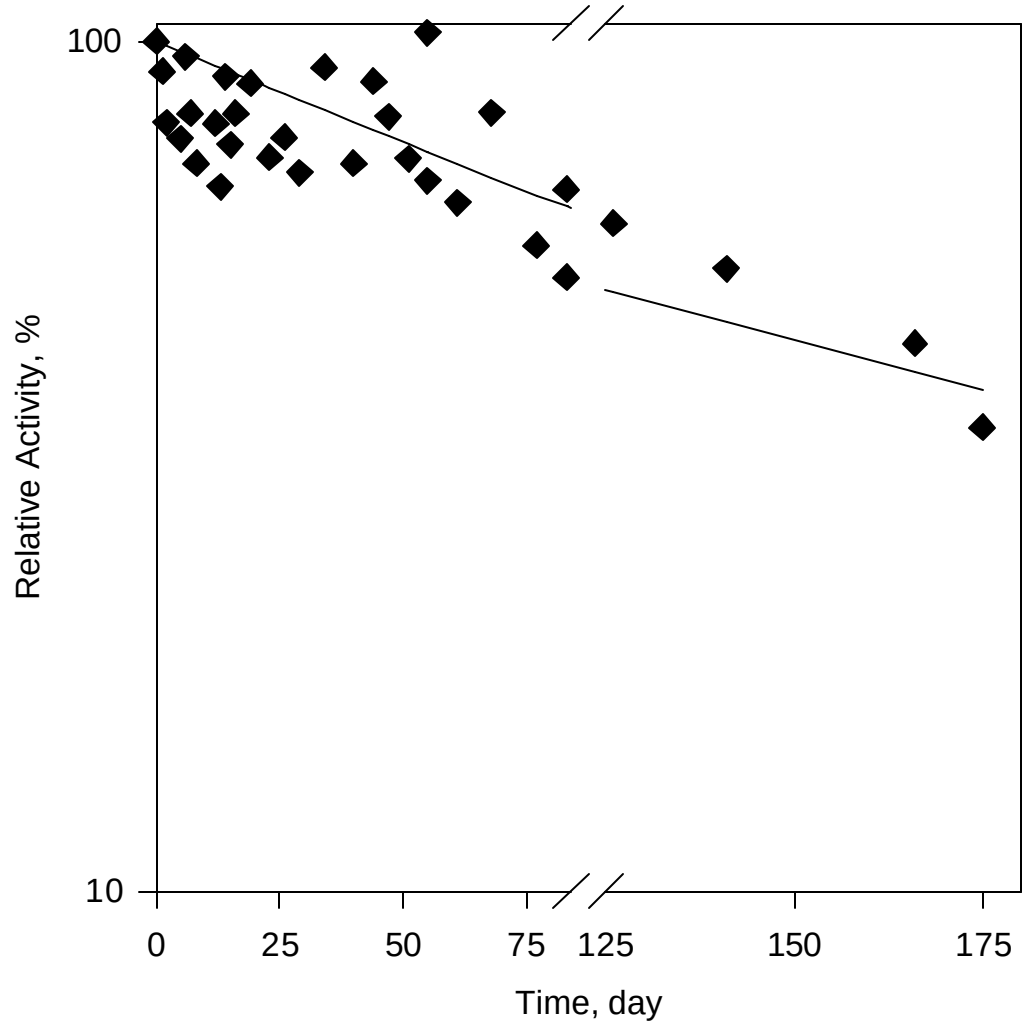

Figure 32 Thermoinactivation of DFPase-containing coating at room temperature

7.0 IMMOBILIZATION OF CA INTO MICHAEL ADDUCT-BASED COATING

7.1 Introduction

In the previous chapter, the covalent immobilization of the nerve agent-degrading enzyme DFPase into waterborne 2K-PU coatings was explored. The resulting enzyme-coating network combined high catalytic efficiency and attractive physico-chemical properties. Given these promising results, it becomes interesting to generate enzyme-containing coatings with other types of polymers.

In this chapter, the incorporation of carbonic anhydrase (CA, EC 4.2.1.1) into Michael adduct coatings was investigated. Native CA catalyzes the reversible hydration of carbon dioxide as well as the hydrolysis of various *p*-nitrophenyl esters.[244,245] To ensure the incorporation of CA into the hydrophobic coatings, the enzyme was modified with the Michael adduct derived from methyl acrylate (MANVF) and further polymerized with MANVF and N-vinyl-formamide (NVF) in aqueous phase (Figures 33 and 34). Native CA and other enzymes are not soluble in the MANVF prepolymer. The degree of modification of the enzyme and the kinetics of enzyme-polymer catalyzed reactions and biocatalyst stability were measured. Enzyme-containing coatings (ECC's) were prepared using the CA polymerized with NVF and MANVF (enzyme-polymer, EP), and the extent of enzyme leakage during activity cycles was determined.

7.2 Material and Methods

7.2.1 Material

An epoxy acrylate oligomer (Ebecryl 3700) and trimethylolpropane triacrylate (TMPTA-N) used in the synthesis and curing of Michael adduct-based coatings, were kindly provided by UCB Chemicals Corporation (Smyrna, GA). Tripropylene glycol diacrylate, (TRPGDA, SR306), and 1-hydroxycyclohexyl phenyl ketone, Irgacure 184, were obtained from Sartomer Company (West Chester, PA) and Ciba Specialty Chemicals Corporation (Tarrytown, NY), respectively. Carbonic anhydrase from bovine erythrocytes (EC. 4.2.2.1; CA; BCA II), *p*-nitrophenyl propionate, *p*-nitrophenyl chloroformate, bovine serum albumin, sodium phosphate mono- and dibasic, acetic acid, triethylamine, neurotensin, boric acid, acetonitrile, α-cyano-4-hydroxy-cinnamic acid, N-vinylformamide (NVF), methyl acylate (MA), sodium methoxide, and ethanolamine were purchased from Sigma-Aldrich Corporation (St Louis, MO).

7.2.2 Michael Adduct Synthesis

The Michael adduct, methyl 3-(N-vinylformamido)propionate (MANVF), was prepared as previously described (Figure 33; step 1). [268]

7.2.3 Synthesis of N—hydroxyethyl 3-(N-vinylformamido)propionamide

N—hydroxyethyl 3-(N-vinylformamido)propionamide was synthesized according to a procedure developed previously Pinschmidt et al. (Figure 33; step 2).[268]

7.2.4 Polymerization of CA with Michael Adducts

7.2.4.1 Activation of N—hydroxyethyl 3-(N-vinylformamido)propionamide. N—hydroxyethyl 3-(N-vinylformamido)propionamide was reacted with p-nitrophenyl chloroformate using the method of Veronese at al.,[269] leading to activated MANVF (Figure 33; step 3).

7.2.4.2 CA- and Neurotensin-MANVF. We followed the procedure initially described by Yang for the modification of enzyme with PEG-OH (Figure 33; step 4). [270] Typically, activated MANVF (70 mg) was added to a borate buffered solution (0.5 M, pH 8.5) containing the enzyme (50 mg). The enzyme and activated MANVF were present in a 1/100 molar ratio. The mixture was stirred at room temperature for 1.5 hrs, followed by dialysis against phosphate buffer (10 mM, pH 7.0) overnight at 6 oC, and lyophilization for 24 hrs on a Labconco freeze dryer 4.5 L. The neurotensin modification was performed in a similar manner.

7.2.4.3 EP Synthesis. CA-MANVF and NVF were polymerized in buffered aqueous media (10 mM phosphate buffer, pH 7.0) (Figure 34; step 1). Typically, NVF (0.2 g), MANVF (0.44 g), buffer (0.8 g), and the photoinitiator, Irgacure 184 (0.013 g), were

poured into a cylindrical vessel, and followed by the addition of CA-MANVF (0-15 mg). The aqueous solution was stirred until complete solubilization of the photoinitiator. The homogeneous mixture was further purged with oxygen-free helium for 30 min at ambient temperature prior to polymerization. Photopolymerization (10 min to 2 hrs) was then performed at room temperature under a helium atmosphere using a longwave ultraviolet lamp (Blak Ray model B100AP) for various period of time. A white emulsion was obtained and lyophilized overnight.

7.2.4.4 <u>ECC's Synthesis.</u> The Michael adduct-based coating formulation and curing were derived from the procedures described by Pinschmidt et al. (Figure 34; step 2).[271,268] Prior to coating synthesis the epoxy acrylate oligomer, Ebecryl 3700, was preheated to 50 ^{o}C, then, typically, Ebecryl 3700 (2 g), MANVF (2.7 g), NVF (0.44 g), TMPTA-N (0.44 g), and TRPGDA (0.44 g), Irgacure 184 (0.113 g) and buffer (0.59 ml; 10 mM phosphate buffer, pH 7.0) were poured into a cylindrical glass vial and mechanically agitated at 400 rpm for 15 min. The lyophilized EP (5-50 mg) was then added to the system and stirred mechanically at 400 rpm until a homogeneous mixture was obtained. After mixing, the latter was applied onto steel panels (Gardner Company, Pompano beach, FL) using a $^{\#}$3 drawing bar (Gardner Company, Pompano beach, FL), and cured with a longwave ultraviolet lamp (Blak Ray model B100AP).

Blanks were prepared by following the same procedure in the absence of enzyme.

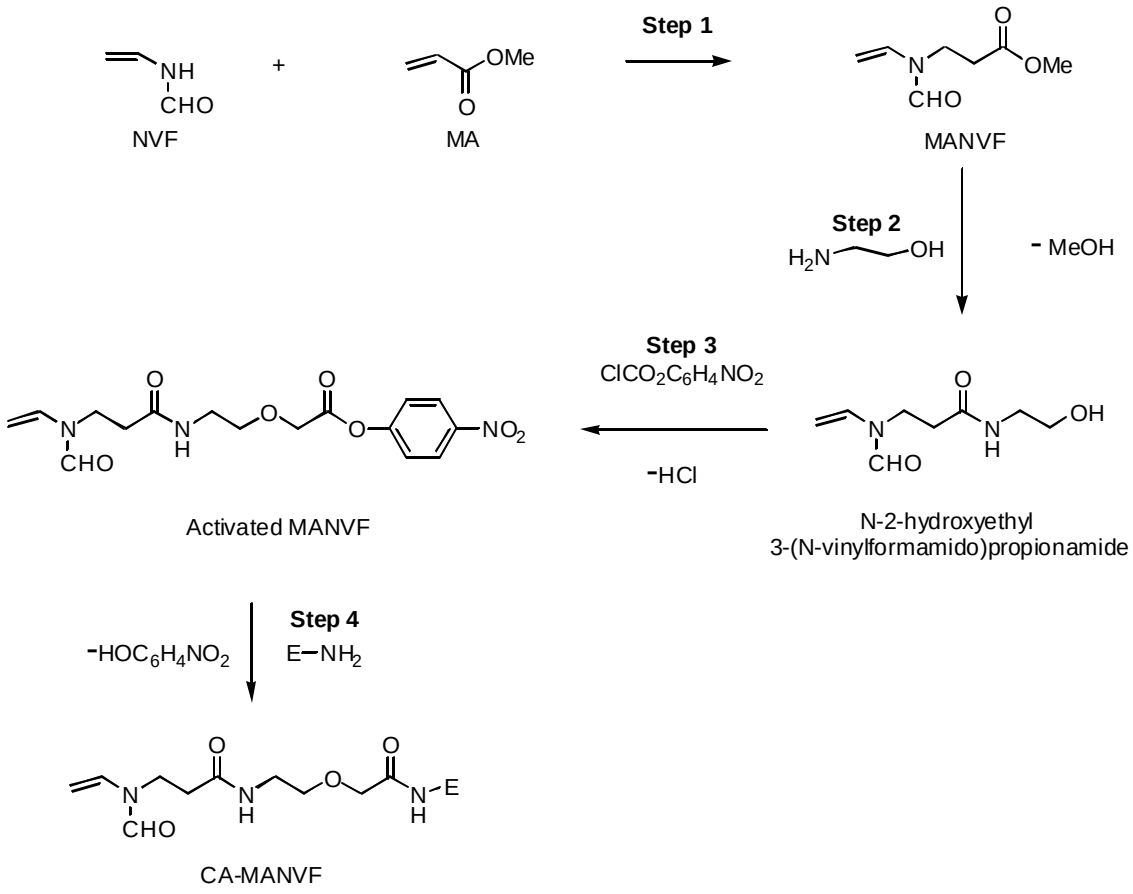

Figure 33 Diagram of enzyme modification with MANVF

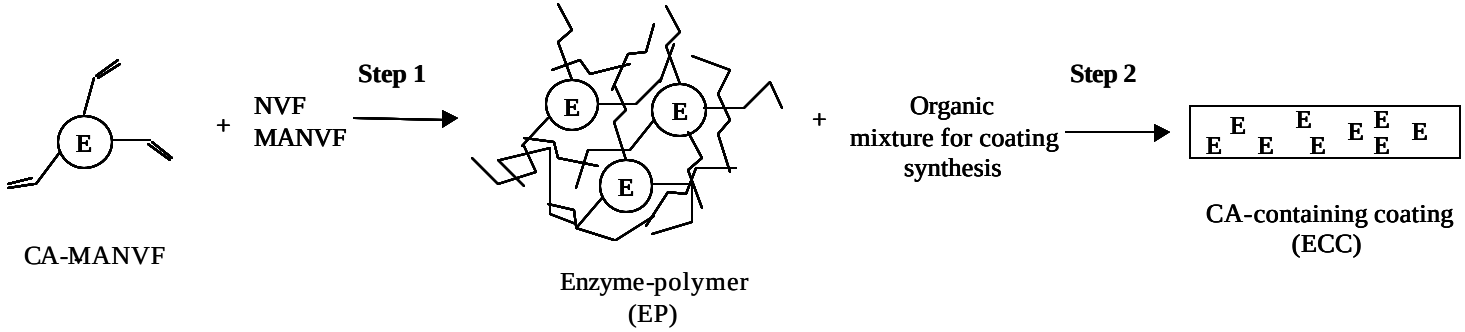

Figure 34 Steps leading to the preparation of ECC's

7.2.5 Immobilization of CA onto Coating Surface

7.2.5.1 Direct coupling Between CA and Coating Surface. The enzyme was immobilized onto the coatings via adsorption. Typically, the coatings were prepared as described above. After curing, the coating (2 g) was peeled off the panel, cut in small pieces and placed in a beaker containing a buffered solution (40 ml; 0.1 M phosphate or borate buffer, 7.5) and CA (2 mg/ml). The biphasic mixture was stirred magnetically for 1 hr at room temperature. The coating pieces were then recovered, washed extensively with buffered media (10 mM phosphate sodium, pH 7.5) and lyophilized overnight.

7.2.5.2 Immobilization onto Coatings by Glow-Discharge and Treatment with Glutaraldehyde. NVF-based coatings were glow discharged with ammonia using a MARCH glow discharge apparatus. The activation of glow-discharged coatings with CA was further performed using glutaraldehyde (Figure 35). The coating pieces were treated with glutaraldehyde according to the procedure described by Kim (Figure 35).[272,140] Typically, coating pieces (4 g) were stirred in the presence of buffered media (80 ml) (50 mM phosphate, pH 7.5) containing 2 % glutaraldehyde for 3 hrs at room temperature. After extensive rinsing with buffer, the coatings pieces were placed in buffer (80 ml) (50 mM phosphate, pH 7.5) containing CA (2 mg/ml) and stirred at room temperature for 3 hrs. The coating pieces were then recovered, washed extensively with buffered media (50 mM phosphate sodium, pH 7.5) and lyophilized overnight.

7.2.5.3 Immobilization onto Partially Hydrolyzed Coating. Coating pieces were incubated in basic media (1 N NaOH) at room temperature for 15 or 30 min under magnetic stirring. This treatment ensured the partial hydrolysis of formamide functionalities into primary amines.[268] Pieces of partially hydrolyzed coating were extensively rinsed and treated with glutaraldehyde and CA as described above (Figure 35).

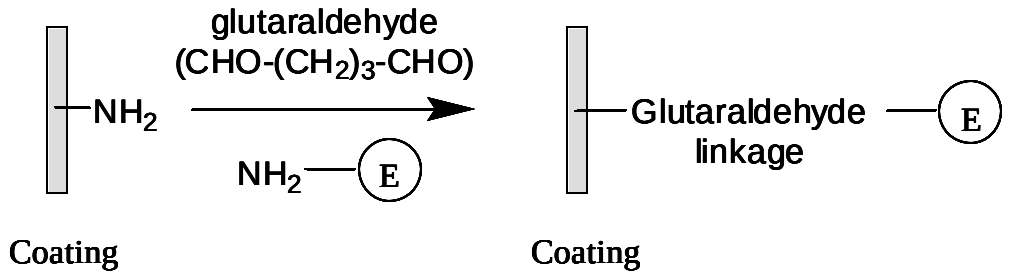

Figure 35: Coupling of the enzyme to the coating surface via Schiff's bases

7.2.6 Activity Assays

7.2.6.1 Native CA and EP's. CA wa assayed for activity as described in section 5.2.2.

7.2.6.2 ECC Activity. The activity of ECC was determined by an end-point assay using pieces of peeled CA-film ranging in weight from 0.11 to 0.13 g. Typically, the pieces were placed in 1.5 ml of 0.4 mM *p*-nitrophenyl propionate in 50 mM sodium phosphate, pH 7.5 and incubated at room temperature for 2 hrs with mixing (500 rpm). After the

incubation period, the 1.5 ml sample was centrifuged, the liquid phase was collected and its absorbance measured spectrophotometrically at 405 nm. Simultaneously, the end-point assay was performed in the presence of coating not containing CA following the same procedure. The absorbance resulting from the background hydrolysis was subtracted from that obtained with the ECC, yielding the rate of enzymatic hydrolysis.

The enzyme concentration in the coatings was varied between 0.05 and 1 $mg/g_{coating}$.

7.2.6.3 ECC Stability. Each sample was used for several cycles of activity measurement performed as described above. Between each assay, the sample was washed twice with buffer (1 ml). The experiment was performed simultaneously with ECC's and coatings not containing CA. At each cycle, the absorbance obtained with coating not containing CA was subtracted from that obtained with ECC.

7.2.6.4 Enzyme Kinetics. The substrate concentration was varied from 0 to 0.4 mM, and the activity assayed as described in the previous section. Given the low substrate solubility in buffer, higher concentrations could not be reached. Since the kinetic constant, K_M, was much higher than 0.4 mM, the enzymatic activity was directly proportional to the substrate concentration, and the resulting slope represented the enzymatic efficiency, $\frac{k_{cat}}{K_M}$.

7.2.6.5 Thermostability. Native CA and EP (0.1 mg/ml) were added to buffer (50 mM phosphate sodium, pH 7.5) incubated at 65 ^{o}C. The aliquots were removed from the incubation bath and placed on ice for 5 min after fixed periods of time (0-230 min). The aliquots were then restored at room temperature to equilibrate before their residual activity was measured as described above.

The thermostability of dry ECC's was determined at room temperature. After fixed periods of storage under ambient conditions, the ECC samples were assayed for activity at room temperature. Similarly, the thermostability of native CA in buffer (50 mM sodium phosphate, pH 7.5) was followed at room temperature.

7.2.7 Characterization of Neurotensin- and CA-MANVF

MALDI-MS analyses were performed with a Perseptive Biosystems Voyager elite MALDI-TOF. CA and neurotensin modifications were analyzed by following the procedure described in the sections 4.2.2.7 and, 5.2.6 respectively.

7.2.8 EP Characterization

7.2.8.1 Aqueous GPC. Solutions of native CA and EP (0.1 w%) were analyzed using an aqueous GPC Waters (Model 600E) equipped with a refractive index detector (Model 2410). A column Waters Ultrahydrogel 250 with a 300-mm × 7.8-mm-id was used. The internal temperature was held at 30 ^{o}C. Runs were performed using 50 µl

injection volumes, a flow rate of 0.8 ml/min, and a mobile phase composed of 90 % phosphate buffer (0.5 M, pH 7.5) and 10 % acetonitrile.

7.2.8.2 Analytic Ultracentrifugation. The procedure for the analysis of EP's with analytic ultracentrifugation is described in section 5.2.8.

7.3 Results and Discussion

7.3.1 CA and Neurotensin Modified with Activated MANVF

Neurotensin was used as a model peptide to demonstrate efficient modification of lysine by activated MANVF (Figure 33; step 4). MALDI-TOF shows an increase of molecular weight, which is predicted from complete modification as described in Figure 33 (step 4) (1,675 Da increasing to 1,887 Da). Similarly, the degree of modification of CA was 100% (no native enzyme remained) with an average of three to five MANVF chains attached per molecule of enzyme. No loss of enzymatic activity was observed upon modification. Since a broad distribution in degree of modification is obtained with CA, we predicted that the synthesis of CA-containing polymers from this prepolymer would yield high polydispersity products.

7.3.2 Activity and Stability of EP

The photopolymerization of CA-MANVF with NVF and MANVF led to the formation of a white gel (EP). As shown in Figure 36, native CA placed under the UV lamp does not undergo any significant activity loss for incubation periods shorter than 80 min. A

substantial activity loss is observed during photopolymerizations in excess of 1 hr. Traces of CA activated with MANVF are still present in the gels obtained after reaction for 10 and 20 min, as determined by MALDI. Longer reaction times ensured that all the enzyme was polymerized within NVF-based polymer, as shown using MALDI and GPC (data not shown). To minimize the activity loss induced by UV light during the photopolymerization process, the time of UV exposure was maintained at 1 hr for further experiments. Analytical ultracentrifugation is a rarely used tool for the analysis of such modifications, but it yields quick and direct results. While in sedimentation rate experiments CA alone showed a single sedimenting species, EP, as expected, exhibited a broad distribution of differently sedimenting species representative for a broad molecular weight distribution. Sedimentation diffusion equilibrium experiments gave a molecular weight of 27 ± 5 kDa for native CA and an average molecular weight of 36 ± 9 kDa for EP.

The catalytic efficiency of immobilized BCA II (bovine carbonic anhydrase purified from red cells) highly depends on the support properties and the type of coupling that links the enzyme and the matrix.[273] For example, BCA II physically absorbed onto colloidal gold retained 70 % of its native activity.[273] When BCA II was encapsulated in sol-gel derived monolith, it lost at least 99 % of its original activity.[274] By comparison, EP is highly active retaining 86 % of the activity of native enzyme (Table 11, Experiments 1^* and 2^*). This activity retention exceeds those observed for a number of other enzymes immobilized into photocurable hydrogels using similar techniques. For example, phosphotriesterase (OPH, EC.3.1.8.1) covalently incorporated into

polyethylene-based hydrogels by photopolymerization exhibited less than 1 % activity retention.[275] The activation of β-glucosidase with itaconic anhydride and subsequent co-polymerization with N,N'-methylenebisacrylamide had less dramatic inactivation effects and led to 33 % catalytic efficiency.[209]

Enzyme thermostability was studied at an elevated temperature of 65 ^{o}C in order to perform experiments on a reasonable time scale. Both native enzyme and EP displayed first order deactivation profiles with half lives of 43.9 and 21.2 min, respectively (Figure 37). Similar deactivation kinetics were observed for native CA by Azari.[276] We found that EP was more unstable than the native enzyme. During the themoinactivation of EP at 65 ^{o}C the immobilized CA was surrounded by NVF-based polymer, which represented 4 (w/w)% of the total buffered media content. To determine whether the decrease in enzyme thermostability resulted from non-covalent interactions between the polymer support and CA, we followed the thermoinactivation of native CA in the presence of NVF-based polymer. To enable direct comparison between native enzyme and EP, the thermostability of native CA was assessed in buffer containing 4 (w/w)% NVF-derived polymer. As shown in Figure 37, the presence of the polymer highly destabilizes the native enzyme decreasing the half-life to 5.9 min. The 21.2 min half-life of EP implies that the multi-point and covalent modification of CA by NVF prevents excessive destabilization by free NVF-based polymer.

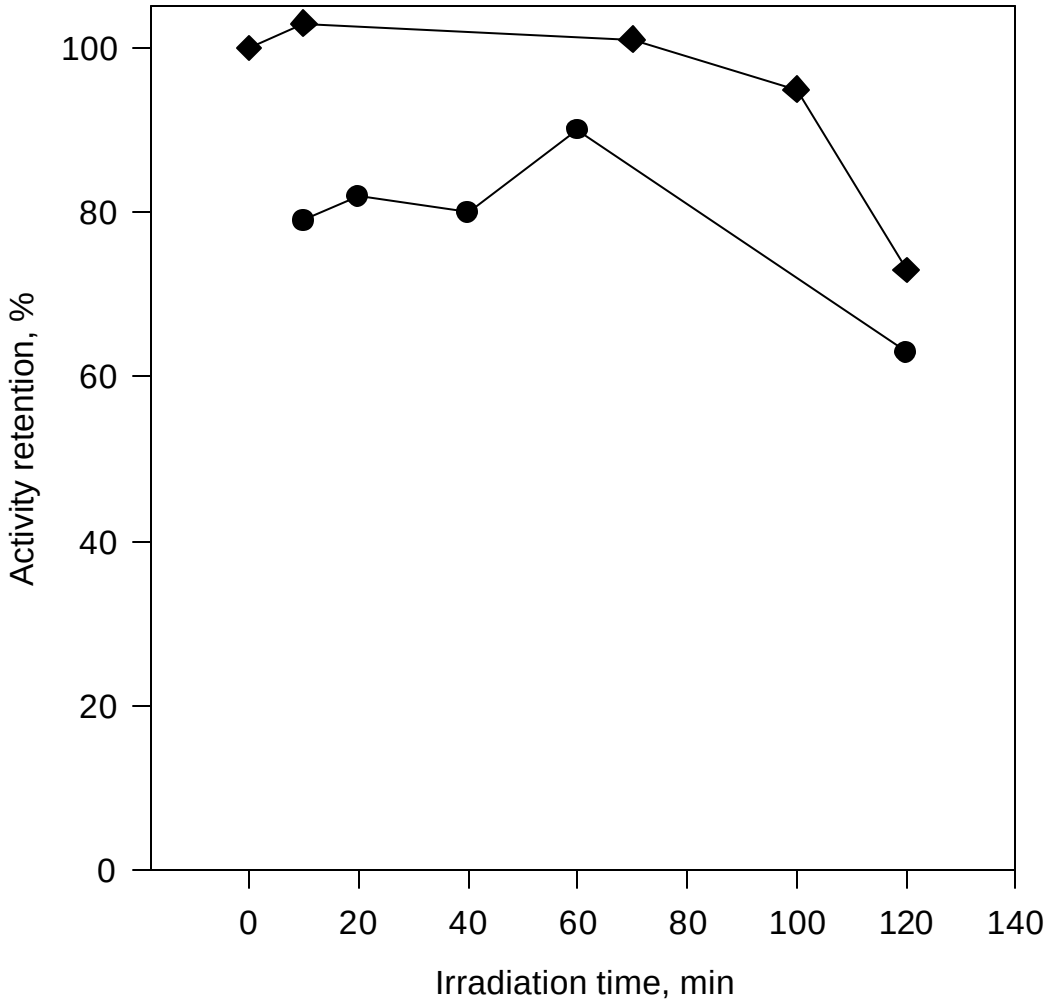

Figure 36 Effect of UV irradiation time on the activity of native CA (closed diamonds) and on the apparent activity retention of EP's (closed circles)

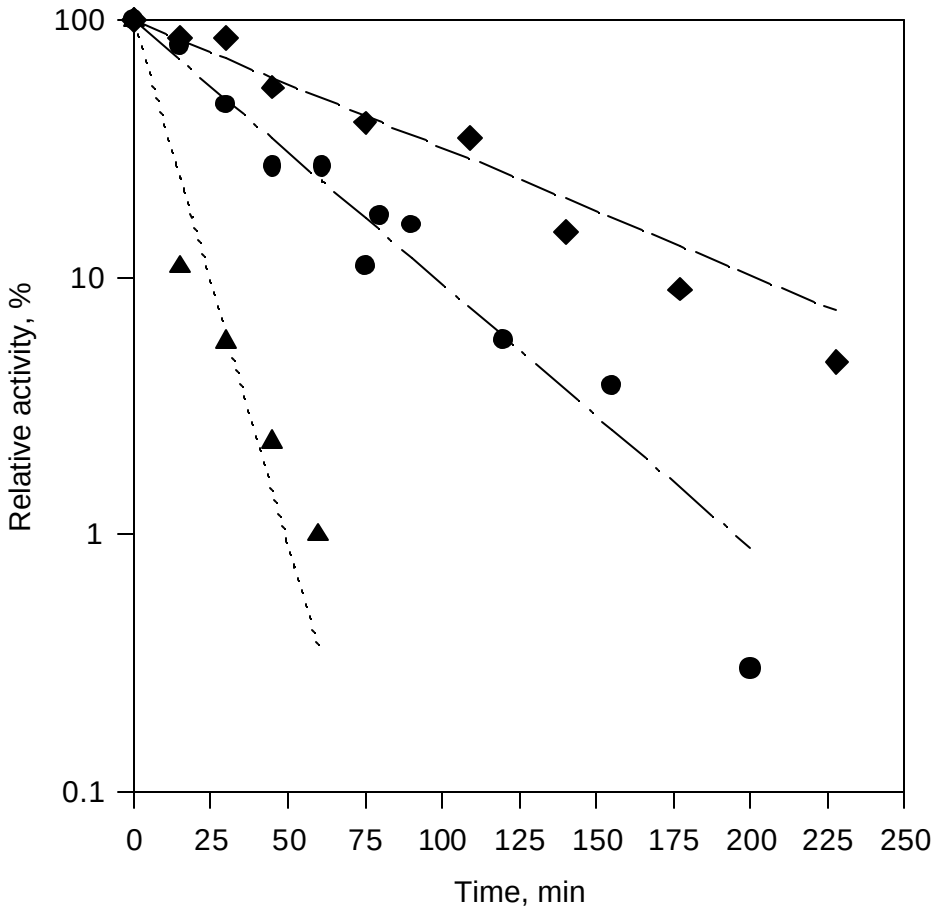

Figure 37 Thermoinactivation of native CA and EP at 65 ^{o}C

Deactivation of native CA was conducted in the presence NVF-and MANVF-derived polymer (4 w%) (closed triangles) and in the absence of NVF-and MANVF-derived polymer (closed diamonds). A 4 w% content of NVF-and MANVF-derived polymer was present during the deactivation of immobilized CA (closed circles).

Table 11

Kinetic parameters for CA immobilized into NVF- and MANVF-derived polymer, ECC's, and native CA

Experiment	k_{cat}/K_M ($min^{-1} mM^{-1}$)	V_{max}/K_M ($\frac{1}{min\, g_{coating}}$)
1[a]; native CA	3.70 ±0.05	-
2[a]; CA incorporated into NVF- and MANVF-derived polymer	3.2±0.1	-
3[b]; ECC	0.26±0.03	4.9±0.6[c]
4[b]; formamide based coatings	-	0.3±0.1
5[b]; glow discharge/glutaraldehyde coatings	-	0.14±0.03
6[b]; short hydrolysis/glutaraldehyde coatings	-	1.4±0.1
7[b]; long hydrolysis/glutaraldehyde coatings	-	56±3

[a]: The initial velocities were determined by following spectrophotometrically (405nm) the product release over 5-15 min at room temperature. [b]: The activity was determined spectrophometrically by end-point assay. [c]: The activity of ECC's is a function of the loading in EP. The highest activity was obtained at [EP]=0.81 $mg/g_{coating}$.

7.3.3 Activity of ECC's

Attempts to disperse native enzyme in the hydrophobic blend used for casting thin films of NVF type polymers resulted in agglomeration of enzyme particles. To ensure the uniform incorporation of enzyme into the Michael adduct-based coatings, EP was used since it was soluble in the organic mixture. ECC's were synthesized as described above and Figure 38 shows the activity of the final film as a function of initial EP loading. The activity is directly proportional to the enzyme concentration, implying that the activity of the immobilized enzyme is not significantly limited by internal mass transfer. Since the Michael adduct-derived coatings are highly cross-linked and non-porous, the enzyme on the interior of the film may not be available to react with substrate (Figure 39).

The extent of enzyme leakage during activity cycles was assessed as shown in Figure 40. Activity loss is mainly observed over the first three activity cycles, for which it fluctuates between 10 and 20 % per cycle. A total activity loss of 46 % was recorded after six activity cycles (12 hrs of incubation in fresh buffer). Similar degrees of leaching have been observed for other enzyme-containing coatings.[141,185] For example, biocatalytic coatings prepared by entrapping α-chymotrypsin into poly(vinyl acetate) were shown to lose 50 % of their activity after 6 reuse cycles.[141] Activity loss was minimal for the subsequent activity cycles.[141]

An observable activity retention of 7 % was calculated (Table 11; Experiment 3**). The efficiency of biocatalytic coatings can significantly fluctuate depending on the

enzyme and the polymer properties. For example, the entrapment of flavin reductase into pyrrole-based coating was reported to lead to 0.13 % activity retention,[161] whereas lipase entrapped into poly(propylene glycol) based coatings exhibited up to 81.6 % activity retention.[186]

7.3.4 Immobilization of CA onto Pre-Formed Coatings

We were interested in comparing the direct incorporation of EP into an ECC to the reaction of CA with an activated pre-formed film. The adsorption of CA onto the coating surface results in films with a the catalytic efficiency ($\frac{V_{max}}{K_M}$)of $3\times10^{-4} \pm 1\times10^{-4}$ $min^{-1}g_{coating}^{-1}$ (Table 11; Experiment 4). By comparison, the apparent efficiency of ECC's is 16 times higher ([EP] = 0.81 $mg/g_{coating}$). The entrapment of enzyme within polymer matrix is a more effective strategy.

An alternative approach is to modify the film with a reactive group prior to exposure to enzyme. We therefore generated primary amines at the coating surface by glow discharge or partial hydrolysis (as described above) prior to coupling to the enzyme via a glutaraldehyde spacer. Glow-discharged coatings reacted poorly with CA, and the resulting film displayed little enzymatic activity (Table 11; Experiment 5). A 15 min partial hydrolysis followed by glutaraldehyde linked immobilization of CA did yield a film with 5 times higher activity than the formamide based film (Table 11; Experiment 6). Further partial hydrolysis of the film (30 min) gave a particularly effective film

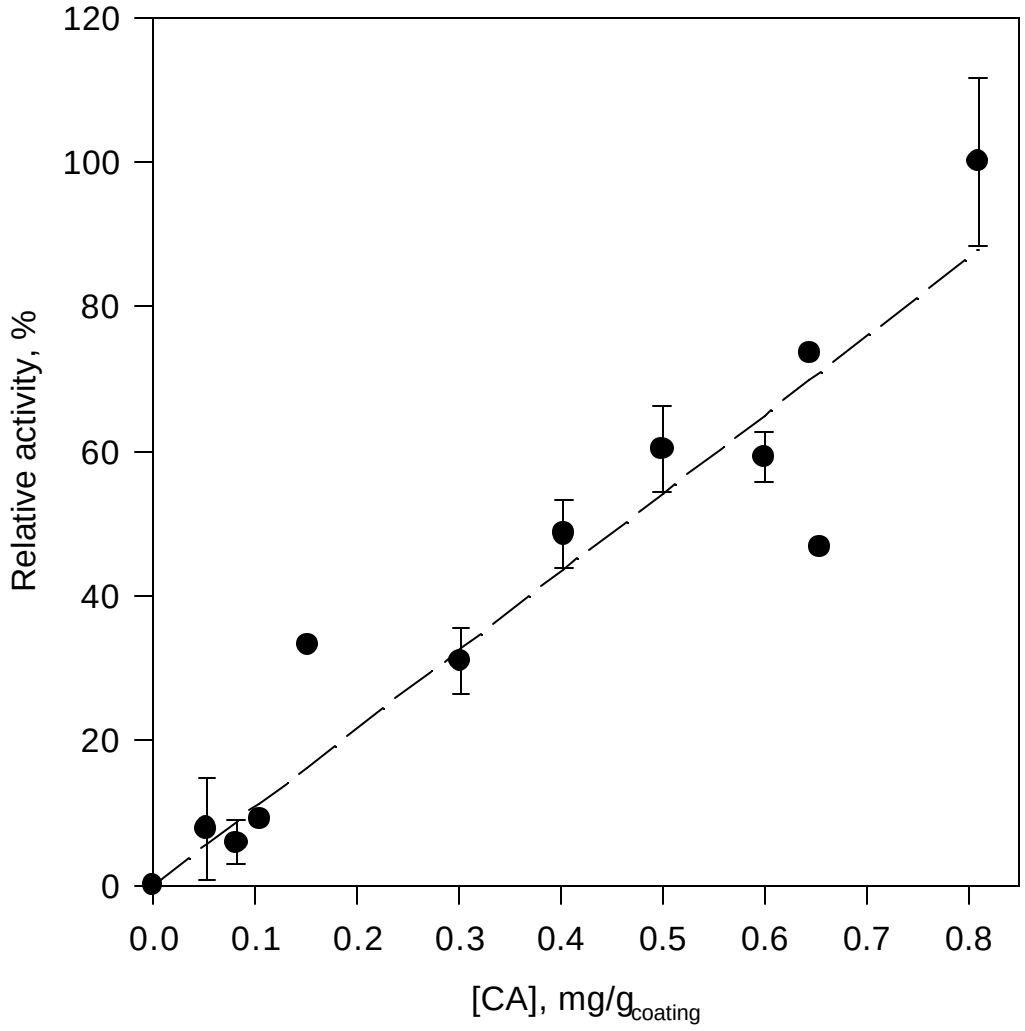

Figure 38 Effect of CA concentration on CA-containing coating apparent efficiency

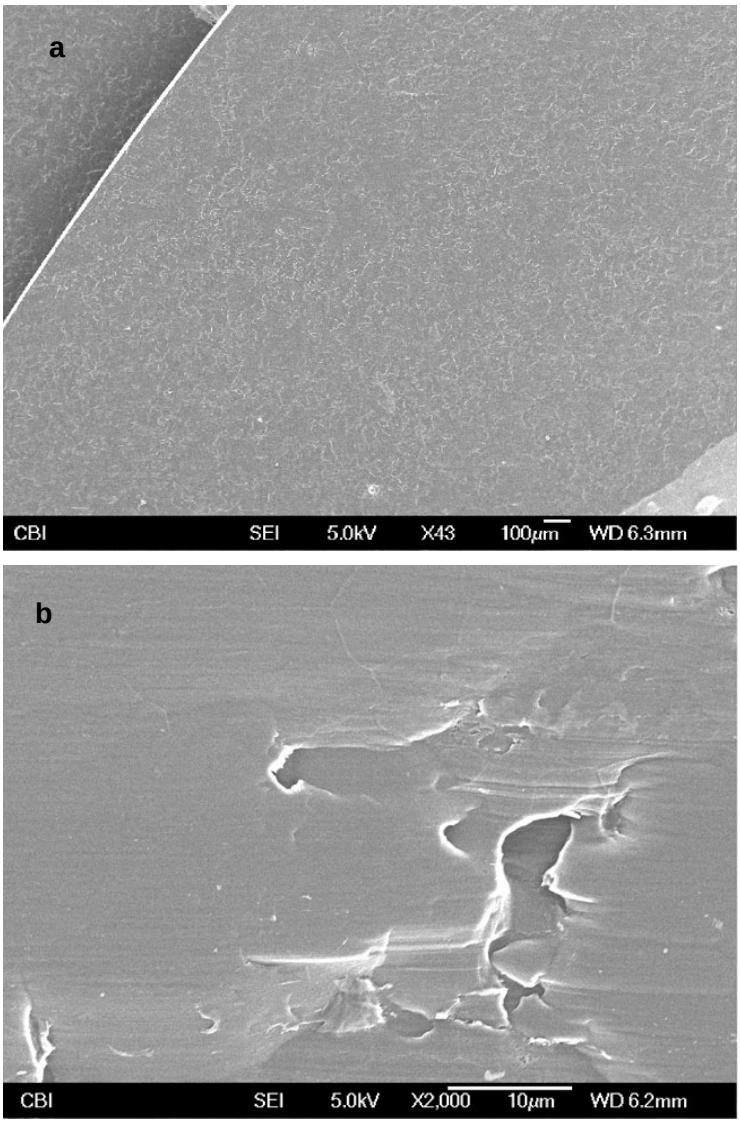

Figure 39 Electron micrographs of Michael adduct derived-coatings

43- and 2000-fold magnifications was used for figures a and b, respectively.

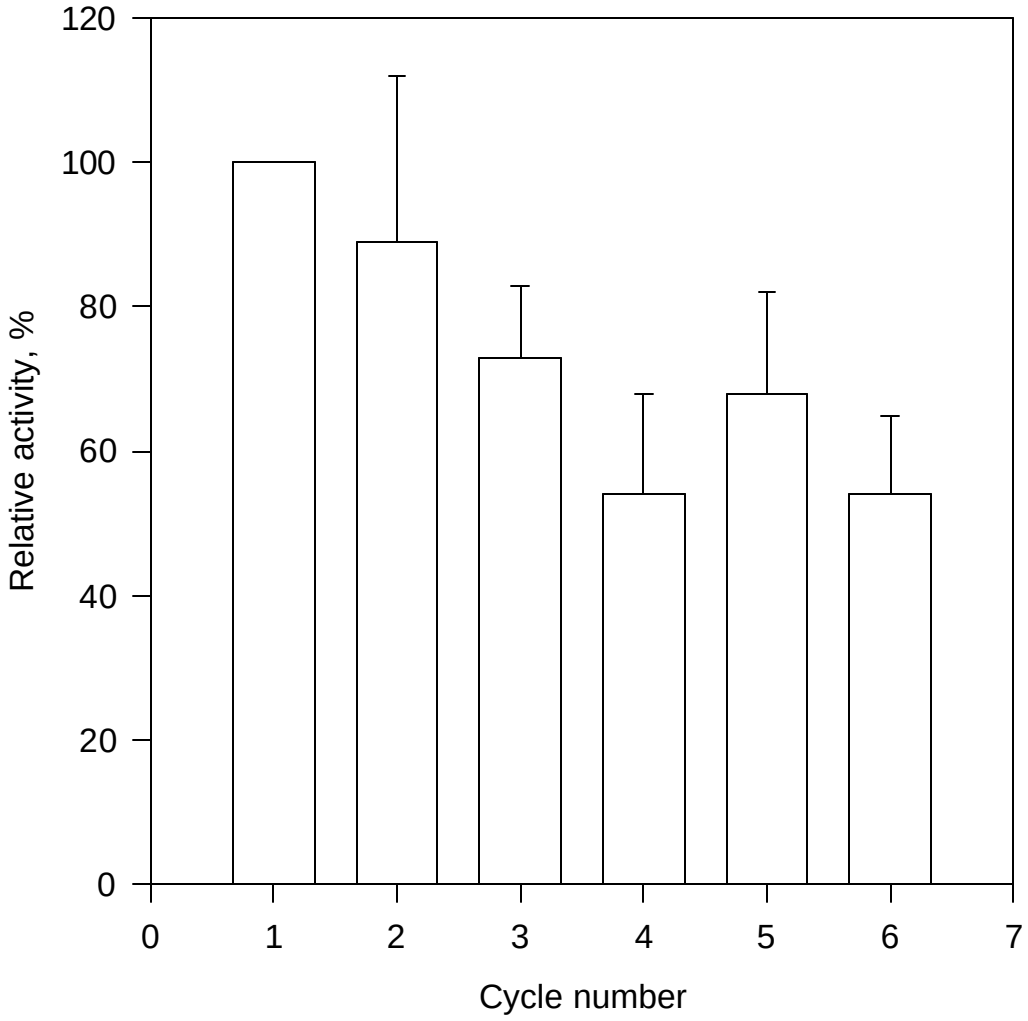

Figure 40 ECC's reusability for activity assays

(Table 11; Experiment 7). However, the 30 min exposure of the film to basic media also destroyed the uniformity and morphology of the coating.

7.3.5 Thermostability of ECC's

Dry ECC's exhibit good stability under ambient conditions with only a 45 % activity loss after 90 days of storage (Figure 41). Native CA stored in buffered solution (50 mM sodium phosphate, pH 7.5) at room temperature exhibits a higher stability with a 40 % activity loss after 90 days. This agrees well with the results reported for BCA II covalently coupled to silica beads via Schiff base linkages.[277] The immobilized enzyme was shown to loose 50 % activity after a 30 day incubation under mixing at 23 ^{o}C in buffered media.[277]

7.4 Conclusion

The incorporation of CA into Michael adduct-based coatings has been performed in a two-step process using MANVF, NVF, and acrylate derivatives. The enzyme was first incorporated into water-soluble NVF-based polymer (Enzyme/Polymer; EP), which was soluble in the hydrophobic blend used for the film casting. Given its high polydispersity, EP could not be analyzed by mass spectrometry techniques including MALDI and electrospray ionization. Analytic ultracentrifugation was the only successful method to characterize the degree of polymerization of EP. CA-ECC's exhibited an apparent activity retention of 7 %. They were highly stable when stored dry at room temperature.

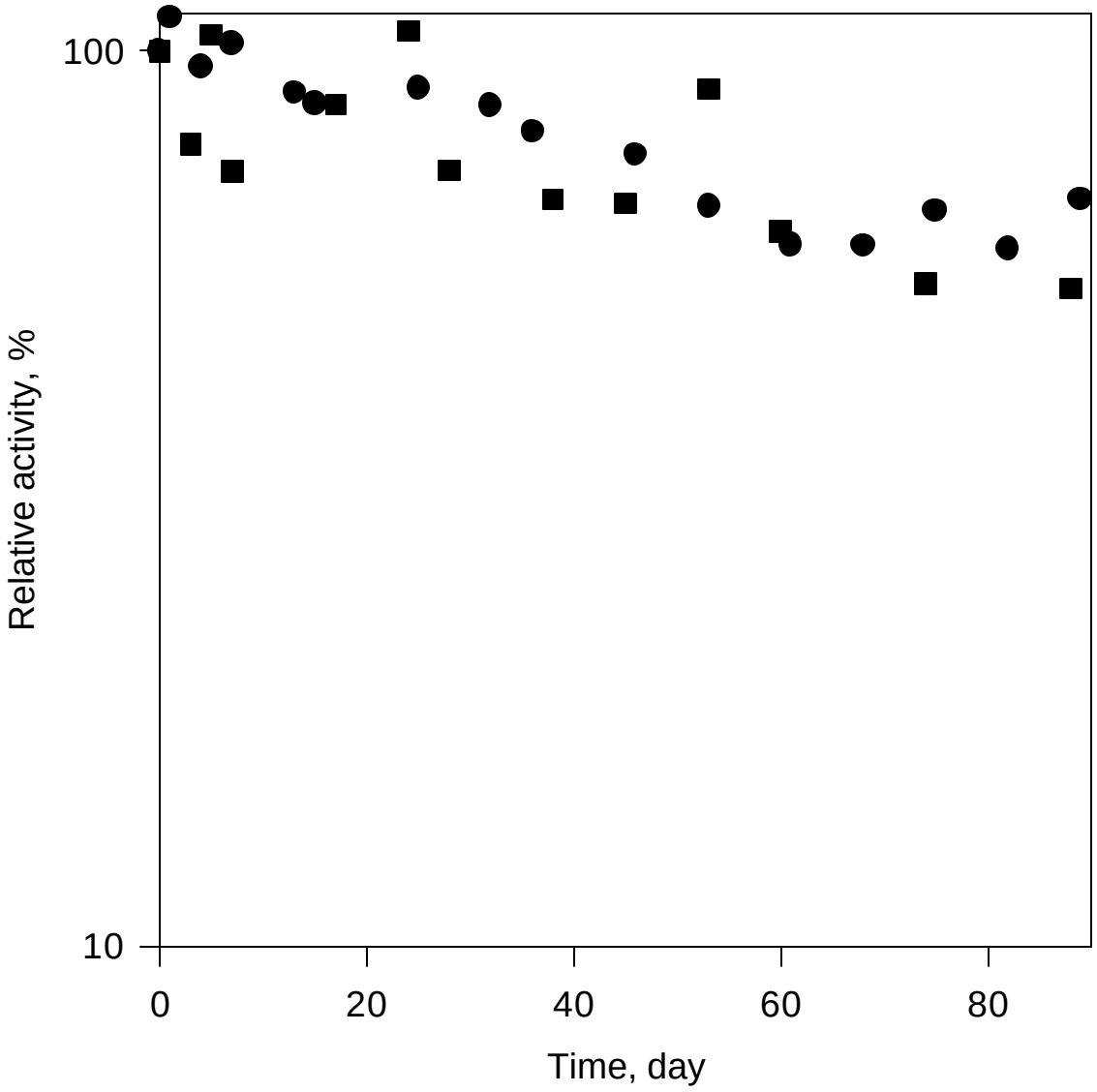

Figure 41 Thermoinactivation of dry CA-containing coating under ambient conditions

Deactivation of native CA wasconducted in buffered solution (closed circles). ECC's were stored dry (closed squares).

BIBLIOGRAPHY

BIBLIOGRAPHY

1. Ahmad F, "Measuring the conformational stability of enzymes," In: Thermostability of Enzymes, editor: Gupta MN, (Berlin: Springer-Verlag, 1993), pp. 96-112.

2. Tanford C, "Protein denaturation." *Protein Chemistry*, vol. 23, 1968, pp.121-282.

3. Ghélis C, Yon J, In Protein Folding, (London: Academic Press, Inc., 1982), pp. 374-418.

4. Zale SE, Klibanov AM, "On the role of reversible denaturation (unfolding) in the irreversible thermal inactivation of enzymes," *Biotechnology and Bioengineering*, vol. 25, 1983, pp. 2231-2242.

5. Henley JP, Sadana A, "Deactivation theory," *Biotechnology and Bioengineering*, vol. 28, 1985, pp. 1277-1285.

6. Sadana A, "Models of enzyme deactivation," In: Thermostability of Enzymes, editor Gupta MN, (Berlin: Springer-Verlag, 1993), pp. 84-93.

7. Klibanov AM, "On the mechanism of irreversible thermoinactivation of enzymes and possibilities for reactivation of "irreversibly" inactivated enzymes," *Biochemical and Biophysical Research Communications*, vol. 83, 1978, pp. 1012-1017.

8. Gupta S, "Mechanisms of irreversible thermoinactivation and medium engineering," In: Thermostability of Enzymes, editor: Gupta MN, (Berlin: Springer-Verlag, 1993), pp. 114-122.

9. Volkin DB, Klibanov AM, "Minimizing protein inactivation," In: Protein Function: A Practical Approach, editor: Creighton TE, (London: IRL Press, 1989), pp. 1-24.

10. Fágáin CÓ, "Studies on denaturation, inactivation and stabilizing interactions," In: Stabilizing Protein Function, editor: Fágáin CÓ, (Berlin: Springer-Verlag, 1997), pp. 21-38.

11. Volkin DB, Mach H, Middaugh CR, "Degradative covalent reactions important to protein stability," *Molecular Biology*, vol. 8, 1997, pp. 105-122.

12. Zale SE, Klibanov AM, "Why does ribonuclease irreversibly inactivate at high temperatures?," *Biochemistry*, vol. 25, 1986, pp. 5432-5444.

13. Inglis AS, "Cleavage at aspartic acid," *Methods in Enzymology*, vol. 91, 1983, pp. 324-332.

14. Hurrell RF, Carpenter KJ, "Nutritional significance of cross-link formation during food processing," In: Protein Crosslinking: Advances in Experimental Medicine and Biology, vol. 86B, editor: Friedman M, (New York:, 1977), pp.225-238.

15. Geiger T, Clarke S, "Deamidation, isomerization, and racemization at asparaginyl and aspartyl residues in peptides," *Journal of Biological Chemistry*, vol. 15, 1987, pp.785-794.

16. Bada JL**,** "*In vivo* racemization in mammalian proteins," *Methods in Enzymology*, vol. 106, 1984, pp. 98-115.

17. Finot PA, Bujard E, Mottu F, Mauron J, "Availability of the true Schiff's bases of lysine. Chemical evaluation of the Schiff's base between lysine and lactose in milk," In: Protein Crosslinking: Advances in Experimental Medicine and Biology, vol. 86B, editor: Friedman M, (New York: Plenum Press, 1977), pp.343-365.

18. Stauffer HCE, Etson D, "The effect on subtilisin activity of oxidizing a methionine residue," *Journal of Biological Chemistry*, vol. 244, 1969, pp. 5333-5338.

19. Schöneich C, "Kinetics of thiol reactions," *Methods in Enzymology,* vol. 251, 1995, pp. 45-55.

20. Hartmann HJ, Sievers C, Weser U, "Thiyl radicals in biochemically important thiols in the presence of metal ions," *Metals Ions in Biological Systems,* vol. 36, 1999, pp. 389-413.

21. Carrea G, Riva S, "Properties and synthetic applications of enzymes in organic solvents," *Angewandte Chemie International Edition*, vol. 39, 2000, pp. 2226-2254.

22. Klikanov AM, "Enzymes that work in organic solvents," *Chemische Technik*, vol. 16, 1986, pp. 354-359.

23. Fágáin CÓ, "Enzymes in organic media," In Stabilizing Protein Function, editor: Fágáin CÓ, (Berlin: Springer-Verlag, 1997), pp. 39-46.

24. Klibanov AM, "Enzymatic catalysis in anhydrous organic solvents," *Trends in Biochemical Sciences*, vol. 14, 1989, pp. 141-144.

25. Klibanov AM, "Improving enzymes by using them in organic solvents," *Nature*, vol. 409, 2001, pp. 241-246.

26. Mozhaev VV, Khmel'nitskii YL, Sergeeva NV, Belova AB, Klyachko NL, Levashov AV, Martinek K, "Catalytic activity and denaturation of enzymes in water/alcohol, water/glycol, water/formamide solvents," *European Journal of Biochemistry*, vol. 184, 1989, pp. 597-602.

27. Khmelnitsky YL, Levashov AV, Klyachko NL, Matinek K, "Engineering biocatalytic systems in organic media with low water content," *Enzyme Microbial Technology*, vol. 10, 1988, pp. 710-724.

28. Ghatorae AS, Guerra MJ, Bell G, Halling PJ, "Immiscible organic solvent inactivation of urease, chymotrypsin, lipase, and ribonuclease: separation of dissolved solvent and interfacial effects," *Biotechnology and Bioengineering*, vol. 44, 1994, pp. 1355-1361.

29. Beverung CJ, Radke CJ, Blanch HW, "Protein adsorption at the oil/eater interface: characterization of adsorption kinetics by dynamic interfacial tension measurements," *Biophysical Chemistry*, vol. 81, 1999, pp. 59-80.

30. Hickel A, Radke CJ, Blanch HW, "Role of organic solvents on pa-hydroxynitrile lyase interfacial activity and stability," *Biotechnology and Bioengineering*, vol. 74, 2001, pp. 18-28.

31. Ghatorae AS, Bell G, Halling PJ, "Inactivation of enzymes by organic solvents: new technique with well-defined interfacial area," *Biotechnology and Bioengineering*, vol. 43, 1994, pp. 331-336.

32. Hickel A, Radke CJ, Blanch HW, "Hydroxynitrile lyase adsorption at liquid/liquid interfaces," *Journal of Molecular Catalysis B: Enzymatic*, vol. B 5, 1998, pp. 349-354.

33. Gray CJ, "Stabilisation of enzymes with soluble additives," In: Thermostability of Enzymes, editor: Gupta MN, (Berlin: Springer-Verlag, 1993), pp. 124-143.

34. Vallee BL, Ulmer DD, "Biochemical effects of mercury, cadmiun, and lead," *Annual Review of Biochemistry*, vol. 41, 1972, pp. 91-128.

35. Habeeb AFSA, "Reaction of sulhydryl groups with Ellman's reagent," *Methods in Enzymology*, vol. 25, 1972, pp. 457-464.

36. Fágáin CÓ, "Use of stabilizing additives," In: Stabilizing Protein Function, editor: Fágáin CÓ, (Berlin: Springer-Verlag, 1997), pp. 69-79.

37. Gross M, Jaenicke R, "Proteins under pressure," *European Journal of Biochemistry*, vol. 221, 1994, pp. 617-630.

38. Mozhaev VV, Heremans K, Frank J, Masson P, Balny C, "Exploiting the effects of high hydrostatic pressure in biotechnological applications," *TIBTECH*, vol. 12, 1994, pp. 493-501.

39. Michels PC, Hei P, Clark DS, "Pressure effects on enzyme activity and stability at high temperatures," *Advances in Protein Chemistry*, vol. 48, 1996, pp.341-376.

40. Marshall CJ, "Cold-adapted enzymes," *TIBTECH*, vol. 15, 1997, pp. 359-364.

41. Franks F, "Protein destabilization at low temperatures," *Advances in Protein Chemistry*, vol. 46, 1995, pp. 105-139.

42. Carpenter JF, Izutsu K-I, "Freeezing- and drying-induced perturbations of protein structure and mechanisms of proteins protection by stabilizing additives," *Drugs in Pharmaceuticals Sciences*, vol. 96, 1999, pp. 123-160.

43. Pikal MJ, "Mechanisms of protein stabilization during freeze-drying and storage: the relative importance of thermodynamic stabilization and glassy state relaxation dynamics," *Drugs in Pharmaceuticals Sciences*, vol. 96, 1999, pp. 161-198.

44. Wang W, "Instability, stabilization, and formulation of liquid protein pharmaceuticals," *International Journal of Pharmacy*, vol. 185, 1999, pp.129-188.

45. Timasheff SN, "Stabilization of protein structure by solvents," In: Protein Function: A Practical Approach, editor: Creighton TE, (London: IRL Press, 1997), pp. 331-345.

46. DeSantis G, Jones JB, "Chemical modification of enzymes for enhanced functionality," *Current Opinion in Biotechnology*, vol. 10, 1999, pp. 324-330.

47. Fágáin CÓ, "Chemical modification of proteins in solution," In: Stabilizing Protein Function, editor: Fágáin CÓ, (Berlin: Springer-Verlag, 1997), pp. 81-114.

48. Tyagi R, Gupta MN, "Chemical modification and chemical crosslinking for enhancing thermostability of enzymes," In: Thermostability of Enzymes, editor: Gupta MN, (Berlin: Springer-Verlag, 1993), pp. 146-160.

49. Shaw E, "Selective chemical modification of proteins," *Physiological Reviews*, vol. 50, 1970, pp. 244-296.

50. Nureddin A, Inagami T, *Biochemistry Journal*, vol. 147, 1975, pp. 71-81.

51. Inada Y, Matsushima A, Hiroto M, Nishimura H, Kodera Y, *Advances in Biochemical Engineering/Biotechnology*, vol. 52, 1995, pp. 129-150.

52. Matusushima A, Kodera Y, Hiroto M, Nishimura H, Inada Y, "Bioconjugates of proteins and polyethylene glycol: potent tools in biotechnological processes," *Journal of Molecular Catalysis B: Enzymatic*, vol. 2, 1996, pp. 1-17.

53. Këstner AI**,** "Immobilised enzymes," *Russian Chemical Reviews*, vol. 43, 1974, pp. 690-705.

54. Kokufuta E, "Novel applications for stimulis-sensitive polymer gels in the preparation of functional immobilized biocatalysts," *Advances in Polymer Sciences*, vol. 110, 1993, pp. 157-177.

55. Liang JF, Li YT, Yang C, "Biomedical application of immobilized enzymes," *Journal of Pharmaceuticals Sciences*, vol. 89, 2000, pp. 979-990.

56. Cabral JMS, In: Thermostability of Enzymes, editor: Gupta MN, (Berlin: Springer-Verlag, 1993), pp. 162-181.

57. Fágáin CÓ, "Immobilization," In: Stabilizing Protein Function, editor: Fágáin CÓ, (Berlin: Springer-Verlag, 1997), pp. 115-128.

58. Chiaratini L, Magnani M, "Immobilization of enzymes and proteins on red blood cells," In Immobilization of enzymes and cells, editor: Bickerstaff GF, (Totowa, NJ: Humana Press, 1997), pp. 143-152.

59. Caldwell SR, Raushel FM, "Detoxification of organophosphate pesticides using a nylon base immobilized phosphotriesterase from *Pseudonomas diminuta*," *Applied Biochemistry and Biotechnology*, vol. 44, 1991, pp. 1018-1022.

60. Ahulekar RV, Prabhune AA, Raman SH, Ponratham S, "Immobilization of penicillin G acylase on functionalized macroporous beads," *Polymer*, vol. 34, 1993, pp. 163-166.

61. Rejikuma S, Devi S, "Immobilization of β-galactosidase onto polymeric supports," *Journal of Apllied Polymer Science*, vol. 55, 1995, pp. 871-878.

62. Li ZF, Kang ET, Neoh KG, Tan KL, "Covalent immobilization of glucose oxidase on the surface of polyaniline films graft copolymerized with acrylic acid," *Biomaterials*, vol. 19, 1997, pp.45-53.

63. LeJeune KE, Russell AJ, "Covalent binding of a nerve agent hydrolyzing enzyme within polyurethane foams," *Biotechnology and Bioengineering*, vol. 51, 1996, pp. 450-457.

64. Bakker M, van de Velde F, van Rantwijk F, Sheldon RA, "Highly efficient immobilization of glycosylated enzymes into polyurethane foams," *Biotechnology and Bioengineering*, vol. 70, 2000, pp. 342-348.

65. Reetz MT, "Entrapment of biocatalysts in hydrophobic sol-gel materials for use in organic chemistry," *Advanced Materials*, vol. 9, 1997, pp. 943-954.

66. Gill I, Ballesteros A, "Bioencapsulation within synthetic polymers (part 1): sol-gel encapsulated biologicals," *TIBTECH*, vol. 18, 2000, pp. 282-296.

67. Böttcher H, "Bioactive sol-gel coatings," *Journal für Praktische Chemie*, vol. 342, 2000, pp. 427-436.

68. Nosoh Y, Sekiguchi T, In: Thermostability of Enzymes, editor: Gupta MN, (Berlin: Springer-Verlag, 1993), pp.182-203.

69. Sterner R, Liebl W, "Thermophilic adaptation of proteins," *Critical Reviews in Biochemistry and Molecular Biology*, vol. 36, 2001, pp. 39-106.

70. Lehmann M, Pasamontes L, Lassen SF, Wyss M, "The consensus concept for thermostability engineering of proteins," *Biochimica and Biophysica Acta*, vol. 1543, 2000, pp. 408-415.

71. Lehmann M, Wyss M, "Engineering proteins for themrostability: the use of sequence alignments versus rational design and directed evolution," *Current Opinion in Biotechnology*, vol. 12, 2001, pp. 371-375.

72. Chirumamilla RR, Muralidhar R, Marchant R, Nigam P, "Improving the quality of industrially important enzymes by directed evolution," *Molecular and Cellular Biochemistry*, vol. 224, 2001, pp. 159-168.

73. Stemmer WPC, "DNA shuffling by random fragmentation and reassembly: in vitro recombination for molecular evolution," *Proceedings of the National*

Academy of Sciences of the United States of America, vol. 91, 1994, pp. 10747-10751.

74. Kurtzman AL, Govindarajan S, Vahle K, Jones JT, Heinrichs V, Patten PA, "Advances in directed protein evolution by recursive genetic recombination; applications to therapeutic proteins," *Current Opinion in Biotechnology*, vol. 12, 2001, pp. 361-370.

75. Arnold FH, Wintrocke PL, Miyazaki K, Gershenson A, "How enzymes adapt: lessons from directed evolution," *Trends in Biochemical Sciences*, vol. 26, 2001, pp. 100-106.

76. DeFrank JJ, "Organophosphorus cholinesterase inhibitors: detoxification by microbial enzymes," In: Applications of Enzyme Biotechnology, editors: Kelly JW, Baldwin TO, (New York: Plenum Press, 1991), pp.165-180.

77. Grimsley JK, Rastogi VK, Wild JR, "Biological detoxification of organophosphorus neurotoxins," In: Bioremediation: Principles and Practice, editors: Sikdar SK, Irvine RL, (Technomic Publishing, Co., Inc., 1997), pp. 577-614.

78. Mazur A, "An enzyme in animal tissue capable of hydrolyzing the phosphorus-fluorine bond of alkyl fluorophosphates," *Journal of Biological Chemistry*, vol. 164, 1946, pp. 271-289.

79. Dumas DP, Caldwell SR, Wild JR, Raushel FM, " Purification and properties of the phosphotriesterase from *Pseudomonas diminuta*," *Journal of Biological Chemistry*, vol. 264, 1989, pp. 19659-19665.

80. Horne I, Sutherland T, Harcourt R, Russell RJ, Oakeshott JG, "Identification of an *opd* (organophosphate degredation) gene in an *Agrobacterium* isolate," *Applied and Environmental Microbiology*, vol. 68, 2002, pp. 3371-3376.

81. Hoskin FCG, Prusch RD, "Characterization of a DFP-hydrolyzing enzyme in squid posterior salivary gland by use of soman, DFP, and manganous Ion," *Comparative Biochemistry and Physiology*, vol. 75C, 2002, pp. 17-20.

82. DeFrank JJ, Cheng T, "Purification and properties of an organophosphorus acid anhydrase from a halophilic bacterial isolate," *Journal of Bacteriology*, vol. 173, 1991, pp. 1938-1943.

83. Mulbry WW, Hams JF, Kearney PC, Nelson JO, McDaniel CS, Wild JR, "Identification of a plasmid-borne parathion hydrolase gene from *Flavobacterium sp.* by southern hydridization with *opd* from *Pseudomonas dismuta*," *Applied and Environmental Microbiology*, vol. 51, 1986, pp. 926-930.

84. Mouches C, Magnin M, Berge JB, De Silvestri M, Beyssat V, Pasteur N, Georghiou GP, "Overproduction of detoxifying esterases in organophosphate-resistant Culex mosquitoes and their presence in other insects," *Proceedings of the National Academy of Sciences USA*, vol. 84, 1978, pp. 2113-2116.

85. Hoskin FCG, Walker JE, Mello CM, "Organophosphorus acid anhydrolase in slime mold duckweed and mung bean: A continuing search for physiological role and a natural substrate," *Chemico-Biological Interactions*, vol. 119-120, 1999, pp. 399-404.

86. Gopal S, Rastogi V, Ashman W, Mulbry W, "Mutagenesis of organophosphorus hydrolase to enhance hydrolysis of the nerve agent VX," *Biochemical and Biophysical Research Communications*, vol. 279, 2000, pp. 516-6519.

87. Lai K, Kave KI, Wild JR, "Bimetallic binding motifs in organophophorus hydrolase are important for catalysis and structural organization," *Journal of Biological Chemistry*, vol. 269, 1994, pp. 16579-16584.

88. Watkins LM, Mahoney HJ, McCulloch JK, Raushel FM, "Augmented hydrolysis of diisopropyl fluorophosphate in engineered mutants of phosphotriesterase," *Journal of Biological Chemistry*, vol. 272, 1997, pp. 25596-25601.

89. DiSioudi B, Grimsley JK, Lai K, Wild JR, "Modification of near active site residues in organophosphorus hydrolase reduces metal stoichiometry and alters substrate specificity," *Biochemistry*, vol. 38, 1999, pp. 2866-2872.

90. DiSioudi BD, Miller CE, Lai K, Grimsley JK, Wild JR, "Rational design of organophosphorus hydrolase for altered substrate specificities," *Chemico-Biological Interactions*, vol. 119-120, 1999, pp. 211-223.

91. Hartleib J, Ruterjans H, "Insights into the reaction mechanism of the diisopropylfluorophosphatase from *Loligo vulgaris* by means of kinetic studies, chemical modification and site-directed mutagenesis," *Biochimica Biophysica Acta*, vol. 1546, 2001, pp. 312-324.

92. Chen W, Bruhlmann F, Richins RD, Mulchandani A, "Engineering of improved microbes and enzymes for bioremediation," *Current Opinion in Biotechnology*, vol. 10, 1999, pp. 137-141.

93. Cho CM, Mulchandani A, Chen W, "Bacterial cell Surface display of organophosphorus hydrolase for selective screening of improved hydrolysis of organophosphorus nerve agents," *Applied Environmental Microbial*, vol. 68, 2002, pp. 2026-2030.

94. Richins RD, Mulchandani A, Chen W, "Expression, immobilization, and enzymatic characterization of cellulose-binding domain-organophosphorus hydrolase fusion enzymes," *Biotechnology Bioengineering*, vol. 69, 2000, pp. 591-596.

95. Wu C, Cha HJ, Valdes JJ, Bentley WE, "GFP-visualized immobilized enzymes: Degredation of paraoxon via organophosphorus hydrolase in a packed column," *Biotechnology Bioengineering*, vol. 77, 2002, pp. 212-218.

96. Walker CH, "The classification of esterases which hydrolyze organophosphates: Recent developments," *Chemico-Bioligical Interactions*, vol. 87, 1993, pp. 17-24.

97. Reiner E, "Recommendations of the IUBMB nomenclature committee: Comments concerning classification and nomenclature of esterase hydrolysing organophosphate compounds," *Chemico-Biological Interactions*, vol. 87, 1993, pp. 15-16.

98. Caldwell S, Newcomb J, Schlecht K, Raushel F, "Limits of diffusion in the hydrolysis of substrates by the phosphotriesterase from *Pseudomonas diminuta*," *Applied Biochemistry and Biotechnology* , vol. 31, 1991, pp. 59-73.

99. Hartleib J, Rutergans H, "High-yield expression, purification, and characterization of the recombinant diisopropylfluorophosphatase from *Loligo vulgaris*," *Protein Expression and Purification*, vol. 21, 2001, pp. 210-219.

100 Wang F, Xiao M, Mu S, "Purification and properties of a diisopropylfluorophoshatase from squid *Todarodes Pacificus Steenstrup*," *Journal of Biochemical Toxicology*, vol. 8, 1993, pp. 161-166.

101. Hoskin CGH, Roush AH, "Hydrolysis of nerve gas by squid-type diisopropyl phosphofluoridate hydrolyzing enzyme on agarose resin," *Science*, vol. 215, 1982, pp. 1255-1257.

102. Crawford DM, "Dynamic mechanical analysis of novel polyurethane coating for military applications," *Thermocimica Acta*, vol. 357-358, 2000, pp. 161-168.

103. Munnecke DM, "Properties of an immobilized pesticide-hydrolyzing enzyme. *Applied and Environmental Microbiology*, vol. 33, 1977, pp. 503-507.

104. Munnecke DM, "Hydrolysis of organophosphate insecticides by an immobilized-enzyme system," *Biotechnology and Bioengineering*, vol. 21, 1971, pp. 2247-2261.

105. Caldwell SR, Raushel FM, "Detoxification of organophosphate pesticides using an immobilized phosphotriesterase from *Pseudomonas diminuta*," *Biotechnology and Bioengineering*, vol. 37, 1991, pp. 103-109.

106. Havens PL, Rase HF, "Detoxification of organophosphate pesticide solutions: Immobilized enzyme systems," In: Hazardous Waste Management II, ACS Symposium Series 468, editors: Tedder DW, Pohland FG, (Washington DC: American Chemical Society,1991), pp. 261-281.

107. Grimsley JK, Singh WP, Wild JR, Giletto A, "A novel, enzyme-based method for the wound-surface removal and decontamination of organophosphorous nerve agents," In: Bioactive fibers and polymers. ACS Symposium Series 742, (American Chemical Society: Washington DC, 2001), pp. 35-49.

108. Gill I, Ballesteros A, "Bioencapulation within synthetic polymers (Part 2): Non-sol-gel protein-polymer composites," *TIBTechnology*, vol. 18, 2000, pp. 469-479.

109. Braatz JA, "Biocompatible polyurethane-based hydrogels," *Journal of Biomaterial Applications*, vol. 9, 1994, pp. 71-96.

110. Havens PL, Rase HF, "Reusable immobilized enzyme/polyurethane sponge for removal and detoxification of localized organophosphate pesticide spills," *Industrial and Engineering Chemistry Research*, vol. 32: 2254-2258.

111. LeJeune KE, Mesiano AJ, Bower SB, Grimsley JK, Wild JR, Russell AJ, "Dramatically stabilized phosphotriesterase-polymers for nerve agent degredation," *Biotechnology and Bioengineering*, vol. 54, 1997, pp. 105-114.

112. LeJeune KE, Swers JS, Hetro AD, Donahey GP, Russell AJ, "Increasing the tolerance of organophosphorus hydrolase to bleach," *Biotechnology and Bioengineering* 64, 1999, pp. 250-254.

113. LeJeune KE, Dravis BC, Yang F, Hetro AD, Doctor BP, Russell AJ, "Fighting nerve agent chemical weapons with enzyme technology," *Annals New York Academy of Science*, vol. 864, 1998, pp. 153-170.

114. Gordon RK, Feaster SR, Russell AJ, LeJeune KE, Maxwell DM, Lenz DE, Ross M, Doctor BP, "Organophosphate skin decontamination using enzymes," *Chemico-Biological Interactions*, vol. 119-120, 1999, pp. 463-470.

115. Gill I, Ballesteros A, "Encapsulation of biologicals with silicate, siloxane, and hybrid sol-gel polymers: An efficient and generic approach," *Journal of the American Chemical Society*, vol. 120, 1998, pp. 8587-8598.

116. Gill I, Ballesteros A, "Degradation of organophosphorous nerve agents by enzyme-polymer nanocomposites: efficient biocatalytic materials for personal protection and large-scale detoxification," *Biotechnology and Bioengineering*, vol. 70, 2000, pp. 400-410.

117. Gill I, Pastor E, Ballesteros A. Lipase-Silicone Biocomposites: Efficient and Versatile Immobilized Biocatalysts," *Journal of the American Chemical Society*, vol. 121, 1999, pp. 9487-9496.

118. Storey KB, Duncan JA, Chakrabarti AC, "Immobilization of amyloglucosidase using two forms of polyurethane polymer," *Applied Biochemistry and Biotechnology*, vol. 23, 1990, pp. 221-236.

119. Dias SF, Vilas-Boas L, Cabral JMS, Fonseca MMR, "Production of ethyl butyrate by *Candida rugosa* lipase immobilized in polyurethane, " *Biocatalysis*, vol. 5, 1991, pp. 21-34.

120. Havens PL, Rase HF, "Reusable immobilized enzyme/polyurethane sponge for removal and detoxification of localized organophosphate pesticide spills," *Industrial and Engineering Chemical Research*, vol. 32, 1993, pp. 2254-2258.

121. LeJeune KE, Wild JR, Russell AJ, "Nerve agent degraded by enzymatic foams," *Nature*, vol. 395, 1998, pp. 27-28.

122. Coessens V, Pintauer T, Matyjaszewski K, "Functional polymers by atom transfer radical polymerization," *Progress in Polymer Science*, vol. 26, 2000, pp. 337-377.

123. Matyjaszewski K, Paik H-J, Shipp DA, Isobe Y, Okamoto Y, 2001, "Free-radical intermediates in atom transfer radical addition and polymerization: study of racemization, halogen exchange, and trapping reactions," *Macromolecules*, vol. 34, pp. 3127-3129.

124. Qiu J, Sipp D, Gaynor SG, Matyjaszewski K, "The effect of ligands on atom transfer radical polymerization in water-borne systems," *Polymer Preprints (American Chemical Society, Division of Polymer Chemistry)*, vol. 40, 1999, pp. 418-419.

125. Wang XS, Armes SP, "Facile atom transfer radical polymerization of methoxy-capped oligo(ethylene glycol) methacrylate in aqueous media at ambient temperature," *Macromolecules*, vol. 33, 2000, pp. 6640-6647.

126. Wange XS-, Armes SP, "Facile atom transfer radical polymerization of methoxy-capped oligo(ethylene glycol) methacrylate in aqueous media at ambient temperature," *Macromolecules*, vol. 33, 2000, pp. 6640-6647.

127. Wang XS-, Lascelles SF, Jacksoon RA, Armes SP, "Facile synthesis of well-defined water-soluble polymers via atom transfer radical polymerization in aqueous media at ambient temperature," *Chemical Communications*, vol. 9, 1999, 1817-1818.

128. Coca S, Jasieczek CB, Beers KL, Matyjaszewski K, "Polymerization of acrylates by atom transfer radical polymerization. Homopolymerization of 2-hydroxyehtyl acrylate," *Journal of Polymer Science: Part A: Polymer Chemistry*, vol. 36, 1998, pp. 1417-1424.

129. Tsarevsky NV, Pintauer T, Glogowski E, Matyjaszewski K, "Atom transfer radical polymerization of 2-hydroxyethyl methacrylate and 2-(N,N-dimethylamino)ethyl methacrylate in aqueous homogeneous media: Synthesis and mechanistic studies," *Polymer Preprints (American Chemical Society, Division of Polymer Chemistry)*, vol. 43, 2002, pp. 201-202.

130. Matyjaszewski K, Shipp DA, Wang J-L, Grimaud T, Patten TE, "Utilizing halide exchange to improve control of atom transfer radical polymerization," *Macromolecules*, vol. 31, 1998, pp. 6836-6840.

131. Matyjaszewski K, Wang J-L, Grimaud T, Shipp DA, "Controlled/"living" atom transfer radical polymerization of methyl methacrylate using various initiation systems," *Macromolecules*, vol. 31, 1998, pp. 1527-1534.

132. Save M, Weaver JVM, Armes SP, "Atom transfer radical polymerization of hydroxy-functional methacrylates at ambient temperature: comparison of glycerol monomethacrylate with 2-hydroxypropyl methacrylate," *Macromolecules*, vol. 35, 2002, pp. 1152-1159.

133. Beddows CG, Guthrie JT, 'The immobilization of enzymes onto hydrolyzed polyethylene-*g*-co-2-HEMA," *Journal of Applied Polymer Science*, vol. 35, 1988, pp. 134-144.

134. Huang W, Kim JB, Bruening ML, Baker GL, "Functionalization of surfaces by water-accelerated atom-transfer radical polymerization of hydroxyethyl methacrylate and subsequent derivatization," *Macromolecules*, vol. 35, 2002, pp. 1175-1179.

135. Bontempo D, Tirelli N, Masci G, Crescenzi V, Hubbell JA, "Thick oating and functionalization of organic surfaces via ATRP in water," *Macromolecular Rapid Communications*, vol. 23, 2002, pp. 417-422.

136. Flickinger MC, Mullick A, Ollis DF, "Method for construction of a simple laboratory-scale nonwoven filament biocatalytic filter," *Biotechnology Progress*, vol. 14, 1998, pp. 664-666.

137. Flickinger MC, Mullick A, Ollis DF, "Construction of a thread coater and use of azocasein release to characterize the sealant coat porosity of fibers coated with latex biocatalytic coatings," *Biotechnology Progress*, vol. 15, 1999, pp. 383-390.

138. Chován T, Guttman A, "Microfabricated devices in biotechnology and biochemical processing," *Trends in Biotechnology*, vol. 20, 2002, pp. 116-122.

139. Kim YD, Park CB, Clark DS, "Stable sol-gel microstructured and microfluidic networks for protein patterning," *Biotechnology and Bioengineering*, vol. 73, 2001, pp. 331-337.

140. Kim YD, Dordick JS, Clark DS, "Siloxane-based biocatalytic films and paints for use as reactive coatings," *Biotechnology and Bioengineering*, vol. 72, 2001, pp. 475-482.

141. Novick SJ, Dordick JS, "Protein-containing hydrophobic coatings and films," *Biomaterials*, vol. 23, 2002, pp. 441-448.

142. Perry TD, Zinn M, Mitchell R, "Settlement inhibition of fouling invertebrate larvae by metabolites of the marine bacterium Halomonas marine within a polyurethane coating," *Biofouling*, vol. 17, 2002, pp. 147-153.

143. Gill IS, Plou F, Ballesteros A, "New avenues to high-performance immobilized biosystems: from biosensors to biocatalysts," In: Stereoselective biocatalysis, editor: Patel RN, (New York: Marcel Dekker, Inc., 2000), pp. 741-773.

144. Piro B, Do V-A, Le LA, Hedayatullah M, Pham MC, "Electrosynthesis of a new enzyme-modified electrode for the amperometric detection of glucose," *Journal of Electroanalytical Chemistry*, vol. 486, 2000, 133-144.

145. Berlin P, Klemm D, Tiller J, Rieseler R, "A novel soluble aminocellulose derivative type: its transparent film-forming properties and its efficient coupling with enzyme proteins for biosensors," *Macromolecular Chemistry and Physics*, vol. 201, 2000, pp. 2070-2082.

146. Koncki R, Wolbeis, "Composite films of Prussian blue and N-substituted polypyrroles: covalent immobilization of enzymes and application to near infrared optical biosensing," *Biosensors and Bioelectronics*, vol. 14, 1999, pp. 87-92.

147. Garjonyte R, Malinauskas A, "Amperometric glucose biosensor based on glucose oxidase immobilized in poly(*o*-phenylenediamine) layer," *Sensors and Actuators B*, vol. 56, 1999, pp. 85-92.

148. Coulet PR, "Polymeric membranes and coupled enzymes in the design of biosensors," *Journal of Membrane Science*, vol. 68, 1992, pp. 217-228.

149. Properties and applications of proteins encapsulated within sol-gel derived materials," *Analytica Chimica Acta*, vol. 461, 2002, pp. 1-36.

150. Ingersoll CM, Bright FV, "Using sol-gel-based platforms for chemical sensors," *CHEMTECH*, vol. , 1997, pp. 26-31.

151. Madaras MB, Popescu IC, Ufer S, Buck RP, "Microfabricated amperometric creatine and creatinine biosensors," *Analytica Chimica Acta*, vol. 319, 1995, pp. 335-345.

152. Wang H, Guan R, Fan C, Zhu D, Li G, "A hydrogen peroxide biosensor based on the bioelectrocatalysis of hemoglobin incorporated in a kieselgubr film," *Sensors Actuators B*, vol. 84, 2002, pp. 214-218.

153. He D, Cai Y, Wei W, Nie L, Yao S, "α-amylase immobilized on bulk acoustic-wave sensor by UV-curing coating," *Biochemical Engineering Journal*, vol. 6, 2000, pp. 7-11.

154. Guerrieri A, De Benedetto GE, Palmisanot F, Zambonin PG, "Electrosynthesized non-conducting polymer as permselective membranes in amperometric enzymes electrodes: a glucose biosensor based on a cross-linked glucose oxidase/overoxidized polypyrole bilayer," *Biosensors and Bioelectronics*, vol. 13, 1998, pp. 103-112.

155. Cosnier S, "Biomolecule immobilization on electrode surfaces by entrapment or attachment to electrochemically polymerized films. A review," *Biosensors and Bioelectronics*, vol. 14, 1999, pp. 443-456.

156. Bartlett PN, "A review of the immobilization of enzymes in electropolymerized films," *Journal of Electroanalytical Chemistry*, vol. 362, 1993, pp. 1-12.

157. Bidan G, "Electroconducting conjugated polymers: new sensitive matrices to build up chemical or electrochemical sensors: a review," *Sensors and Actuators*, vol. 6, 1992, pp. 45-56.

158. He D, Cai Y, Wei W, Nie L, Yao S, "α-Amylase immobilized on bulk acoustic-wave sensor by UV-curing coating," *Biochemical Engineering Journal*, vol. 6, 2000, pp. 7-11.

159. Novick SJ, Dordick JS, "Protein-containing hydrophobic coatings and films," *Biomaterials*, vol. 23, 2002, pp. 441-448.

160. Arai G, Noma T, Hayashi M, Yasumori I, "Electrochemical characteristics of D-amino acid oxidase immobilized in a conductive redox polymer," *Journal of Electroanalytical Chemistry*, vol. 452, 1998, pp. 43-48.

161. Cosnier S, Fontecave M, Limosin D, Nivière V, "A poly(amphiphilic pyrrole)-flavin reductase electrode for amperometric determination of flavins," *Analytical Chemistry*, vol. 69, 1997, pp. 3095-3099.

162. Cosnier S, Décout J-L, Fontecave M, Frier C, Innocent C, "A reagentless biosensor for the amperometric determination of NADH," *Electroanalysis*, vol. 10, 1998, pp. 521-525.

163. Shaolin M, "Bioelectrochemical response o the polyaniline galactose oxidase electrode," *Journal of Electroanalytical Chemistry*, vol. 370, 1994, pp. 135-139.

164. Künzelmann U, Böttcher H, "Biosensor properties of glucose oxidase immobilized within SiO^2 gels," *Sensors and Actuators B*, vol. 38-39, 1997, pp. 222-228.

165. Zhang Z, Liu H, Deng J, "A glucose biosensor based on immobilization of glucose oxidase in electropolymerized *o*-aminophenol film on platinized glassy carbon electrode," *Analytical Chemistry*, vol. 68, 1996, pp. 1632-1638.

166. Shaolin M, Huaiguo X, Bidong Q, "Bioelectrochemical responses of the polyaniline glucose oxidase electrode," *Journal of Electroanalytical Chemistry*, vol. 304, 1991, pp. 7-16.

167. Malitesta C, Palmisano F, Torsi L, Zambonin PG, "Glucose fast-response amperometric sensor based on glucose oxidase immobilized in an electropolymerized poly(*o*-phenylenediamine) film," *Analytical Chemistry*, vol. 62, 1990, pp. 2735-2740.

168. Yon-Hin BFY, Smolander M, Crompton T, Lowe CR, "Covalent electropolymerization of glucose oxidase in polypyrrole. Evaluation of methods of pyrrole attachment to glucose oxidase on the performance of electropolymerized glucose sensors," *Analytical Biochemistry*, vol. 65, 1993, pp. 2067-2071.

169. Foulds NC, Lowe CR, "Enzyme entrapment in electrically conducting polymers," *Journal of the Chemical Society, Faraday Transaction I*, vol. 1, 1986, pp. 1259-1264.

170 Marchesiello M, Geniès E, "A theoretical model for an amperometric glucose sensor using polypyrrole as the immobilization matrix," *Journal of Electroanalytical Chemistry*, vol. 258, 1993, pp. 35-48.

171. Umana M, Waller J, "Protein-modified electrodes. The glucose oxidase/polypyrrole system," *Analytical Chemistry*, vol. 58, 1986, pp. 2979-2983.

172. Yon-Hin BFY, Lowe CR, "An investigation of 3–functionalized pyrrole-modified glucose oxidase for the covalent electropolymerization of enzyme films," *Journal of Electroanalytical Chemistry*, vol. 374, 1994, pp. 167-172.

173. Wolowacz SE, Yon Hin BFY, Lowe CR, "Covalent electropolymerization of glucose oxidase in polypyrrole," *Analytical Chemistry*, vol. 64, 1992, pp. 1541-1545.

174. Cosnier S, Senillou A, Grätzel M, Comte P, Vlachopoulos N, Renault NJ, Martelet C, "A glucose biosensor based on enzyme entrapment within polypyrrol film electrodeposited on mesoporous titanium dioxide," *Journal of Electroanalytical Chemistry*, vol. 469, 1999, pp. 176-181.

175. Pandey PC, "A new conducting polymer-coated glucose sensor," *Journal of the Chemical Society, Faraday Transactions I*, vol. 84, 1988, pp. 2259-2265.

176. Scheller F, Schubert F, Biosensors (Amsterdam: Elsevier, 1992), pp. 50-64.

177. Dumont J, Fortier G, "Behavior of glucose oxidase immobilized in various electropolymerized thin films," *Biotechnology and Bioengineering*, vol. 49, 1996, pp. 544-552.

178. Almeida NF, Beckman EJ, Mohammad MA, "Immobilization of glucose oxidase in thin polypyrrole films: influence of polymerization conditions and film thickness on the activity and stability of the immobilized enzyme," *Biotechnology and Bioengineering*, vol. 42, 1993, pp. 1037-1045.

179. Deng Q, Dong S, "Mediators hydrogen peroxide electrode based on horseradish peroxidase entrapped in poly(*o*-phenylenediamine)," *Journal of Electroanalytical Chemistry*, vol. 377, 1994, pp. 191-195.

180. Tatsuma T, Gondaira M, Watanabe T, "Peroxidase-incorporated polypyrrole membrane electrodes," *Analytical Chemistry*, vol. 64, 1992, pp. 1183-1187.

181. Yang Y, Mu S, "Bioelectrochemical responses of the polyaniline horseradish peroxidase electrodes," *Analytical Chemistry*, vol. 432, 1997, pp. 71-78.

182. Chen X, Wang B, Dong S, "Amperometric biosensor for hydrogen peroxide based on sol-gel/hydrogel composite thin film," *Electroanalysis*, vol. 13, 2001, pp. 1149-1152.

183. Wang B, Zhang J, Cheng G, Dong S, "Amperometric enzyme electrode for the determination of hydrogen peroxide based on sol-gel/hydrogel composite film," *Analytica Chimica Acta*, vol. 407, 200, pp. 111-118.

184. Wang B, Dong S, "Sol-gel derived amperometric biosensor for hydrogen peroxide based on methylene green incorporated in Nafion film," *Talanta* 51, 2000, pp. 565-572.

185. Kuncová G, Šivel M, "Lipase immobilized in organic-inorganic matrices," *Journal of Sol-Gel Science and Technology*, vol. 8, 1997, pp. 667-671.

186. Fukunaga K, Minamijima N, Sugimura Y, Zhang Z, Nakao K, "Immobilization of organic solvent-soluble lipase in nonaqueous conditions and properties of the immobilized enzymes," *Journal of biotechnology*, vol. 52, 1996, pp. 81-88.

187. Yu L, Urban G, Moser I, Jobst G, Gruber H, "Photolithographically patternable modified poly(HEMA) hydrogel membrane, *Polymer Bulletin*, vol. 35, 1995, pp. 759-765.

188. Schubert F, Scheller FW, "Organelles electrodes," *Methods in Enzymology*, vol. 137, 1988, pp. 152-160.

189. Gill I, Ballesteros A, "Degradation of organophosphorous nerve agents by enzyme-polymer nanocomposites: efficient biocatalytic materials for personal protection and large-scale detoxification," *Biotechnology and Bioengineering*, vol. 70, 2000, pp. 400-410.

190. Cosnier S, Lepellec A, Guidetti B, Rico-Lattes I, "Enhancement of biosensor sensitivity in aqueous and organic solvents using a combination of poly(pyrrole-ammonium) and poly(pyrrole-lactobionamide) films as host matrices," *Journal of Electroanalytical Chemistry*, vol. 449, 1998, pp. 165-171.

191. Xue H, Shen Z, "A highly stable biosensor for phenols prepared by immobilizing polyphenol oxidase into polyaniline-polyacronitrile composite matrix," *Talanta*, vol. 57, 2002, pp. 289-295.

192. Wang B, Li B, Wang Z, Xu G, Wang Q, Dong S, "Sol-gel thin-film immobilized soybean peroxidase biosensor for the amperometric determination of hydrogen peroxide in acid medium, " *Analytical Chemistry*, vol. 71, 1999, pp. 1935-1939.

193. Deng Q, Guo Y, Dong S, "Cryo-hydrogel for the construction of a tyrosinase-based biosensor," *Analytica Chimica Acta*, vol. 319, 1996, pp. 71-77.

194. Deng Q, Dong S, "Construction of a tyrosinase-based biosensor in pure organic phase," *Analytical Chemistry*, vol. 67, 1995, pp. 1357-1360.

195. Cosnier S, Innocent, "A new strategy for the construction of a tyrosinase-based amperometric phenol and *o*-diphenol sensor," *Bioelectrochemistry and Bioenergetics*, vol. 31, 1993, pp. 147-160.

196. Cosnier S, Innocent C, "A novel biosensor elaboration by electropolymerization of an adsorbed amphiphilic pyrrole-tyrosinase enzyme layer," *Journal of Electroanalytical Chemistry*, vol. 328, 1992, pp. 361-366.

197. Boudraux CJ, Niroomand A, Jeannette T, "Waterborne 2K acrylic polyurethanes: novel low –NCO/-OH systems," *European Coatings Journal*, vol. 6, 1999, pp. 30-35.

198. Feng SX, Dvorchak M, Hudson KE, Renk C, Morgan T, Stanislawczyk V, Shuster DT, Bender H, Papenfuss J, "New high performance two-component wood coatings comprised of a hydroxy functional acrylic emulsion and a water dispersible polyicocyanate," *Journal of Coatings Technology*, vol. 71, 1999, pp. 51-57.

199. Melchiors M, Sonntag M, Kobusch C, Jürgens E, "Recent developments in aqueous two-component polyurethane (2K-PUR) coatings," *Progress in Organic Coatings*, vol. 40, 2000, pp. 99-109.

200. Schaffar BPH, "Thick film biosensors for metabolites in undiluted whole blood and plasma samples," *Analytical and Bioanalytical Chemistry*, vol. 372, 2002, pp. 254-260.

201. Pinschmidt RK, Chen N, "New N-vinylformamide derivatives as reactive monomers and polymers," In Symposium Series 755: Specialty, monomers and polymers: synthesis, properties, and applications, editors: Havelka KO, McCormick CL, (Washington DC: ACS, 2000) pp.119-131.

202. Tischer W, Wedekind F, "Immobilized enzymes: methods and applications," In Biocatalysis-from discovery to application, editor: Fessner WD, (Berlin: Springer-Verlag, 1999) pp. 95-126.

203. Fernández-Lorente G, Fernández-Lafluente R, Armisén P, Sabuquillo P, Mateo C, Guisán JM, "Engineering of enzymes via immobilization and post-immobilization techniques: preparation of enzyme derivatives with improved stability in organic media," In Methods in non-aqueous enzymology, editor: Gupta MN, (Basel: Birkhäuser Verlarg, 2000) pp. 36-51.

204. Bosley JA, Peilow AD, "Immobilization of lipases for use in non-aqueous reaction systems," In Methods in non-aqueous enzymology, editor: Gupta MN, (Basel: Birkhäuser Verlarg, 2000) pp. 52-69.

205. Liu Y, Yu T, "Polymers and enzyme biosensor," *Reviews in Macromolecular Chemistry and Physics*, vol. C7, 1997, pp. 459-500.

206. Dumitriu S, Chornest E, "Polysaccharide as support for enzyme and cell immobilization," In Polysaccharides, editor: Dumitriu S, (New York: Marcel Dekker, Inc., 1998) pp. 629-748.

207. Scouten WH, "A survey of enzyme coupling techniques," *Methods in Enzymology*, vol. 135, 1987, pp. 30-65.

208. Weetall HH, "Enzymes immobilized on inorganic supports," *Trends in Biotechnology*, vol. 3, 1985, pp. 276-280.

209. Fischer L, Peißker F, "A covalent two-step immobilization technique using itaconic anhydride," *Applied Microbiology and Biotechnology*, vol. 49, 1998, pp. 129-135.

210. Kim J, Delio R, Dordick JS, "Protease-containing silicates as active antifouling materials," *Biotechnology Progress*, vol. 18, 2002, pp. 551-555.

211. Yang Z, Williams D, Russell AJ, "Synthesis of protein-containing polymers in organic solvents," *Biotechnology and Bioengineering*, vol. 45, 1994, pp. 10-17.

212. Fulcrand V, Jacquier R, Lazaro R, Viallefont P, "Enzymatic peptide synthesis in organic solvent mediated by gels of copolymerized acrylic derivatives of α-chymotrypsin and polyoxyethylene," *International Journal of Peptide and Protein Research*, vol. 38, 1991, pp. 273-277.

213. Hartleib J, Geschwinder S, Scharff E, Rüterjans H,."Role of calcium ions in the structure and function of the di-isopropylfluorophosphatase from *Loligo vulgaris*," *Biochemical Journal*, vol. 353, 2001, pp. 579-589.

214. Scharff EI, Lücke C, Fritzsch G, Koepke J, Hartleib J, Dierl S, Rüterjans H,. "Crystallization and preliminary x-ray crystallographic analysis of DFPase from *Loligo vulgaris*," *Acta Crystallography*, vol. D57, 2001, pp. 148-149.

215. Scharff E I, Koepke J, Fritzsch G, Lucke C, Ruterjans H, "Crystal structure of diisopropylfluorophosphatase from Loligo vulgaris," *Structure*, vol. 9, 2001, pp. 493-502.

216. Price NRA, "Circular dichroism protein analysis," In Molecular biology and biotechnology, editor: Meyers RA, (New York: VCH publishers, 1995) pp. 179-185.

217. De Filippis V, Vangelista L, Schiavo G, Tonello F, Montecucco C, "Structural studies on the zinc-endopeptidase light chain of tetanus neurotoxin," *European Journal of Biochemistry*, vol. 229, 1995, pp. 61-69.

218. Yang Y, Chen R, Zhou H-M, "Comparison of inactivation and conformational changes of native and apo yeast dehydrogenase during denaturation," *Biochemistry and Molecular Biology International*, vol. 45, 1998, pp. 475-487.

219. Bullbock J, Chowdhury S, Johnston D, "Characterization of poly(ethylene glycol)-modified superoxide dismutase: comparison of capillary electrophoresis and matrix-assisted laser desorption/ionization mass spectrometry," *Analytical Chemistry*, vol. 68, 1996, pp. 3258-3264.

220. Roberts MJ, Harris JM, "Attachment of degradable poly(ethylene glycol) to proteins has the potential to increase therapeutic efficacy," *Journal of Pharmaceutical Sciences*, vol. 87, 1998, pp. 1440-1445.

221. Chowdhury SK, Doleman M, Johnston D, "Fingerprinting proteins coupled with polymers by mass spectrometry: Investigation of polyethylene glycol-conjugated superoxide dismutase," *Journal of the American Society for Mass Spectrometry*, vol. 6, 1995, pp. 478-487.

222. Hillenkamp F, Karas M, Beavis RC, Chalt BT, "Matrix-assisted laser desorption/ionization mass spectrometry of biopolymers," *Analytical Chemistry*, vol. 63, 1991, pp. 1193-1202.

223. Korsmeyer KK, Guan S, Yang Z-C, Falick AM, Ziegler DM, Cashman JR, "N-glycosylation of pig flavin-containing monooxygenase form 1: determination of the site of protein modificiation by mass spectrometry," *Chemical Research in Toxicology*, vol. 11, 1998, pp. 1145-1153.

224. Exterkate FA, Alting AC, "Role of calcium in activity and stability of the Latococcus lactis cell envelope proteinase," *Applied and Environmental Microbiology*, vol. 65, 1999, pp. 1390-1396.

225. Dragani B, Cocco R, Ridderström M, Stenberg G, Mannervik B, Aceto A, "Unfolding and refolding of human Glyoxalase II and single-tryptophan mutants," *Journal of Molecular Biology*, vol. 291, 1999, pp. 481-490.

226. Dolashka-Angelova P, Angelova M, Genova L, Stoeva S, Voelter W, "A novel Cu, Zn superoxide dismutase from the fungal strain Humicola lutea 110: isolation and physico-chemical characterization," *Spectrochimica Acta Part A*, vol. 55, 1999, pp. 2249-2260.

227. Tanzawa K, Berger J, Prockop DJ, "Type I procollagen N-proteinase from whole chick embryos," *Journal of Biological Chemistry*, vol. 260, 1985, pp. 1120-1126.

228. Czerwinski SE, Maxwell DM, Lenz DE, "A method for measuring octanol:water partition coefficients of highly toxic organophosphorus compounds," *Toxicology Methods*, vol. 8,1998, pp. 139-149.

229. Sedmak JJ, Grossberg SE, "A rapid method, sensitive and versatile assay for protein using coomassie brilliant blue G250," *Analytical Biochemistry*, vol. 79, 1977, pp. 544-552.

230. Bradford MM, "A rapid and sensitive method for the quantitation of microgram quantities of protein utilizing the principle of protein-dye binding," *Analytical Chemistry*, vol. 72, 1976, pp. 248-254.

231. Yang JT, Wu C, Martinez H, "Calculation of protein conformation from circular dichroism," *Methods in Enzymology*, vol. 130, 1986**,** pp. 208-269.

232. Hu Z, Korus RA, Stormo KE, "Characterization of immobilized enzymes in polyurethane foams in a dynamic bed reactor," *Applied Microbiology Biotechnology*, vol. 39, 1993, pp. 289-295.

233. Storey KB, Duncan JA, Chakrabarti AC, "Immobilization of amyloglucosidase using two forms of polyurethane polymer," *Applied Biochemistry Biotechnology*, vol. 23, 1990, pp. 221-236.

234. Wang P, Sergeeva MV, Lim L, Dordick JS, "Biocatalytic plastics as active and stable materials for biotransformations," *Nature Biotechnology*, vol. 115, 1997, pp. 789-793.

235. Cheng T-C, Calorimis JJ, "A cloned bacterial enzyme for nerve agent decontamination," *Enzyme Microbial Technology*, vol. 18, 1996, pp. 597-601.

236. Arroyo MA, Sánchez-Montero JM, Sinisterra JV, "Thermal stabilization of immobilized lipase B from *Candida Antarctica* on different supports: effect of water activity on enzymatic activity in organic media," *Enzyme Microbial Technology*, vol. 24, 1999, pp. 3-12.

237. Henley JP, Sadana A, "A mathematical model analysis of enzyme stabilization by a series-type mechanism: influence of chemical modifiers," *Biotechnology and Bioengineering*, vol. 26, 1984**,** pp. 959-969.

238. Frömmel C, Höhne WE, "Influence of calcium binding on the thermal stability of thermitase, a serine protease from *Thermoactinomyces vulgaris*," *Biochimica Biophysica Acta*, vol. 670, 1981, pp. 25-31.

239. Benov L, Sage H, Fridovich I, "The copper- and zinc-containing superoxide dismutase from *Escherichia coli*: molecular weight and stability," *Archives of Biochemistry and Biophysics*, vol. 340, 1997**,** pp. 305-310.

240. Cowan DA, Daniel RM, "Purification and some properties of an extracellular protease (caldolysin) from an extreme thermophile," *Biochimica Biophyisa Acta*, vol. 705, 1982, pp. 293-305.

241. Freeman SA, Peek K, Prescott M, Daniel R, "Characterization of a chelator-resistant proteinase from *Thermus* strain Rt4A2," *Biochemistry Journal*, vol. 195, 1993**,** pp. 463-469.

242. Toogood H.S, Prescott M, Daniel RM, "A pepstatin-intensive aspartic proteinase from a thermophilic *Bacillus* sp.," *Biochemistry Journal*, vol. 307, 1995**,** pp. 783-789.

243. Mabrouk PA, "Effect of pegylation on the structure and function of horse cytochrom c," *Bioconjugate Chemistry*, vol. 5, 1994, pp., 236-241.

244. Pocker Y, Sarkanen S, "Carbonic anhydrase: structure, catalytic versatility, and inhibition," *Advances in Enzymology*, vol. 47, 1978, pp. 149-274.

245. Pocker Y, Strom DR, "The catalytic versatility of erythrocyte carbonic anhydrase. IV. Kinetic studies of enzyme-catalyzed hydrolyses of *p*-nitrophenyl esters," *Biochemistry*, 1968, vol. 7, pp.1202-1214.

246. Lindskog S, "Structure and mechanism of carbonic anhydrase," *Pharmacology Therapy*, vol. 74, 1997, pp. 1-20.

247. Fersht A, In: Structure and mechanism in protein science: a guide to enzyme catalysis and protein folding, (New York: WH Freeman and Company, 1998), pp.76-77.

248. Tsarevsky NV, Pintauer T, Matyjaszewski K, "Atom transfer radical polymerization of ionic monomers in aqueous solution: mechanistic studies and synthesis," *Polymer preprints*, vol. 43, 2002, pp. 203-204.

249. Lynn M, "Inorganic support intermediates: covalent coupling of enzymes on inorganic supports," In: Immobilized enzymes, antigens, antibodies, and peptides, editor: Weetall HH, (New York: Marcel Dekker, Inc., 1975), pp. 1-47.

250. Yoshimoto T, Mihama T, Takahashi K, Saito Y, Tamaura Y, Inada Y, "Chemical modification of enzymes with activated magnetic modifier," *Biochemical and Biophysical Research Communications*, vol. 145, 1987, pp. 908-914.

251. Šuškovic B, Vajtner Z, Naumski R, "Synthesis and biological activities of some peptidoglycan monomer derivatives," *Tetrahedron*, vol. 47, 1991, pp. 8407-8416.

252. Alomirah HF, Alli I, Konishi Y, "Applications of mass spectrometry to food proteins and peptides," *Journal of chromatography A*, vol. 893, 2000, pp. 1-21.

253. Andreopoulos FM, Roberts MJ, Bentley MD, Harris JM, Beckman EJ, Russell AJ, "Photoimmobilization of organophosphorous hydrolase within a PEG-based hydrogel," *Biotechnology and Biotechnology*, vol. 65, 1999, pp.579-588.

254. Teodorescu M, Matyjaszewski K, "Atom transfer radical polymerization of meth(acrylamides)," *Macromolecules*, vol. 32, 1999, pp. 4826-4831.

255. Rademacher JT, Braum M, Pallack ME, Brittain WJ, "Atom transfer radical polymerization of N,N-dimethylacrylamdie," *Macromolecules*, vol. 33, 2000, pp. 284-288.

256. Yang Z, Mesiano AJ, Venkatasubramanian , Gross SH, Harris JM, Russell AJ, "Activity and stability of enzymes incorporated into acrylic polymers," *Journal of the American chemical Society*, vol. 117, 1995, pp. 4843-4850.

257. Wang P, Sergeeva MV, Lim L, Dordick JS, "Biocatalytic plastics as active and stable materials for biotransformaitons," *Nature Biotechnology*, vol. 15, 1997, pp. 789-793.

258. Lococq J, "Particulate markers for immunoelectron microscopy," In Fine structure immunocytochemistry, editor: Griffiths G, (Berlin: Springer-Verlag, 1993), pp. 279-306.

259. Albrecht RA, Simmons SR, Pawley JB, "Correlative video-enhanced light microscopy, high voltage transmission electron microscopy, and field emission scanning electron microscopy for the localization of colloidal gold labels," In Immunocytochemistry, editor: Beesley J, (New York: IRL Press, 1993), pp. 151-176.

260. Andreopoulos FM, Beckman EJ, Russell AJ, "Light-induced tailoiring of PEG-hydrogel properties," *Biomaterials*, vol. 19, 1998, pp. 1343-1352.

261. Page CL, Short NR, El Tarras A, "Diffusion of chloride ions in hardened cement pastes," *Cement Concrete Research*, vol. 11, 1981, pp. 395-406.

262. Van Stroe-Biezen SAM, van der Loo JMH, Janssen LJJ, Eveaerts FM, "Determination of the inherent kinetics of immobilized glucose oxidase using a diffusion cell," *Bioprocess Engineering*, vol. 15, 1996, pp. 87-94.

263. Bird RB, Stewart WE, Lightfoot EN, In Transport phenomena, editors:, (New York: John Wiley & Sons, Inc., 1966), Chapter 17.

264. Gray WG, "A derivation of the equations for multi-phase transport," *Chemical Engineering Sciences*, vol. 30, 1975, pp. 229-233.

265. Hu ZC, Korus RA, Storno KE, "Characterization of immobilized enzymes in polyurethane foams in a dynamic bed reactor," *Applied Microbiology and Biotechnology*, vol. 39, 1993, pp. 289-295.

266. Reid RC, Prausnitz JM, Poling BE, Diffusion coefficients. In: The properties of gases and liquids, editors: Sun B et al., (New York: McGraw-Hill Book Company, 1987), pp.577-631.

267. Buenfeld NR, Zhang JZ, "Chloride diffusion through surface-treated mortar specimens," *Cement Concrete Research*, vol. 28, 1998, pp. 665-674.

268. Pinschmidt RK, Jr, Walter LR, Carroll E, Yacouh K, Drescher J, Nordquist AF, Chen N, "N-vinylformamide-building lock for novel polymer structures," *Journal of Macromoleculaes Science-Pure Applied Chemistry*, vol. A34, 1997, pp. 1885-1905.

269. Veronese FM, Largajolli R, Boccù E, Benassi CA, Schiavo O, "Surface modification of proteins: Activation of monomethoxy-polyethylene glycols by phenylchloroformates and modification of ribonuclease and superoxide dismutase," *Applied Biochemical Biotechnology*, vol. 11, 1984, pp. 141-152.

270. Yang Z, Domach M, Auger R, Yang FX, AJ Russell, "Polyethylene glycol-induced stabilization of Subtilisin," *Enzyme Microbial Technology*, vol. 18, 1996, pp. 82-89.

271. Pinschmidt RK, Jr, Chen N, "New N-vinylformamide derivatives and their use in radiation cure coatings," *Polymer Preprints*, vol. 39, 1998, pp. 639-640.

272. Ford DJ, Fesce AJ. "Reaction of glutaraldehyde with proteins," In: Enzyme immunoassay, (Tokyo: Igaku-Shoin, 1981), pp. 54-66.

273. Crumbliss AL, Stonehuerner J, Henkens RW. “The use of inorganic materials to control or maintain immobilized enzyme activity,” *New Journal of Chemistry*, vol. 18, 1994, pp. 327-339.

274. Badjic JD, Kostic NM. “Effects of encapsulation in sol-gel silica glass on esterase activity, conformational stability, and unfolding of bovine carbonic anhydrase II,” *Chemistry of Materials*, vol. 11, 1999, pp. 3671-3679.

275. Andreopoulos F.M, Roberts MJ, Bentley MD, Harris JM, Beckman EJ, Russell AJ. “Photoimmobilization of orpganophosphorus hydrolasse within a PEG-based hydrogel,” *Biotechnology and Bioenginering*, vol. 65, 1999, pp. 579-588.

276. Azari F, Nemat-Gorgani M. “Reversible denaturation of carbonic anhydrase provides a method for its adsorptive immobilization,” *Biotechnology and Bioengineering*, vol. 62, 1999, pp. 193-199.

277. Crumbliss AL, McLachlan KL, O’Daly J.P, Henkens RW. “Preparation and activity of carbonic anhydrase immobilized on porous silica beads and graphite rods,” *Biotechnology and Bioengineering*, vol. 31, 1987, pp. 796-801.